PURINERGIC P2X7 RECEPTOR: PATHOPHYSIOLOGICAL ROLE IN ALVEOLAR FUNCTIONS

By
Dr. AMARJIT MISHRA
Bachelor of Veterinary Science & Animal Husbandry
West Bengal University of Animal and Fishery Sciences,
Kolkata, India.
2003

Master of Veterinary Science (Animal Biochemistry)
Indian Veterinary Research Institute,
Bareilly, India.
2005

Submitted to the Faculty of the
Graduate College of the
Oklahoma State University
in partial fulfillment of
the requirements for
the Degree of
DOCTOR OF PHILOSOPHY
December, 2011.

PURINERGIC P2X7 RECEPTOR: PATHOPHYSIOLOGICAL ROLE IN ALVEOLAR FUNCTIONS

Thesis Approved:

Dr. Lin Liu

Dr. Carey Pope

Dr. Myron Hinsdale

Dr. Jeffrey Hadwiger

Dr. Sheryl Tucker

(Dean of the Graduate College)

TABLE OF CONTENTS

LIST OF TABLES

LIST OF FIGURES

LIST OF ABBREVIATIONS

AEC I	Alveolar type I epithelial cell
AEC II	Alveolar type II epithelial cell
ATP	Adenosine triphosphate
ADAM	A Disintegrin and Metalloproteinase
ARDS	Acute Respiratory Distress Syndrome
ALI	Acute Lung Injury
BzATP	2’ (3’)-O-(4-Benzoylbenzoyl) adenosine ’triphosphate
CaMK	Ca2+–calmodulin-dependent protein kinase
COPD	Chronic obstructive pulmonary Disease
DAG	Diacylglycerol
DMEM	Dulbecco's Modified Eagle's Medium
DPPC	Dipalmitoylphosphatidylcholine
DAMP	Damage-associated molecular patterns
EDTA	Ethylene Diamine Tetraacetic Acid
FBS	Fetal Bovine Serum
GPI	Glycosylphosphatidylinositol
HEK	Human Embryonic Kidney
IP3	Inositol triphosphate
Ig	Immunoglobulin
IL-1β	Interleukin -1-beta

MAPK	Mitogen Activated Protein Kinase
OxATP	Oxidized ATP
PAMP	Pathogen-associated molecular patterns
PLD	Phospholipase D
PKC	Protein kinase C
PKA	Protein kinase A
ROS	Reactive oxygen species
sVCAM-1	Soluble Vascular cell adhesion molecule -1
SPA	Surfactant Protein A
TNF-α	Tumor Necrosis Factor- alpha
VCAM-1	Vascular Cell adhesion molecule -1

CHAPTER I

INTRODUCTION

1. Purinergic receptors

1.1 Classification and basic structures

Purinergic receptors were first recognized by Burnstock in 1978, when he proposed the two classes of purinoceptors termed P1 and P2 purinoceptors (Burnstock *et al.*, 1978a;Burnstock *et al.*, 1978b). P1 purinoceptors couple to adenylate cyclase and are competitively antagonized by low concentrations of methylxanthines. P2-puriniceptors are preferentially activated by ATP or ADP and other nucleotides. This agonist-based classification is the fundamental part of purinergic receptor research (Ziganshin *et al.*, 2002).

A1 and A2 subtypes in the adenosine/P1 receptor family were soon described by van Calker et al. in 1979 and Londos et al. in 1980 (Vancalker *et al.*, 1979;Londos *et al.*, 1980). The stimulation of A1 and A2 receptors results in the inhibition and activation of adenylate cyclase, respectively. A2 receptors are further subdivided into A2A and A2B, with high- and low- affinity of A2 agonist, respectively. A3 receptor was later proposed following its cloning from rat striatum (Zhou *et al.*, 1992).

P2 purinoceptors are broadly subdivided into P2X and P2Y based on pharmacological characteristics in that α, β-meATP was the most potent agonist for the P2X purinoceptors, and 2-meSATP for P2Y purinoceptors (Burnstock &

Kennedy, 1985). ATP acts as a ligand for P2X purinoceptors and opens a cation selective channel (ionotropic receptors). ATP or UTP serves as a ligand for P2Y purinoceptors and causes the activation of the phosphoinositide signaling cascade, i.e. formation of inositol (1, 4, 5) triphosphate and release of Ca^{2+} from intracellular stores (metabotropic receptors).

The purinoceptors are further classified by molecular biology approach (Dubyak, 1991;Pirotton *et al.*, 1991;Harden *et al.*, 1995). Based on sequence homology seven subclasses of the P2X receptor family (P2X1-7) was reported. These subclasses have 30-40% homology in their primary structure (Khakh *et al.*, 2001), but differ considerably in the length of their carboxy-termini ranging from as short as 30 and 48 amino acids for P2X6 and P2X1, respectively to as long as 240 amino acids for P2X7 (North, 2002). The structural features are predicted from the amino acids sequences of the cloned P2X receptors. The P2X receptor subunits have two hydrophobic transmembrane domains with intra-cellular amino and carboxyl-termini and an ATP-binding pocket within the extracellular intervening hydrophilic loop. However, one subunit with two transmembrane domains alone is unlikely to form an ion channel. They are organized in a homo or hetero-trimeric or larger complexes (Cusack, 1993a;Nicke *et al.*, 1998). The extracellular loop of the seven receptors (P2X1 to P2X7) comprises of 10 conserved cysteine residues, 14 conserved glycine residues, and 2-6 potential N-linked glycosylation sites. The 10 cysteines form 5 disulfide bridges and impose structural constraints needed to couple the ATP-binding site to the ion channel. Majority of the conserved region are in the extra-cellular loop with the

transmembrane domains being less conserved. P2X receptors can also be divided into two broad groups according to the speed of desensitization: one group (P2X1 and P2X3) desensitize rapidly within 50-300 ms and another group (P2X2, P2X4, P2X5, P2X6, P2X7) slowly up to several seconds. The mechanism of P2X receptor desensitization is not completely understood. The interactions between the two transmembrane domains, but not the extracellular loop of the P2X1 receptor, are required for the receptor desensitization. However, the desensitization for P2X3 is controlled by Ca^{2+}-dependent calcineurin-mediated dephosphorylation involving N-terminal residues.

P2Y recptor family consists of 8 members (P2Y1, P2Y2, P2Y4, P2Y6, P2Y11, P2Y12, P2Y13 and P2Y14), all of which are 7-transmembrane G-protein coupled receptors (Cusack, 1993a). The positively charged amino acid residues in transmembrane domains (residues III, VI and VII) are involved in the ligand binding by electrostatic interactions with the phosphates of ATP (von Kugelgen & Harden, 2011). Other P2Y receptors including P2Y3, P2Y7, P2Y8, P2Y9 and P2Y10, were found identical with other P2Y receptor proteins and only exists in non-mammalian species. These P2Y receptors are not able to activate phospholipase-C (PLC) or adenylate cyclase (AC). Therefore, these receptors were eventually removed from the P2Y purinoceptor family. The signaling pathway initiated through all P2Y receptors is the activation of PLC, leading to IP3 formation and Ca^{2+} mobilization. This stimulates a variety of signaling pathways including PKC, PLA_2 and Ca^{2+}-dependent K^+ channels. The second signaling pathway is the inhibition of adenylate cyclase in almost all P2Y

subtypes, except in P2Y11 which stimulates adenylate cyclase. ATP and UTP activate almost all P2Y with variable potency. For example the positively charged amino acids of the P2Y2 receptor in the transmembrane regions VI and VII contributes from part of the ATP or UTP binding sites (Garrand *et al.*, 1995). P2Y2 receptor couples to Gi/o and Gq/11 and mediate phospholipid breakdown and IP3 generation as well as Ca^{2+} mobilization via PLCβ. Moreover, inhibition of adenylate cyclase by P2Y2 receptor has been shown in some cell system.

1.2. Extracellular ATP and purinergic signaling

Over the last two decades, a total of 19 different purinergic receptor subtypes (including 7 P2X receptors, 8 P2Y receptors, and 4 adenosine receptors) that can recognize extracellular ATP and adenosine have been cloned and characterized (Ralevic & Burnstock, 1998). In addition, several families of ectonucleotidases that hydrolyse ATP to ADP, AMP and adenosine have been found (Zimmermann, 2000). These distinct sets of purinergic receptors and ectonucleotidases are expressed on the cell surface of the different mammalian cells and regulate cellular activities through cell-type specific purinergic signaling systems (Burnstock, 2008;Corriden & Insel, 2010).

Controlled ATP release from intact cells was first identified in neurons (Abbracchio *et al.*, 2009). ATP is also released from non-neuronal cells through vesicular transport (Praetorius & Leipziger, 2009). Additional mechanisms for ATP release has been reported including release through stretch-activated channels, voltage-dependent and multi-channel anion transporter or permeases (Alawqati, 1995), cystic fibrosis transmembrane conductance regulator (CFTR)

(Braunstein *et al.*, 2001), and P2X7 receptor associated connexin and pannexin hemichannels (Praetorius & Leipziger, 2009). ATP release from mouse neutrophil occurs through connexin-43 hemi channels (Eltzschig *et al.*, 2006).

Extracellular ATP has two fates before being degraded by the ectonucleotidases. The released ATP either acts on the purinoceptors of the same cell (autocrine) or the neighboring cells (paracrine). Autocrine signaling through the purinergic receptors regulates the neutrophil chemotaxis via ATP release from polarized neutrophil in response to chemotactic mediators (Chen *et al.*, 2006). The activated T cells also induces the release of ATP through pannexin 1 channels. These hemichannels translocate with P2X receptors to the immune synapse, where they promote Ca^{2+} influx and cell activation through autocrine purinergic signaling (Schenk *et al.*, 2008;Yip *et al.*, 2009). The activation of purinergic receptors in immune cells can elicit either positive or negative feedback mechanisms and thus tighly regulate immune responses.

Paracrine purinergic signaling regulates a wide range of physiological process, including immune cell functions (Bours *et al.*, 2006;Corriden & Insel, 2010). ATP released from damaged or stressed host cells serves as an important function in the recognition of 'danger signals' and guides phagocytes to inflammatory sites. Thus promotes clearance of damaged and apoptotic cells (Elliott *et al.*, 2009). In response to damage-associated molecular patterns (DAMPs) and pathogen-associated molecular patterns (PAMPs), activation of inflammasome and the subsequent release of interleukin-1β (IL-1β) require purinergic singnalling. In the cytoplasm nucleotides are concentrated in the

micomolar or even millimolar level, while the extracellular concentration is extremely low, usually in the nanomolar range (Dubyak, 2002). ATP is rapidly released upon damage of plasma membrane and diffuses throughout the pericellular space and bind to specific receptors expressed by virtually all immune cells (Di Virgilio *et al.*, 2001). Diffusion of nucleotides is drastically controlled via degradation by ecto-nucleotidases expressed on the plasma membranes of most cells. Rapid metabolism of extracellular ATP generates the anti-inflammatory metabolite adenosine and terminates the alert-signal to a checkpoint (Ohta & Sitkovsky, 2001).

2. P2X7 receptor

2.1. Distribution

P2X7 receptors are expressed on the cells of hematopoietic lineage. The distribution of P2X7 receptor has been studied by permeability and RT-PCR analysis in cultured monocytes/macrophages (Hickman *et al.*, 1994), phagocytes (CoutinhoSilva *et al.*, 1996), dendritic cells (Coutinho-Silva *et al.*, 1999), T lymphocytes (Baricordi *et al.*, 1996), B lymphocytes (Wiley *et al.*, 1992), mast cells (Tatham & Lindau, 1990) and eosinophils (Ferrari *et al.*, 2000). In the central nervous system functional P2X7 receptors are localized on microglia, Schwann cells and astrocytes (Ferrari *et al.*, 1996;Collo *et al.*, 1997). In dorsal root ganglia, P2X7 receptor appears to be selectively localized on glia cells, but not neurons. P2X7 receptor has also been identified in fibroblasts (Ferrari *et al.*, 1996;Solini *et al.*, 2000), endothelial cells (Ray *et al.*, 2002) and epithelial cells

(Slater *et al.*, 2000). Our laboratory has reported previously specific expression of P2X7 receptors in alveolar type I epithelial cells (AEC I) (Chen *et al.*, 2004).

2.2. Structure

The cytolytic P2Z receptor previously described in mast cells, macrophages and lymphocytes was re-classified as the P2X7 receptor on the basis of homology with the 6 described members of P2X family of receptors. ATP-sensitive P2X7 receptors are the latest cloned member of the P2X family. The P2X7 receptor, first cloned from rat brain and human monocytes, is the most disparate from other P2X subtypes, in terms of structure and function (Rassendren *et al.*, 1997;Surprenant *et al.*, 1996).

The human P2X7 receptor gene comprises 13 exons and is located on chromosome 12q24.31. It is about 52 Kb long, and 23.7 Kb away from the P2X4 gene (Buell *et al.*, 1998). There are 32 non-synonymous, amino acid-altering single nucleotide polymorphisms (SNPs) currently documented for the P2X7 gene in dbSNP. However, none of these SNPs alters P2X7 receptor expression or function. There has been no report of other types of gene mutations, such as deletion or splicing variants of mRNA, in P2X7 receptor.

As other P2X receptor member, the P2X7 receptor has two transmembrane domains with intracellular amino and carboxy termini. Oligomeric structure in the plasma membrane is formed by trimerization or larger complexes of identical subunits. The P2X7 receptor appear not to form hetero-oligomers with other P2X receptors (Kim *et al.*, 2001). The unique feature of native P2X7 receptor is that it has a longer intracellular C-terminus (240 amino

acids) and forms pore in the plasma membrane. At least 177 amino acids take part in the pore formation (Surprenant *et al.*, 1996). Two lysine residues in the extracellular loop of P2X7 receptor (K193 and K311) are considered important for ATP binding (Worthington *et al.*, 2002). Alanine substitution of these residues abolished both BzATP and ATP- induced pore formation independent of the surface expression. A potential lipopolysaccharide (LPS)-binding motif (573-CRWRIRKEFPKSEGQYSG) has been found at the end of the C-terminus of the P2X7 receptor (Denlinger *et al.*, 2001). P2X7 receptor has also been shown to couple with extracellular matrix protein laminin α3, 3 cytoskeletal proteins (β-actin, α-actinin4 and supevillin), an integrin subunit (β2), a scaffolding protein (MAGuK, membrane-associated guanylate kinase P55 subfamily member 3), three chaperones (heat shock protein 90 'hsp 90', heat shock protein 70 'HSP 70' and heat shock cognate 71,'Hsc 71') and two signaling molecules (protein tyrosine phosphatase β 'RPTPβ' and phosphatidylinositol 4-kinase 'PI4K') (Kim *et al.*, 2001). However, the exact role of these components to the phosphorylation, glycosylation, trafficking, membrane expression and function of P2X7 receptor is still unknown and needs further investigation.

2.3 Pharmacology

The non-desensitizing P2X7 purinoceptor is the most sensitive to steric aspects of ATP structure among all P2X receptors (Cusack, 1993b). The active agonist requires the adenine base, D-ribose sugar and the 5'-triphosphate side chain. 2', 3'-O-(4-benzoylbenzoyl)-ATP (BzATP), a photoactivatable ATP analogue, is 10-100 times more potent than ATP in activating both native and

cloned P2X7 receptors (Dubyak & Elmoatassim, 1993). BzATP has significant greater potency (EC_{50}= 20 μM) than ATP (EC_{50} > 100 μM). The rank order of agonist potency of ATP and its analogues for P2X7 receptors is BzATP>ATP>>2-meSATP>ATPγS (Gargett *et al.*, 1997) and differs from other P2X receptors (Surprenant, 1996;Wiley *et al.*, 1998). However, species differences between human and murine P2X7 receptors have been observed, based on different sensitivities to membrane permeabilzation by ATP, BzATP and ATPγS (Hickman *et al.*, 1994). Brief agonist activation (< 10 s) of the P2X7 receptor results in rapid and reversible channel opening and expediate Na^+, K^+ and Ca^{2+} permeability (Surprenant, 1996). Under the conditions of hypoxia or tissue injury, ATP is released into the extracellular spaces (North, 2002). Therefore, in metabolically compromised tissues extracellular Na^+ is replaced by K^+ and enhances the efficacy and potency of ATP on P2X7 receptors. K^+ efflux enhances the ATP effect on P2X7 receptor–expressing cells. Thus, even low concentrations of ATP may activate the P2X7 receptor to a substantial extent (Riedel *et al.*, 2007). P2X7 receptor-operated channels are highly Ca^{2+} selective, although Ba^{2+} as well as fluorescent intercalator dyes such as YO-PRO-1 (375 Da), ethidium$^+$ (314 Da) are also permeable (Wiley *et al.*, 1998). BzATP-stimulated pore dilation and YO-PRO-1 dye uptake is one of the unique features of P2X7 receptors under physiological conditions. P2X7 receptor-mediated YO-PRO-1 uptake does not occur in all cell types and is dependent upon receptor density (North, 2002). P2X7 receptor upon priming undergoes agonist plasticity such that brief agonist exposure resulting in an apparent increase in potency to

subsequent agonist exposure (Chakfe *et al.*, 2002). However, prolonged P2X7 receptor activation triggers a series of cellular responses, such as activation of caspases, cytokine release, cell proliferation and apoptosis (Panenka *et al.*, 2001;Perregaux *et al.*, 2000).

Novel series of P2X7 receptor antagonists, composed of cyclic imides have been shown to be effective in inhibiting P2X7 receptor (Stokes *et al.*, 2006). For example, the cyclic imide member of this family, AZ10606120, potently blocks human P2X7 receptor-mediated cation influx and interleukin-1β (IL-1β) release. The AZD9056, have been shown to be effective against patients with chronic obstructive pulmonary disease (Stockley *et al.*, 2008). The 2', 3'-dialdehyde derivative of ATP, also known as oxidized ATP (OxATP), reacts with lysine residues at the ATP binding site to form a covalent schiff base. The reaction with OxATP gives total and irreversible inhibition of P2X7 receptor on mouse macrophages without affecting P2Y receptors (Murgia *et al.*, 1993). OxATP are 20-500-fold more potent for P2X7 receptor in human than that in mouse. However, OxATP has many other pharmacological off-targets including P2X1 and P2X2 receptors (Evans *et al.*, 1995) and nuclear factor-κB (NF-κB) and also inhibits cytokine release (Beigi *et al.*, 2003). The isoquinoline sulfonamide derivative KN-62, a potent inhibitor of calcium and calmodulin-dependent kinase II (CaMKII), also acts on P2X7 receptor (Gargett & Wiley, 1997). Brilliant Blue G selectively blocks ATP-gated rat and human P2X7 receptors with IC_{50} of 10 and 200 nM, respectively (Jiang *et al.*, 2000). All three of these noncompetitive

antagonists, KN-62, OxATP and BBG are highly selective for P2X7 receptors, with different potency at P2X7 orthologs.

2.4. Functions

Activation of P2X7 receptor results in a rapid but reversible channel opening that is permeable to cations such as Ca^{2+}, Na^{+} and K^{+} ions. Recent evidence suggests that channel opening is distinct from the P2X7 receptor-mediated pore formation. Firstly, the truncation of C-terminus (from residue 413) of rat P2X7 receptor results in loss of YO-PRO-1 uptake, but not BzATP-induced current, suggesting the long C-terminus is required for pore formation (Surprenant, 1996). Secondly, extracellular calmidazolium inhibits the BzATP-induced current by up to 90%, but has no effect on YO-PRO-1 uptake, indicating that blockade of the ionic channel does not prevent the pore formation (Virginio *et al.*, 1997). Thirdly, pore formation but not the ion channel opening is temperature-dependent (Nuttle *et al.*, 1993). However, a number of signaling events have been demonstrated to follow the primary signal events (ionic channel opening/pore formation) following ATP activation of P2X7 receptor.

2.4.1. Mature IL-1β, IL-18 and Nitric Oxide release

IL-1β and IL-18 are pro-inflammatory cytokines that requires processing by interleukin converting enzyme (ICE, also known as caspase-1) at specific aspartic residues for mature molecule production. Activation of P2X7 receptor on human macrophages triggers the release of these two cytokines (Ferrari *et al.*, 1997a;Mehta *et al.*, 2001;Perregaux *et al.*, 2000). P2X7 receptor is also required for inflammasome assembly and caspase activation (Perregaux & Gabel, 1998).

Studies on P2X7 receptor knock-out mice have shown that absence of P2X7 receptor leads to an inability to release IL-1β in response to ATP stimulation from peritoneal macrophages (Solle *et al.*, 2001). P2X7 null mice therefore have impaired cytokine signaling cascade *in vivo*. This suggests that P2X7 receptor activation provides signals for maturation and release of IL-1β and initiation of a cytokine cascade.

Both ATP and BzATP show a concentration-dependent stimulation of LPS-stimulated nitric oxide (NO) release in macrophages. This effect is blocked by OxATP, strongly suggesting that P2X7 receptor plays a crucial role in LPS-dependent NO release in macrophages (Sperlagh *et al.*, 1998). Furthermore, LPS-induced endogenous ATP release from macrophages could be the major source of ATP which activates P2X7 receptor in macrophages.

2.4.2. Activation of NF-κB and Phospholipase D (PLD)

ATP and BzATP can induce activation of a transcription factor controlling cytokine expression and apoptosis. This delayed ATP-effect is blocked by OxATP, indicating the involvement of P2X7 receptor. ATP induced-activation requires both reactive oxygen intermediates (ROIs) and caspase-1. The unique NF-κB-DNA complex induced by ATP is transcriptionally active and induces expression of NF-κB target genes (Ferrari *et al.*, 1997b). This suggests that P2X7 receptor control the expression of subsets of NF-κB target gene distinct from the classical proinflammatory mediators.

Membrane phospholipase D (PLD) catalyses the phosphotidylcholine hydrolysis into phosphatidic acid and choline. ATP stimulates both Ca^{2+}-

dependent and -independent phospholipase D activity following brief exposure in macrophages and lymphocytes. Stimulation of Ca^{2+}-dependent PLD is directly proportional to bivalent cation influx through P2X7 receptor (Elmoatassim & Dubyak, 1993;Fernando *et al.*, 1999).

2.4.3. Cell membrane blebbing

BzATP stimulation of HEK293 cells transfecteed with P2X7 receptor shows an irreversible loss of plasma membrane. This phenomenon does not occur in P2X2 receptor transfected cells. The unprocessed and mature form of IL-1β was found in the shed microvesicles (MacKenzie *et al.*, 2001). P2X7–mediated microvesicle formation and shedding might be a crucial pathway for secretory protein release from cytoplasm.

2.4.4. Shedding of L-selectin and CD23

L-selectin (CD62L; a C-type lectin) and CD23 (low affinity IgE receptor) are involved in the adhesive interaction and rolling behavior of lymphocytes on endothelial cells (Gu *et al.*, 1998). P2X7 receptor contributes to the regulation of intercellular interactions and to the generation of soluble markers. Elevated levels of CD62L and CD23 in sera have been reported from B-cell chronic lymphocytic leukaemia (B-CLL) patients (Wiley *et al.*, 2002). ATP-induced shedding process of these molecules are metalloproteinase-mediated (Gu *et al.*, 1998;Jamieson *et al.*, 1996). ATP-induced L-selectins and CD23 shedding have also been shown to decrease in P2X7 receptor knock-out mice, indicating the pathophysiological role of P2X7 receptor (Labasi *et al.*, 2001).

2.4.5. ATP-induced cytotoxicity

Involvement of P2X7 receptor in ATP-induced apoptosis is well documented in lymphocytes (Chused *et al.*, 1996), monocytes (Grahames *et al.*, 1999), macrophages (Blanchard *et al.*, 1991), murine thymocytes (Pizzo *et al.*, 1992), and dendritic cells (Coutinho-Silva *et al.*, 1999). P2X7 receptor activation has been shown to stimulate the activity of intracellular caspases prior to ATP-induced apoptosis. K^+ efflux through the P2X7 receptor ion channel leads to cell shrinkage and activation of caspase cascades (Bortner *et al.*, 1997).

2.5. Diseases

P2X7 receptor plays important roles in immunity, inflammation, bone homeostasis, neurological function and neoplasia (Di Virgilio *et al.*, 1998;Hughes *et al.*, 2007). There is increase body of evidence implicating P2X7 receptor in various pathological conditions of pulmonary, cardiac, renal, skeletal muscle and central nervous system (CNS) disorders, where inflammation is the corner stone of these disorders.

Studies in animal models have implicated a close connection of P2X7 receptor to Alzheimer disease (McLarnon & Ryu, 2009), Parkinson's disease (Takenouchi *et al.*, 2010), multiple sclerosis, sensory neuropathies and neuropathic pain (Abbracchio *et al.*, 2009). P2X7 receptor with its direct effect in apoptosis plays significant role as it was shown in prostate cancers (Maianski *et al.*, 2007), uterine epithelial cancers (Li *et al.*, 2009) as compared to healthy tissues.

P2X7 receptors are expressed in cells of the cardiovascular system and have been shown to be associated with hypertensions and thrombotic events (Furlan-Freguia *et al.*, 2011). Production of cytokines and apoptosis of endothelial cells are critical phenomenon during vascular remodeling in hypertension. The hypotensive responses in inflammatory diseases via IL-1β release with nitric oxide synthesis are linked to P2X7 receptor function in the pathogenesis of cardiac disorders.

The involvement of P2X7 receptor in the pathogenesis of pulmonary emphysema (Lucattelli *et al.*, 2011), and COPD (Eltom *et al.*, 2011;Cicko *et al.*, 2010) has been well documented. Pulmonary fibrosis is characterized by inflammation and fibrosis of the interstitium and destruction of alveolar histoarchitecture. Recent animal studies have identified the importance of P2X7 receptor and pannexin-1 complex in IL-1β maturation, inflammation and evolution to pulmonary fibrosis (Riteau *et al.*, 2010).

3. Lung surfactant secretion

3.1. Lung surfactant

Lung surfactant is a lipid-enriched substance comprising of 80% glycerophospholipids, 10% cholestrol and about 5-10% proteins. Di-palmitoylphosphatidyl choline (DPPC) is the major glycerophospholipid present in surfactant. The major function of surfactant is to reduce surface tension in the lung. There are 4 major surfactant proteins. SP-B and SP-C are synthesized in endoplasmic reticulumn and further processed by Golgi apparatus. These proteins are stored in lamellar bodies preceeding exocytosis (Clark *et al.*, 1995). However,

SP-A and SP-D secretes constitutively independent of lamellar bodies (Rooney, 2001). Alveolar epithelial type II cells (AEC II) stores and secrete surfactant. Physiologically, mechanical stretch, labor, and ventilation induce surfactant secretion from AEC II. However, recent experiments suggests that lung distensions rather than systemic changes accompanying hyperventilation (Pco_2, Po_2, and pH) increases surfactant secretion (Tschumperlin & Margulies, 1999). The mechanical stretch of the AEC II during an enhanced inspiration ('sigh') is a direct stimulus for surfactant secretion.

3.2. Regulation of surfactant secretion

The commonly held view of regulated surfactant secretion from AEC II involves cell membrane receptors including β_2-adrenergic, adenosine A2B, and purinergic P2Y2. ATP, UTP, adenosine, platelet activating factor, LPS, and IL-1β are the known agonists to stimulate surfactant secretion (Andreeva *et al.*, 2007). Stimulation of these receptors ultimately leads to activation of protein kinase A (PKA), protein kinase C (PKC) and calcium and calmodulin kinase (CaMK) and their downstream partners. The purinergic metabotropic receptor, P2Y2, is coupled to the G protein Gq, which stimulates phospholipase C (PLC) and hydrolyzes phosphotidylinositol biphosphate into diacylglycerol (DAG) and inositol triphosphate (IP_3) (Rooney *et al.*, 1992). The increase in intracellular Ca^{2+} concentration results in enhanced surfactant secretion (Ashino *et al.*, 2000). Surfactant exocytosis in AEC II is extremely sensitive to perturbations of Ca^{2+}. *In vitro,* secretagogues including β_2-adrenergic agonists (terbutaline), A_{2B} receptor agonists (adenosine), $P2Y_2$ receptor agonists (ATP and UTP), PKC activators

(phorbol esters) and calcium ionophores (A23187) have been shown to stimulate surfactant exocytosis. Terbutaline and adenosine activate adenyl cyclase which further stimulates PKA-mediated signaling. Moreover, ATP and phorbol esters activate PKC and downstream signaling molecules. The ionophores increase the intracellular calcium concentrations which further activates PKC and CAMK II. Activation of various kinases leads to phosphorylation of various proteins resulting in surfactant exocytosis. However, the mechanism of how the phosphorylation induces secretion is incompletely understood.

3.3. Contribution of AEC I to surfactant secretion

The alveolar epithelium has two specialized epithelial cell types: the terminally differentiated squamous AEC I and the surfactant producing cuboidal AEC II. The AEC I cover 95% of the alveolar surface and form a tight epithelial barrier with the AEC II to facilitate gas and water exchange. Alveolar epithelial cells are closely associated with endothelial cells, stromal fibroblasts, inflammatory cells, and the accompanying extracellular matrix. The function of AEC I has been relatively unexplored because it has been extremely difficult to isolate and culture viable AEC I (Williams, 2003). Our lab and other labs have developed methods to isolate AEC I (Williams, 2003;Wang & Hubmayr, 2011;Chen *et al.*, 2005).

AEC I respond to the forces generated by mechanical ventilation *i.e.* conversion of physical forces on the cell membranes and/or receptors into activation of intracellular signaling pathway leading to Ca^{2+} wave generation. The intracellular Ca^{2+} contributes to integrate signaling in lung epithelium. The

mechanisms underlying the coordination of intracellular Ca^{2+} changes in AEC I to neighboring AEC II involve diffusion of ions/second messenger molecules through gap junctions and release of ATP or UTP in the extracellular spaces. This subsequently activates Ca^{2+} signaling pathways in AEC II through purinergic receptors and induces surfactant release. Recent studies using the *in situ* technique confirm that calcium waves passed from AEC I to AEC II result in the release of surfactant from AEC II (Ashino *et al.*, 2000). Mechanical stimulation of AEC I-like cells in heterocellular culture propagated calcium to neighboring AEC II-like cells mainly via an apyrase-sensitive mechanism, suggesting that ATP is an extracellular mediator of alveolar cell communications (Boitano *et al.*, 2004;Isakson *et al.*, 2003). ATP is produced by AEC I in response to mechanical stimulation and in turn triggers surfactant secretion from AEC II (Patel *et al.*, 2005). However, the mechanism of ATP release from AEC I has not been established.

3.4. Mechanism of surfactant secretion

The regulated surfactant secretion is a slow and multiphasic process. Surfactant secretion consists of two phases, a prefusion and a postfusion phase, and is clearly separated in time (Dietl & Haller, 2005). The prefusion steps include transport of lamellar body to the plasma membrane and docking followed by a postfusion phase of fusion pore formation in the plasma membrane (Lindau & Gomperts, 1991). Surfactant exocytosis involves interaction of proteins present on the lamellar bodies and plasma membrane. During membrane fusion, the proteins residing on vesicle or v-SNAREs (on lamellar bodies in AEC II) interact

with those on plasma or target membrane to form a highly stable coiled-coil ternary SNARE complex (Chander *et al.*, 2006). The coil is contributed by proteins including VAMP, syntaxin and SNAP proteins. Previously, from our lab we have reported the membrane fusion machinery of AEC II such as t-SNAREs syntaxin-2, SNAP-23, and annexin A2 (Abonyo *et al.*, 2004;Wang *et al.*, 2007). *In vitro* the formation of SNARE complex is sufficient for the close apposition and membrane fusion.

The vesicular contents of the lamellar body are released through fusion pore formation in the AEC II plasma membrane. The half time for the secretion of lung surfactant and its removal from the alveolar space in normal rat is approximately 4-10 hour (King & Martin, 1980;Young *et al.*, 1981). However, *in vivo* surfactant release through fusion pores, permeation and spreading are more rapid than *in vitro*. Albeit the fusion of lamellar body with the plasma membrane occurs rapidly, the delivery of lamellar body contents to air-liquid interface is considerably slower.

4. Acute Lung Injury

Acute Respiratory Disease Syndrome (ARDS) is acute lung injury (ALI) of the alveolar/capillary membrane. ARDS is characterized by permeability pulmonary edema (fluid in the alveolar space) and acute respiratory failure. It is defined as acute respiratory distress with diffuse alveolar infiltrates on chest X-ray, severe hypoxemia (PaO_2/F_IO_2 <200). The etiology of ARDS includes aspiration of gastric contents, pneumonia, smoke inhalation, sepsis, trauma, drug overdose, multiple transfusions, pancreatitis, and venous air embolism. Sepsis is

an important predisposing factor, present in 40% of ARDS patients. Multiple risk factors increase the chance of developing ARDS.

ALI is a common complication of mechanical ventilated patients and often synergized the upshots with sepsis background. Mechanical ventilation augments the acute lung injury caused by bacterial products. The molecular pathogenesis of this synergistic interaction *per se* remains incompletely understood *hitherto*. Mechanical stretch on alveolar walls produce several different consequences in injured lungs including the physical shear of alveolar epithelial and endothelial cells, disruption of the alveolar basement membrane, and activation of stretch-responsive receptors and signaling pathways. A range of bacterial products activates a series of Toll like receptors, which induces ROS generation through oxidized phospholipids (OxPAPC) and increase in microvascular permeability. Thus, innate immune mechanisms are likely activated in the lungs of most patients before and after the onset of ALI. Alveolar cells produce a range of proinflammatory cytokines when exposed to bacterial products. Importantly, ATP is a potent candidate to activate the innate immune response. There is a significant degree of purinergic interplay in the prognosis of the ALI pathogenecity.

The cardinal pathological findings in the lungs of patients with ALI were best described in a classic study in 1977 (Bachofen & Weibel, 1977). The pathogenesis of the disease can be inferred by concentering on the factors that are responsible for the accumulation of protein-rich and neutrophillic pulmonary edema in the lung and, the mechanisms that impair the removal of pulmonary edema fluid. Inflammatory cells from the lung are the inciting factors in the

pathogenesis of ALI. The protein –rich edema fluid in ALI is associated with large numbers of neutrophils, denuded alveolar epithelial cells and proinflammatory markers including cytokines, oxidants procoagulant factors and proteases.

The initial cause of ALI is the lung vascular injury. An increase in lung vascular permeability occurs primarily at the level of lung microcirculation, which in turn results in the accumulation of protein-rich pulmonary edema fluid, even in the presence of normal lung vascular pressure (Brigham & Staub, 1998). A sustained loss of normal endothelial barrier function is best described in neutrophil-dependent lung injury (Matthay & Zimmerman, 2005). Neutrophil sequestration and activation in the lung microvasculature leads to degranulation and release of several toxic mediators, including ROS, proinflammatory cytokines and procoagulant molecules, resulting in increase of vascular permeability.

Alveolar epithelial injury is another cardinal characteristic of ALI. Although the mechanisms responsible for epithelial injury in ALI are poorly understood, it appears that neutrophil and their products are primarily responsible for the increased paracellular alveolar permeability in ALI. However, neutrophil can cross the alveolar epithelium without affecting the lung epithelial permeability (Martin *et al.*, 1989;Wienerkronish *et al.*, 1991). In pathological states the migration of a large number of neutrophils results in increased epithelial injury (Downey *et al.*, 1993). Furthermore, the degree of neutrophil activation (priming) by exposure to chemokines and other proinflammatory cytokines seems to play a crucial role in the alveolar epithelial injury as neutrophils crawl into the

distal airspaces. Transepithelial migration of neutrophils into the distal airspaces involves three distinct and sequential steps of adhesion, migration and post-migration. Neutrophils adhere to the basolateral epithelial surface by β2-integrins (Folkesson & Matthay, 1997;Gao *et al.*, 2001). The initial adhesion of neutrophils to the basolateral surface is primarily mediated by CD11b/CD18 molecules (Parkos *et al.*, 1991). However, CD18-independent transmigration of neutrophils has also been documented. The paracellular route of neutrophil migration to the distal airspaces is also associated with CD47, a cell-surface molecule expressed on epithelial cells and neutrophils (Su *et al.*, 2008). Once they traverse the epithelium and enter the airspaces, neutrophils adhere to the apical surface, where they phagocytize and kill bacteria. The release of toxic intracellular molecules from activated neutrophils induces dissolution of tight junction and necrosis of AEC I. Finally, apoptosis and phagocytosis of inflammatory cells are critical for the resolution of inflammation and mitigation of lung tissue damage.

5. VCAM-1

5.1. Biology

Vascular cell adhesion molecule-1 (VCAM-1) is a type1 membrane glycoprotein belonging to the immunoglobulin (Ig) superfamily of cell adhesion molecules. The long isoform of VCAM-1 is a 110 kDa protein containing a 674-amino acid extracellular domain organized into seven C2-type Ig domains, a 22-amino acid transmembrane domain and a 19-amino acid cytoplasmic domain. The short isoform is a 45 kDa glycophosphatidylinositol (GPI)-linked protein containing the first three amino- terminal Ig domains of the transmembrane

isoform. Both the transmembrane and the GPI-anchored VCAM-1 isoforms can be released from cells to yield soluble VCAM-1 (sVCAM-1) that is detectable in serum and other body fluids. VCAM-1 expression has been reported on inflammed vascular endothelium by a number of stimuli (Carter & Wicks, 2001). VCAM-1 is also expressed on non-vascular cells, including dendritic cell in lymphoid tissues and skin, tissue macrophages, fibroblast (Meng *et al.*, 1995), smooth muscle cells (Ardehali *et al.*, 1995), bone marrow stromal cells (Feuerbach & Feyen, 1997), liver kupffer cells (van Oosten *et al.*, 1995), renal tubular epithelial cells (Oertli *et al.*, 1998) and lung epithelial cells (Popper *et al.*, 2002).

The counter-ligands for VCAM-1 are heterodimeric α4 or α9-integrins noncovalently linked to either β1 or β7 chain (Newham *et al.*, 1997;Feng *et al.*, 2000). Previous studies have shown the expression of functional α4-integrin in activated neutrophils which roll and adhere on VCAM-1 substrate, independent of selectins and β2-integrin (Ibbotson *et al.*, 2001). The essential interactions between circulating neutrophil and activated endothelium permit effective egress of the neutrophil to the site of infection. The binding of the VCAM-1 to integrins allows tight association and diapedesis preceding initial events of rolling and lose tethering. Nevertheless, neutrophils in the lungs adhere to capillaries where the shear forces are greatly reduced. α4β1-integrin mediated tethering and adhesion is likely to support the endothelial transmigration in inflammation.

5.2. Contribution of sVCAM-1 in inflammation

sVCAM-1 has been shown to mediate angiogenesis and is chemotactic to T-lymphocytes and monocytes (Tokuhira *et al.*, 2000). sVCAM-1 levels are correlated with various diseases. Elevated sVCAM-1 levels have been documented in synovial fluids (SF) from patients with rheumatoid arthritis (RA) (Navarro-Hernandez *et al.*, 2009), cerebrospinal fluid of patients with active multiple sclerosis (Rieckmann *et al.*, 2005), serum from patients with advanced cancers (Okugawa *et al.*, 2009), and inflammatory bowel disease and type II diabetes (Magro *et al.*, 2004;Nakamura *et al.*, 2008), alveolar lining fluid from pneumonia and asthma patients(Janson *et al.*, 2005;Matsuno *et al.*, 2007).

VCAM-1 shedding from transmembrane has been studied extensively in different cell systems. Regulated ectodomain shedding of VCAM-1 is cell specific (Rose *et al.*, 2000) and involves mainly proteases from activated endothelium, epithelium, macrophages and/or neutrophils (Garton *et al.*, 2003;Redondo-Munoz *et al.*, 2008). The proteolytic release of sVCAM-1 is mediated by the zinc metalloproteases of the type I transmembrane protein ADAM17 (TNFα-conveting enzyme; TACE) from stimulated endothelial cells, and elastase and cathepsin G released from activated neutrophils (Scheller *et al.*, 2011). The proteolytic cleavage by ADAM17 can be regulated by transactivation of the G-protein coupled receptors (GPCR). Phosphorylation of the cytoplasmic domain of ADAM17, stimulation-dependent internalization, partitioning of the ADAM17 and its substrates within lipid raft microdomains and regulated intramembrane proteolysis contributes to ectodomain shedding of VCAM-1

(Levine, 2008). Thus, sVCAM-1 resembles an important regulatory component of the inflammatory response.

6. Objectives

The present study was designed to elucidate the role of P2X7 receptor in AEC I and AEC II communications to surfactant exocytosis. The role of P2X7 receptor in AEC I was studied for the regulation of surfactant secretion. The signaling pathway coupling AEC I and AEC II in surfactant release was further studied using different selective inhibitors. Next, series of conditioned-media experiments using stably and endogenously expressing P2X7 receptor, respectively were performed for the surfactant secretion from AEC II. Selective knock-down experiment for P2X7 receptor was also performed. Physiological stimulus like hyperventilation was employed and compared between wild-type and P2X7 receptor knock-out mice to evaluate the function of P2X7 receptor in hyperventilation-induced surfactant increase. Additionally, the involvement of P2X7 receptor in the pathogenesis of ALI has also been studied. Employing an experimental strategy of clinically relevant two-hit model of LPS and mechanical ventilation, we tested this idea using P2X7 receptor knock-out mice and selective P2X7 receptor inhibitor. Finally, attempts were made to study the mechanism of P2X7 receptor-mediated signaling events in ALI. One of the identified proteins, the soluble form of VCAM-1 (sVCAM-1), was further studied for their role in neutrophil chemotaxis in ALI. The study hence would be the first of its kind to implicate the pathophysiological role of P2X7 receptor in alveolar functions (Figure 1).

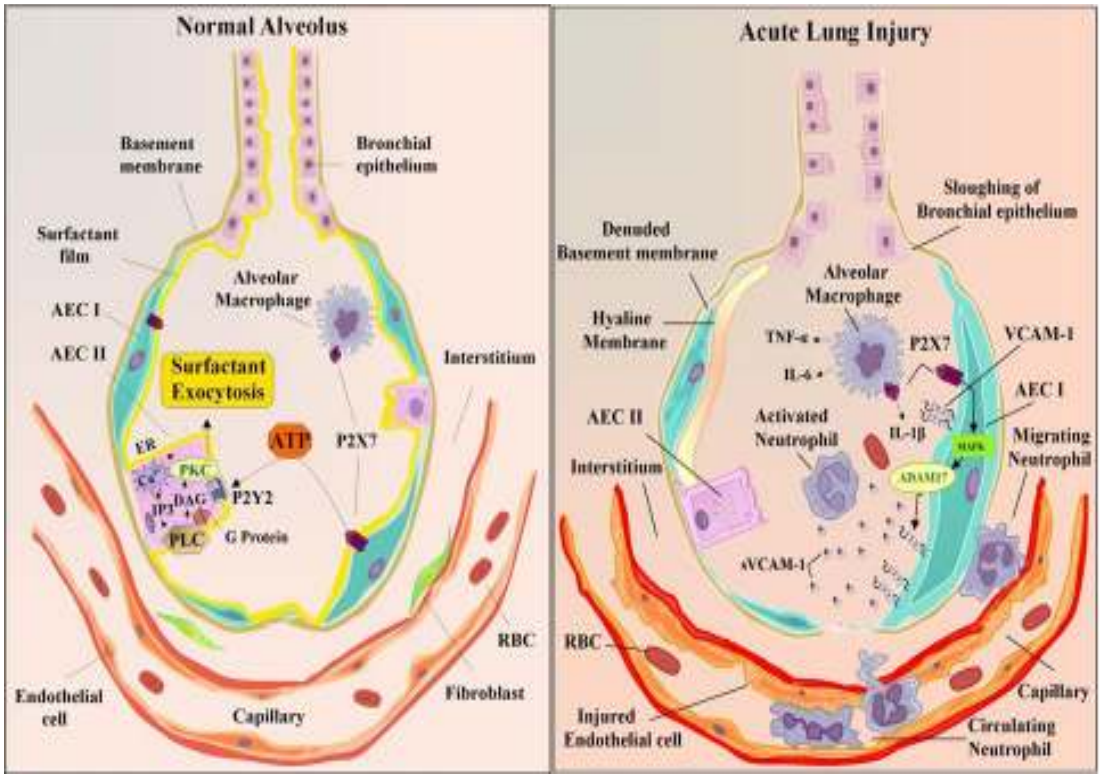

Figure 1.1. Proposed pathophysiological role of P2X7 receptor in the normal and injured alveolus.

In the normal alveolus, activation of P2X7 receptor in AEC I cell surface leads to ATP release. ATP in the extracellular space activates neighboring AEC II and stimulates surfactant secretion through P2Y2 receptor signaling pathway. In the ALI, there is sloughing of both bronchial and alveolar epithelial cells, denuded alveolar basement membrane. Alveolar macrophages secrete cytokines; IL-1β, IL-6, and TNF-α, that act locally on AEC I. This increases the VCAM-1 expression in AEC I membrane. P2X7 receptor stimulation on AEC I modulate ADAM17 activity

through MAPK activation. ADAM17 shed VCAM-1 from the AEC I surface. sVCAM-1 in the alveolar space stimulate neutrophil chemotaxis and sequestrations.

7. References

1. Abbracchio MP, Burnstock G, Verkhratsky A, & Zimmermann H (2009). Purinergic signalling in the nervous system: an overview. *Trends in Neurosciences* **32**, 19-29.

2. Abonyo BO, Gou DM, Wang PC, Narasaraju T, Wang ZX, & Liu L (2004). Syntaxin 2 and SNAP-23 are required for regulated surfactant seeretion. *Biochemistry* **43**, 3499-3506.

3. Alawqati Q (1995). Regulation of Ion Channels by Abc Transporters That Secrete Atp. *Science* **269**, 805-806.

4. Andreeva AV, Kutuzov MA, & Voyno-Yasenetskaya TA (2007). Regulation of surfactant secretion in alveolar type II cells. *American Journal of Physiology-Lung Cellular and Molecular Physiology* **293**, L259-L271.

5. Ardehali A, Laks H, Drinkwater DC, Ziv E, & Drake TA (1995). Vascular Cell-Adhesion Molecule-1 Induced on Vascular Endothelia and Medial Smooth-Muscle Cells in Experimental Cardiac Allograft Vasculopathy. *Circulation* **92**, 450-456.

6. Ashino Y, Ying XY, Dobbs LG, & Bhattacharya J (2000). [Ca2+](i) oscillations regulate type II cell exocytosis in the pulmonary alveolus. *American Journal of Physiology-Lung Cellular and Molecular Physiology* **279**, L5-L13.

7. Bachofen M & Weibel ER (1977). Alterations of Gas-Exchange Apparatus in Adult Respiratory Insufficiency Associated with Septicemia. *American Review of Respiratory Disease* **116**, 589-615.

8. Baricordi OR, Ferrari D, Melchiorri L, Chiozzi P, Hanau S, Chiari E, Rubini M, & DiVirgilio F (1996). An ATP-activated channel is involved in mitogenic stimulation of human T lymphocytes. *Blood* **87**, 682-690.

9. Beigi RD, Kertesy SB, Aquilina G, & Dubyak GR (2003). Oxidized ATP (oATP) attenuates proinflammatory signaling via P-2 receptor-independent mechanisms. *British Journal of Pharmacology* **140**, 507-519.

10. Blanchard DK, Mcmillen S, & Djeu JY (1991). IFN-Gamma Enhances Sensitivity of Human Macrophages to Extracellular Atp-Mediated Lysis. *Journal of Immunology* **147**, 2579-2585.

11. Boitano S, Isakson BE, Seedorf GJ, & Lubman RL (2004). Functional coupling and cell signaling between alveolar type I and type II epithelial cells. *Faseb Journal* **18**, A1051.

12. Bortner CD, Hughes FM, & Cidlowski JA (1997). A primary role for K+ and Na+ efflux in the activation of apoptosis. *Journal of Biological Chemistry* **272**, 32436-32442.

13. Bours M, Swennen E, Di Virgilio F, Cronstein B, & Dagnelie P (2006). Adenosine 5 '-triphosphate and adenosine as endogenous signaling molecules in immunity and inflammation. *Pharmacology & Therapeutics* **112**, 358-404.

14. Braunstein GM, Roman RM, Clancy JP, Kudlow BA, Taylor AL, Shylonsky VG, Jovov B, Peter K, Jilling T, Ismailov II, Benos DJ, Schwiebert LM, Fitz JG, & Schwiebert EM (2001). Cystic fibrosis transmembrane conductance regulator facilitates ATP release by stimulating a separate ATP release channel for autocrine control of cell volume regulation. *Journal of Biological Chemistry* **276**, 6621-6630.

15. Brigham KL & Staub NC (1998). Pulmonary edema and acute lung injury research. *American Journal of Respiratory and Critical Care Medicine* **157**, S109-S113.

16. Buell GN, Talabot F, Gos A, Lorenz J, Lai E, Morris MA, & Antonarakis SE (1998). Gene structure and chromosomal localization of the human P2X(7) receptor. *Receptors & Channels* **5**, 347-+.

17. Burnstock G, Cocks T, & Crowe R (1978a). Evidence for Purinergic Innervation of Anococcygeus Muscle. *British Journal of Pharmacology* **64**, 13-20.

18. Burnstock G, Cocks T, Kasakov L, & Wong HK (1978b). Direct Evidence for Atp Release from Non-Adrenergic, Non-Cholinergic (Purinergic) Nerves in Guinea-Pig Taenia-Coli and Bladder. *European Journal of Pharmacology* **49**, 145-149.

19. Burnstock G & Kennedy C (1985). Is There A Basis for Distinguishing 2 Types of P2-Purinoceptor. *General Pharmacology* **16**, 433-440.

20. Burnstock G (2008). Unresolved issues and controversies in purinergic signalling. *Journal of Physiology-London* **586**, 3307-3312.

21. Carter RA & Wicks IP (2001). Vascular cell adhesion molecule 1 (CD106) - A multifaceted regulator of joint inflammation. *Arthritis and Rheumatism* **44**, 985-994.

22. Chakfe Y, Seguin R, Antel JP, Morissette C, Malo D, Henderson D, & Seguela P (2002). ADP and AMP induce interleukin-1 beta release from microglial cells through activation of ATP-primed P2X(7) receptor channels. *Journal of Neuroscience* **22**, 3061-3069.

23. Chander A, Naidu DG, & Chen XL (2006). Lamellar body fusion for surfactant secretion: Deletion of the 10-20 domain in the N-terminus decreases fusion activity of annexin A7. *Faseb Journal* **20**, A1439.

24. Chen JW, Chen ZM, Narasaraju T, Jin N, & Liu L (2005). Isolation of highly pure alveolar epithelial type I and type II cells from rat lungs (vol 84, pg 727, 2004). *Laboratory Investigation* **85**, 1181.

25. Chen Y, Corriden R, Inoue Y, Yip L, Hashiguchi N, Zinkernagel A, Nizet V, Insel PA, & Junger WG (2006). ATP release guides neutrophil chemotaxis via P2Y2 and A3 receptors. *Science* **314**, 1792-1795.

26. Chen ZM, Jin NL, Narasaraju T, Chen JW, McFarland LR, Scott M, & Liu L (2004). Identification of two novel markers for alveolar epithelial type I and II cells. *Biochemical and Biophysical Research Communications* **319**, 774-780.

27. Chused TM, Apasov S, & Sitkovsky M (1996). Murine T lymphocytes modulate activity of an ATP-activated P-2z-type purinoceptor during differentiation. *Journal of Immunology* **157**, 1371-1380.

28. Cicko S, Lucattelli M, Muller T, Lommatzsch M, De Cunto G, Cardini S, Sundas W, Grimm M, Zeiser R, Durk T, Zissel G, Boeynaems JM, Sorichter S, Ferrari D, Di Virgilio F, Virchow JC, Lungarella G, & Idzko M (2010). Purinergic Receptor Inhibition Prevents the Development of Smoke-Induced Lung Injury and Emphysema. *Journal of Immunology* **185**, 688-697.

29. Clark JC, Wert SE, Bachurski CJ, Stahlman MT, Stripp BR, Weaver TE, & Whitsett JA (1995). Targeted Disruption of the Surfactant Protein-B Gene Disrupts Surfactant Homeostasis, Causing Respiratory-Failure in Newborn Mice. *Proceedings of the National Academy of Sciences of the United States of America* **92**, 7794-7798.

30. Collo G, Neidhart S, Kawashima E, KoscoVilbois M, North RA, & Buell G (1997). Tissue distribution of the P2X(7) receptor. *Neuropharmacology* **36**, 1277-1283.

31. Corriden R & Insel PA (2010). Basal Release of ATP: An Autocrine-Paracrine Mechanism for Cell Regulation. *Science Signaling* **3**.

32. Coutinho-Silva R, Persechini PM, Bisaggio RD, Perfettini JL, Neto ACTD, Kanellopoulos JM, Motta-Ly I, Dautry-Varsat A, & Ojcius DM (1999). P-2Z/P2X(7) receptor-dependent apoptosis of dendritic cells. *American Journal of Physiology-Cell Physiology* **276**, C1139-C1147.

33. CoutinhoSilva R, Alves LA, deCarvalho ACC, Savino W, & Persechini PM (1996). Characterization of P-2Z purinergic receptors on phagocytic cells of the thymic reticulum in culture. *Biochimica et Biophysica Acta-Biomembranes* **1280**, 217-222.

34. Cusack NJ (1993a). P-2 Receptor - Subclassification and Structure-Activity-Relationships. *Drug Development Research* **28**, 244-252.

35. Cusack NJ (1993b). P-2 Receptor - Subclassification and Structure-Activity-Relationships. *Drug Development Research* **28**, 244-252.

36. Denlinger LC, Fisette PL, Sommer JA, Watters JJ, Prabhu U, Dubyak GR, Proctor RA, & Bertics PJ (2001). Cutting edge: The nucleotide receptor P2X(7) contains multiple protein- and lipid-interaction motifs including a potential binding site for bacterial lipopolysaccharide. *Journal of Immunology* **167**, 1871-1876.

37. Di Virgilio F, Chiozzi P, Ferrari D, Falzoni S, Sanz JM, Morelli A, Torboli M, Bolognesi G, & Baricordi OR (2001). Nucleotide receptors: an emerging family of regulatory molecules in blood cells. *Blood* **97**, 587-600.

38. Di Virgilio F, Falzoni S, Mutini C, Sanz JM, & Chiozzi P (1998). Purinergic P2X(7) receptor: A pivotal role in inflammation and immunomodulation. *Drug Development Research* **45**, 207-213.

39. Dietl P & Haller T (2005). *Exocytosis of lung surfactant: From the secretory vesicle to the air-liquid interface*, pp. 595-621.

40. Downey GP, Worthen GS, Henson PM, & Hyde DM (1993). Neutrophil Sequestration and Migration in Localized Pulmonary Inflammation - Capillary Localization and Migration Across the Interalveolar Septum. *American Review of Respiratory Disease* **147**, 168-176.

41. Dubyak GR (1991). Signal Transduction by P2-Purinergic Receptors for Extracellular Atp. *American Journal of Respiratory Cell and Molecular Biology* **4**, 295-300.

42. Dubyak GR (2002). Focus on "Extracellular ATP signaling and P2X nucleotide receptors in monolayers of primary human vascular endothelial cells". *American Journal of Physiology-Cell Physiology* **282**, C242-C244.

43. Dubyak GR & Elmoatassim C (1993). Signal-Transduction Via P2-Purinergic Receptors for Extracellular Atp and Other Nucleotides. *American Journal of Physiology* **265**, C577-C606.

44. Elliott MR, Chekeni FB, Trampont PC, Lazarowski ER, Kadl A, Walk SF, Park D, Woodson RI, Ostankovich M, Sharma P, Lysiak JJ, Harden T, Leitinger N, & Ravichandran KS (2009). Nucleotides released by apoptotic cells act as a find-me signal to promote phagocytic clearance. *Nature* **461**, 282-U165.

45. Elmoatassim C & Dubyak GR (1993). Dissociation of the Pore-Forming and Phospholipase-D Activities Stimulated Via P(2Z) Purinergic Receptors in Bac1.2F5 Macrophages - Product Inhibition of Phospholipase-D Enzyme-Activity. *Journal of Biological Chemistry* **268**, 15571-15578.

46. Eltom S, Stevenson CS, Rastrick J, Dale N, Raemdonck K, Wong S, Catley MC, Belvisi MG, & Birrell MA (2011). P2X7 Receptor and Caspase 1 Activation Are Central to Airway Inflammation Observed after Exposure to Tobacco Smoke. *Plos One* **6**.

47. Eltzschig HK, Eckle T, Mager A, Kueper N, Karcher C, Weissmueller T, Boengler K, Schulz R, Robson SC, & Colgan SP (2006). ATP release from activated neutrophils occurs via connexin 43 and modulates adenosine-dependent endothelial cell function. *Circulation Research* **99**, 1100-1108.

48. Evans RJ, Lewis C, Buell G, Valera S, North RA, & Surprenant A (1995). Pharmacological Characterization of Heterologously Expressed Atp-Gated Cation Channels (P-2X Purinoceptors). *Molecular Pharmacology* **48**, 178-183.

49. Feng CG, Britton WJ, Palendira U, Groat NL, Briscoe H, & Bean AGD (2000). Up-regulation of VCAM-1 and differential expansion of beta integrin-expressing T lymphocytes are associated with immunity to pulmonary Mycobacterium tuberculosis infection. *Journal of Immunology* **164**, 4853-4860.

50. Fernando KC, Gargett CE, & Wiley JS (1999). Activation of the P2Z/P2X(7), receptor in human lymphocytes produces a delayed permeability lesion: Involvement of phospholipase D-1. *Archives of Biochemistry and Biophysics* **362**, 197-202.

51. Ferrari D, Chiozzi P, Falzoni S, DalSusino M, Melchiorri L, Baricordi OR, & DiVirgilio F (1997a). Extracellular ATP triggers IL-1 beta release by activating the purinergic P2Z receptor of human macrophages. *Journal of Immunology* **159**, 1451-1458.

52. Ferrari D, Idzko M, Dichmann S, Purlis D, Virchow C, Norgauer J, Chiozzi P, Di Virgilio F, & Luttmann W (2000). P2 purinergic receptors of human eosinophils: characterization and coupling to oxygen radical production. *Febs Letters* **486**, 217-224.

53. Ferrari D, Villalba M, Chiozzi P, Falzoni S, RicciardiCastagnoli P, & DiVirgilio F (1996). Mouse microglial cells express a plasma membrane pore gated by extracellular ATP. *Journal of Immunology* **156**, 1531-1539.

54. Ferrari D, Wesselborg S, Bauer MKA, & Schulze-Osthoff K (1997b). Extracellular ATP activates transcription factor NF-kappa B through the P2Z purinoreceptor by selectively targeting NF-kappa B p65 (RelA). *Journal of Cell Biology* **139**, 1635-1643.

55. Feuerbach D & Feyen JHM (1997). Expression of the cell-adhesion molecule VCAM-1 by stromal cells is necessary for osteoclastogenesis. *Febs Letters* **402**, 21-24.

56. Folkesson HG & Matthay MA (1997). Inhibition of CD18 or CD11b attenuates acute lung injury after acid instillation in rabbits. *Journal of Applied Physiology* **82**, 1743-1750.

57. Furlan-Freguia C, Marchese P, Gruber A, Ruggeri ZM, & Ruf W (2011). P2X7 receptor signaling contributes to tissue factor-dependent thrombosis in mice. *Journal of Clinical Investigation* **121**, 2932-2944.

58. Gao XP, Xu N, Sekosan M, Mehta D, Ma SY, Rahman A, & Malik AB (2001). Differential role of CD18 integrins in mediating lung neutrophil sequestration and increased microvascular permeability induced by Escherichia coli in mice. *Journal of Immunology* **167**, 2895-2901.

59. Gargett CE, Cornish JE, & Wiley JS (1997). ATP, a partial agonist for the P2Z receptor of human lymphocytes. *British Journal of Pharmacology* **122**, 911-917.

60. Gargett CE & Wiley JS (1997). The isoquinoline derivative KN-62 a potent antagonist of the P2Z-receptor of human lymphocytes. *British Journal of Pharmacology* **120**, 1483-1490.

61. Garrand R, Erb L, Weisman GA, & Turner JT (1995). Investigation of the Ligand-Binding Site of the P2y Purinoceptors. *Faseb Journal* **9**, A117.

62. Garton KJ, Gough PJ, Philalay J, Wille PT, Blobel CP, Whitehead RH, Dempsey PJ, & Raines EW (2003). Stimulated shedding of vascular cell adhesion molecule 1 (VCAM-1) is mediated by tumor necrosis factor-alpha-converting enzyme (ADAM 17). *Journal of Biological Chemistry* **278**, 37459-37464.

63. Grahames CBA, Michel AD, Chessell IP, & Humphrey PPA (1999). Pharmacological characterization of ATP- and LPS-induced IL-1 beta release in human monocytes. *British Journal of Pharmacology* **127**, 1915-1921.

64. Gu B, Bendall LJ, & Wiley JS (1998). Adenosine triphosphate-induced shedding of CD23 and L-selectin (CD62L) from lymphocytes is mediated by the same receptor but different metalloproteases. *Blood* **92**, 946-951.

65. Harden TK, Boyer JL, & Nicholas RA (1995). P-2-Purinergic Receptors - Subtype-Associated Signaling Responses and Structure. *Annual Review of Pharmacology and Toxicology* **35**, 541-579.

66. Hickman SE, Elkhoury J, Greenberg S, Schieren I, & Silverstein SC (1994). P2Z Adenosine-Triphosphate Receptor Activity in Cultured Human Monocyte-Derived Macrophages. *Blood* **84**, 2452-2456.

67. Hughes JP, Hatcher JP, & Chessell IP (2007). The role of P2X(7) in pain and inflammation. *Purinergic Signalling* **3**, 163-169.

68. Ibbotson GC, Doig C, Kaur J, Gill V, Ostrovsky L, Fairhead T, & Kubes P (2001). Functional alpha(4)-integrin: A newly identified pathway of neutrophil recruitment in critically ill septic patients. *Nature Medicine* **7**, 465-470.

69. Isakson BE, Seedorf GJ, Lubman RL, Evans WH, & Boitano S (2003). Cell-cell communication in heterocellular cultures of alveolar epithelial cells. *American Journal of Respiratory Cell and Molecular Biology* **29**, 552-561.

70. Jamieson GP, Snook MB, Thurlow PJ, & Wiley JS (1996). Extracellular ATP causes loss of L-selectin from human lymphocytes via occupancy of P(2)Z purinoceptors. *Journal of Cellular Physiology* **166**, 637-642.

71. Janson C, Ludviksdottir D, Gunnbjornsdottir M, Bjornsson EH, Hakansson L, & Venge P (2005). Circulating adhesion molecules in allergic and non-allergic asthma. *Respiratory Medicine* **99**, 45-51.

72. Jiang LH, Mackenzie AB, North RA, & Surprenant A (2000). Brilliant Blue G selectively blocks ATP-gated rat P2X(7) receptors. *Molecular Pharmacology* **58**, 82-88.

73. Khakh BS, Burnstock G, Kennedy C, King BF, North RA, Seguela P, Voigt M, & Humphrey PPA (2001). International union of pharmacology. XXIV. Current status of the nomenclature and properties of P2X receptors and their subunits. *Pharmacological Reviews* **53**, 107-118.

74. Kim M, Jiang LH, Wilson HL, North RA, & Surprenant A (2001). Proteomic and functional evidence for a P2X(7) receptor signalling complex. *Embo Journal* **20**, 6347-6358.

75. King RJ & Martin H (1980). Intracellular Metabolism of the Apoproteins of Pulmonary Surfactant in Rat Lung. *Journal of Applied Physiology* **48**, 812-820.

76. Labasi JM, Donovan CB, Wicks JR, Audoly L, & Gabel CA (2001). Absence of the P2X(7) receptor alters leukocyte function and attenuates an inflammatory response. *Molecular Biology of the Cell* **12**, 202A.

77. Levine SJ (2008). Molecular mechanisms of soluble cytokine receptor generation. *Journal of Biological Chemistry* **283**, 14177-14181.

78. Li X, Qi XP, Zhou LY, Fu W, Abdul-Karim FW, MacLennan G, & Gorodeski GI (2009). P2X(7) receptor expression is decreased in epithelial cancer cells of ectodermal, uro-genital sinus, and distal paramesonephric duct origin. *Purinergic Signalling* **5**, 351-368.

79. Lindau M & Gomperts BD (1991). Techniques and Concepts in Exocytosis - Focus on Mast-Cells. *Biochimica et Biophysica Acta* **1071**, 429-471.

80. Londos C, Cooper DMF, & Wolff J (1980). Subclasses of External Adenosine Receptors. *Proceedings of the National Academy of Sciences* **77**, 2551-2554.

81. Lucattelli M, Cicko S, Muller T, Lommatzsch M, De Cunto G, Cardini S, Sundas W, Grimm M, Zeiser R, Durk T, Zissel G, Sorichter S, Ferrari D, Di Virgilio F, Virchow JC, Lungarella G, & Idzko M (2011). P2X(7) Receptor Signaling in the Pathogenesis of Smoke-Induced Lung Inflammation and Emphysema. *American Journal of Respiratory Cell and Molecular Biology* **44**, 423-429.

82. MacKenzie A, Wilson HL, Kiss-Toth E, Dower SK, North RA, & Surprenant A (2001). Rapid secretion of interleukin-1 beta by microvesicle shedding. *Immunity* **15**, 825-835.

83. Magro F, Araujo F, Pereira P, Meireles E, Diniz-Ribeiro M, & Velosom FT (2004). Soluble selectins, sICAM, sVCAM, and angiogenic proteins in different activity groups of patients with inflammatory bowel disease. *Digestive Diseases and Sciences* **49**, 1265-1274.

84. Maianski Z, Pedersen J, Chabert C, Barden J, & Stricker PD (2007). Evaluation of a new monoclonal antibody targeting the apoptotic purinergic receptor P2X7, as a diagnostic tool for prostate cancer. *Journal of Urology* **177**, 474.

85. Martin TR, Pistorese BP, Chi EY, Goodman RB, & Matthay MA (1989). Effects of Leukotriene-B4 in the Human-Lung - Recruitment of Neutrophils Into the

Alveolar Spaces Without A Change in Protein Permeability. *Journal of Clinical Investigation* **84**, 1609-1619.

86. Matsuno O, Miyazaki E, Nureki S, Ueno T, Ando M, Ito K, Kumamoto T, & Higuchi Y (2007). Elevated soluble ADAM8 in bronchoalveolar lavage fluid in patients with eosinophilic pneumonia. *International Archives of Allergy and Immunology* **142**, 285-290.

87. Matthay MA & Zimmerman GA (2005). Acute lung injury and the acute respiratory distress syndrome - Four decades of inquiry into pathogenesis and rational management. *American Journal of Respiratory Cell and Molecular Biology* **33**, 319-327.

88. McLarnon J & Ryu J (2009). A P2X7 Receptor Antagonist Inhibits Inflammation and Is Neuroprotective in An Animal Model of Alzheimer's. *Journal of Neurochemistry* **108**, 7.

89. Mehta VB, Hart J, & Wewers MD (2001). ATP-stimulated release of interleukin (IL)-1 beta and IL-18 requires priming by lipopolysaccharide and is independent of caspase-1 cleavage. *Journal of Biological Chemistry* **276**, 3820-3826.

90. Meng H, Marchese MJ, Garlick JA, Jelaska A, Korn JH, Gailit J, Clark RAF, & Gruber BL (1995). Mast-Cells Induce T-Cell Adhesion to Human Fibroblasts by Regulating Intercellular-Adhesion Molecule-1 and Vascular Cell-Adhesion Molecule-1 Expression. *Journal of Investigative Dermatology* **105**, 789-796.

91. Murgia M, Hanau S, Pizzo P, Rippa M, & DiVirgilio F (1993). Oxidized Atp - An Irreversible Inhibitor of the Macrophage Purinergic-P2Z Receptor. *Journal of Biological Chemistry* **268**, 8199-8203.

92. Nakamura K, Yamagishi SI, Adachi H, Matsui T, Kurita-Nakamura Y, Takeuchi M, Inoue H, & Imaizumi T (2008). Serum levels of soluble form of receptor for advanced glycation end products (sRAGE) are positively associated with circulating AGEs and soluble form of VCAM-1 in patients with type 2 diabetes. *Microvascular Research* **76**, 52-56.

93. Navarro-Hernandez RE, Oregon-Romero E, Vazquez-Del Mercado M, Rangel-Villalobos H, Palafox-Sanchez CA, & Munoz-Valle JF (2009). Expression of ICAM1 and VCAM1 serum levels in rheumatoid arthritis clinical activity. Association with genetic polymorphisms. *Disease Markers* **26**, 119-126.

94. Newham P, Craig SE, Seddon GN, Schofield NR, Rees A, Edwards RM, Jones EY, & Humphries MJ (1997). alpha 4 integrin binding interfaces on VCAM-1 and MAdCAM-1 - Integrin binding footprints identify accessory binding sites that play a role in integrin specificity. *Journal of Biological Chemistry* **272**, 19429-19440.

95. Nicke A, Baumert HG, Rettinger J, Eichele A, Lambrecht G, Mutschler E, & Schmalzing G (1998). P2X(1) and P2X(3) receptors form stable trimers: a novel structural motif of ligand-gated ion channels. *Embo Journal* **17**, 3016-3028.

96. North RA (2002). Molecular physiology of P2X receptors. *Physiological Reviews* **82**, 1013-1067.

97. Nuttle LC, Elmoatassim C, & Dubyak GR (1993). Expression of the Pore-Forming P(2Z)-Purinoreceptor in Xenopus-Oocytes Injected with Poly(A)+ Rna from Murine Macrophages. *Molecular Pharmacology* **44**, 93-101.

98. Oertli B, Beck-Schimmer B, Fan XH, & Wuthrich RP (1998). Mechanisms of hyaluronan-induced up-regulation of ICAM-1 and VCAM-1 expression by murine kidney tubular epithelial cells: Hyaluronan triggers cell adhesion molecule expression through a mechanism involving activation of nuclear factor-kappa B and activating protein-1. *Journal of Immunology* **161**, 3431-3437.

99. Ohta A & Sitkovsky M (2001). Role of G-protein-coupled adenosine receptors in downregulation of inflammation and protection from tissue damage. *Nature* **414**, 916-920.

100. Okugawa Y, Miki C, Toiyama Y, Koike Y, Inoue Y, & Kusunoki M (2009). Serum Level of Soluble Vascular Cell Adhesion Molecule 1 Is a Valuable Prognostic Marker in Colorectal Carcinoma. *Diseases of the Colon & Rectum* **52**, 1330-1336.

101. Panenka W, Jijon H, Herx LM, Armstrong JN, Feighan D, Wei T, Yong VW, Ransohoff RM, & MacVicar BA (2001). P2X7-like receptor activation in astrocytes increases chemokine monocyte chemoattractant protein-1 expression via mitogen-activated protein kinase. *Journal of Neuroscience* **21**, 7135-7142.

102. Parkos CA, Delp C, Arnaout MA, & Madara JL (1991). Neutrophil Migration Across A Cultured Intestinal Epithelium - Dependence on A Cd11B Cd18-Mediated Event and Enhanced Efficiency in Physiological Direction. *Journal of Clinical Investigation* **88**, 1605-1612.

103. Patel AS, Reigada D, Mitchell CH, Bates SR, Margulies SS, & Koval M (2005). Paracrine stimulation of surfactant secretion by extracellular ATP in response to mechanical deformation. *American Journal of Physiology-Lung Cellular and Molecular Physiology* **289**, L489-L496.

104. Perregaux DG & Gabel CA (1998). Human monocyte stimulus-coupled IL-1 beta posttranslational processing: modulation via monovalent cations. *American Journal of Physiology-Cell Physiology* **275**, C1538-C1547.

105. Perregaux DG, McNiff P, Laliberte R, Conklyn M, & Gabel CA (2000). ATP acts as an agonist to promote stimulus-induced secretion of IL-1 beta and IL-18 in human blood. *Journal of Immunology* **165**, 4615-4623.

106. Pirotton S, Verjans B, Boeynaems JM, & Erneux C (1991). Metabolism of Inositol Phosphates in Atp-Stimulated Vascular Endothelial-Cells. *Biochemical Journal* **277**, 103-110.

107. Pizzo P, Murgia M, Zambon A, Zanovello P, Bronte V, Pietrobon D, & DiVirgilio F (1992). Role of P(2Z) Purinergic Receptors in Atp-Mediated Killing of Tumor-Necrosis-Factor (Tnf)-Sensitive and Tnf-Resistant L929 Fibroblasts. *Journal of Immunology* **149**, 3372-3378.

108. Popper HH, Pailer S, Wurzinger G, Feldner H, Hesse C, & Eber E (2002). Expression of adhesion molecules in allergic lung diseases. *Virchows Archiv* **440**, 172-180.

109. Praetorius HA & Leipziger J (2009). ATP release from non-excitable cells. *Purinergic Signalling* **5**, 433-446.

110. Ralevic V & Burnstock G (1998). Receptors for purines and pyrimidines. *Pharmacological Reviews* **50**, 413-492.

111. Rassendren F, Buell GN, Virginio C, Collo G, North RA, & Surprenant A (1997). The permeabilizing ATP receptor, P2X(7) - Cloning and expression of a human cDNA. *Journal of Biological Chemistry* **272**, 5482-5486.

112. Ray FR, Huang W, Slater M, & Barden JA (2002). Purinergic receptor distribution in endothelial cells in blood vessels: a basis for selection of coronary artery grafts. *Atherosclerosis* **162**, 55-61.

113. Redondo-Munoz J, Terol MJ, Garcia-Marco JA, & Garcia-Pardo A (2008). Matrix metafloproteinase-9 is up-regulated by CCL21/CCR7 interaction via extracellular signal-regulated kinase-1/2 signaling and is involved in CCL21-driven B-cell chronic lymphocytic leukemia cell invasion and migration. *Blood* **111**, 383-386.

114. Rieckmann P, Kruse N, Nagelkerken L, Beckmann K, Miller D, Polman C, Dahlke F, Toyka KV, Hartung HP, & Sturzebecher S (2005). Soluble vascular cell adhesion molecule (VCAM) is associated with treatment effects of Interferon beta-1b in patients with Secondary Progressive Multiple Sclerosis. *Journal of Neurology* **252**, 526-533.

115. Riedel T, Schmalzing G, & Markwardt F (2007). Influence of extracellular monovalent cations on pore and gating properties of P2X(7) receptor-operated single-channel currents. *Biophysical Journal* **93**, 846-858.

116. Riteau N, Gasse P, Fauconnier L, Gombault A, Couegnat M, Fick L, Kanellopoulos J, Quesniaux VFJ, Marchand-Adam S, Crestani B, Ryffel B, & Couillin I (2010). Extracellular ATP Is a Danger Signal Activating P2X(7) Receptor in Lung Inflammation and Fibrosis. *American Journal of Respiratory and Critical Care Medicine* **182**, 774-783.

117. Rooney SA (2001). Regulation of surfactant secretion. *Comparative Biochemistry and Physiology A-Molecular and Integrative Physiology* **129**, 233-243.

118. Rooney SA, Gobran LI, & Griese M (1992). Signal-Transduction Mechanisms of Atp Stimulated Surfactant Phosphatidylcholine (Pc) Secretion in Rat Type-Ii Pneumocytes. *Faseb Journal* **6**, A365.

119. Rose DM, Cardarelli PM, Cobb RR, & Ginsberg MH (2000). Soluble VCAM-1 binding to alpha 4 integrins is cell-type specific and activation dependent and is disrupted during apoptosis in T cells. *Blood* **95**, 602-609.

120. Scheller J, Chalaris A, Garbers C, & Rose-John S (2011). ADAM17: a molecular switch to control inflammation and tissue regeneration. *Trends in Immunology* **32**, 380-387.

121. Schenk U, Westendorf AM, Radaelli E, Casati A, Ferro M, Fumagalli M, Verderio C, Buer J, Scanziani E, & Grassi F (2008). Purinergic Control of T Cell Activation by ATP Released Through Pannexin-1 Hemichannels. *Science Signaling* **1**.

122. Slater M, Barden JA, & Murphy CR (2000). Distributional changes of purinergic receptor subtypes (P2X(1-7)) in uterine epithelial cells during early pregnancy. *Histochemical Journal* **32**, 365-372.

123. Solini A, Chiozzi P, Falzoni S, Morelli A, Fellin R, & Di Virgilio F (2000). High glucose modulates P2X(7) receptor-mediated function in human primary fibroblasts. *Diabetologia* **43**, 1248-1256.

124. Solle M, Labasi J, Perregaux DG, Stam E, Petrushova N, Koller BH, Griffiths RJ, & Gabel CA (2001). Altered cytokine production in mice lacking P2X(7) receptors. *Journal of Biological Chemistry* **276**, 125-132.

125. Sperlagh B, Hasko G, Nemeth Z, & Vizi ES (1998). ATP released by LPS increases nitric oxide production in raw 264.7 macrophage cell line via P2Z/P2X7 receptors. *Neurochemistry International* **33**, 209-215.

126. Stockley RA, Snell NJC, Donovan L, Perrett J, Wang M, Newbold P, Entwistle N, & Keeler S (2008). Effects of Azd9056, A P2X7 Antagonist, in Patients with Chronic Obstructive Pulmonary Disease. *Thorax* **63**, A41-A42.

127. Stokes L, Jiang LH, Alcaraz L, Bent J, Bowers K, Fagura M, Furber M, Mortimore M, Lawson M, Theaker J, Laurent C, Braddock M, & Surprenant A (2006). Characterization of a selective and potent antagonist of human P2X(7) receptors, AZ11645373. *British Journal of Pharmacology* **149**, 880-887.

128. Su X, Johansen M, Looney MR, Brown EJ, & Matthay MA (2008). CD47 deficiency protects mice from lipopolysaccharide-induced acute lung injury and Escherichia coli pneumonia. *Journal of Immunology* **180**, 6947-6953.

129. Surprenant A (1996). *Functional properties of native and cloned P2X receptors.Ciba foundation symposia*, pp. 208-222.

130. Surprenant A, Rassendren F, Kawashima E, North RA, & Buell G (1996). The cytolytic P-2Z receptor for extracellular ATP identified as a P-2X receptor (P2X(7)). *Science* **272**, 735-738.

131. Takenouchi T, Sekiyama K, Sekigawa A, Fujita M, Waragai M, Sugama S, Iwamaru Y, Kitani H, & Hashimoto M (2010). P2X7 Receptor Signaling Pathway as a Therapeutic Target for Neurodegenerative Diseases. *Archivum Immunologiae et Therapiae Experimentalis* **58**, 91-96.

132. Tatham PER & Lindau M (1990). Atp-Induced Pore Formation in the Plasma-Membrane of Rat Peritoneal Mast-Cells. *Journal of General Physiology* **95**, 459-476.

133. Tokuhira M, Hosaka S, Volin MV, Haines GK, Katschke KJ, Kim S, & Koch AE (2000). Soluble vascular cell adhesion molecule 1 mediation of monocyte chemotaxis in rheumatoid arthritis. *Arthritis and Rheumatism* **43**, 1122-1133.

134. Tschumperlin DJ & Margulies SS (1999). Alveolar epithelial surface area-volume relationship in isolated rat lungs (vol 86, pg 2026, 1999). *Journal of Applied Physiology* **87**, U34.

135. van Oosten M, van de Bilt E, de Vries HE, van Berkel TJ, & Kuiper J (1995). Vascular adhesion molecule-1 and intercellular adhesion molecule-1 expression on rat liver cells after lipopolysaccharide administration in vivo. *Hepatology (Baltimore, Md)* **22**, 1538-1546.

136. Vancalker D, Muller M, & Hamprecht B (1979). Adenosine Regulates Via 2 Different Types of Receptors, the Accumulation of Cyclic-Amp in Cultured Brain-Cells. *Journal of Neurochemistry* **33**, 999-1005.

137. Virginio C, Church D, North RA, & Surprenant A (1997). Effects of divalent cations, protons and calmidazolium at the rat P2X(7) receptor. *Neuropharmacology* **36**, 1285-1294.

138. von Kugelgen I & Harden TK (2011). Molecular pharmacology, physiology, and structure of the P2Y receptors. *Advances in pharmacology (San Diego, Calif)* **61**, 373-415.

139. Wang PC, Chintagari NR, Gou DM, Su LJ, & Liu L (2007). Physical and functional interactions of SNAP-23 with annexin A2. *American Journal of Respiratory Cell and Molecular Biology* **37**, 467-476.

140. Wang SH & Hubmayr RD (2011). Type I Alveolar Epithelial Phenotype in Primary Culture. *American Journal of Respiratory Cell and Molecular Biology* **44**, 692-699.

141. Wienerkronish JP, Albertine KH, & Matthay MA (1991). Differential Responses of the Endothelial and Epithelial Barriers of the Lung in Sheep to Escherichia-Coli Endotoxin. *Journal of Clinical Investigation* **88**, 864-875.

142. Wiley JS, Chen R, Wiley MJ, & Jamieson GP (1992). The Atp4- Receptor-Operated Ion Channel of Human-Lymphocytes - Inhibition of Ion Fluxes by Amiloride Analogs and by Extracellular-Sodium Ions. *Archives of Biochemistry and Biophysics* **292**, 411-418.

143. Wiley JS, Dao-Ung LP, Gu BJ, Sluyter R, Shemon AN, Li CP, Taper J, Gallo J, & Manoharan A (2002). A loss-of-function polymorphic mutation in the cytolytic P2X7 receptor gene and chronic lymphocytic leukaemia: a molecular study. *Lancet* **359**, 1114-1119.

144. Wiley JS, Gargett CE, Zhang W, Snook MB, & Jamieson GA (1998). Partial agonists and antagonists reveal a second permeability state of human lymphocyte P2Z/P2X(7) channel. *American Journal of Physiology-Cell Physiology* **275**, C1224-C1231.

145. Williams MC (2003). Alveolar type I cells: Molecular phenotype and development. *Annual Review of Physiology* **65**, 669-695.

146. Worthington RA, Smart ML, Gu BJ, Williams DA, Petrou S, Wiley JS, & Barden JA (2002). Point mutations confer loss of ATP-induced human P2X(7) receptor function. *Febs Letters* **512**, 43-46.

147. Yip L, Woehrle T, Corriden R, Hirsh M, Chen Y, Inoue Y, Ferrari V, Insel PA, & Junger WG (2009). Autocrine regulation of T-cell activation by ATP release and P2X(7) receptors. *Faseb Journal* **23**, 1685-1693.

148. Young SL, Kremers SA, Apple JS, Crapo JD, & Brumley GW (1981). Rat Lung Surfactant Kinetics - Biochemical and Morphometric Correlation. *Journal of Applied Physiology* **51**, 248-253.

149. Zhou QY, Li CY, Olah ME, Johnson RA, Stiles GL, & Civelli O (1992). Molecular-Cloning and Characterization of An Adenosine Receptor - the A3 Adenosine Receptor. *Proceedings of the National Academy of Sciences* **89**, 7432-7436.

150. Ziganshin AU, Ziganshina LE, & Burnstock G (2002). P2 receptors: Theoretical background for the use in clinical practice. *Bulletin of Experimental Biology and Medicine* **134**, 313-317.

151. Zimmermann H (2000). Extracellular metabolism of ATP and other nucleotides. *Naunyn-Schmiedebergs Archives of Pharmacology* **362**, 299-309.

CHAPTER II

PURINERGIC P2X7 RECEPTOR REGULATES LUNG SURFACTANT SECRETION IN A PARACRINE MANNER

2.1 Abstract

Alveolar epithelium is composed of alveolar epithelial type I (AEC I) and type II (AEC II) cells. AEC II secretes lung surfactant via exocytosis. The P2 purinergic receptor, $P2X_7$ receptor ($P2X_7R$) has been implicated in the regulation of synaptic transmission and inflammation. Here, we report that AEC I-specific $P2X_7R$ is a novel mediator for the paracrine regulation of surfactant secretion in AEC II. In primary culture of AEC I and AEC II, BzATP, an agonist of $P2X_7R$, increased surfactant secretion, which was blocked by the $P2X_7R$ antagonist, Brilliant Blue G. This effect was observed in AEC II co-cultured with the HEK293 cells stably expressing rat $P2X_7R$, but not with the $P2X_7R$ knocked down AEC I or in isolated AEC I and AEC II from $P2X7R^{-/-}$ mice. BzATP-mediated secretion involved $P2Y_2$ receptor signaling since it was reduced by the addition of the ATP scavengers, apyrase and adenosine deaminase and the $P2Y_2$ receptor antagonist, suramin. $P2X_7R^{-/-}$ mice failed to increase surfactant secretion in response to hyperventilation, pointing to the physiological relevance of $P2X_7R$ in maintaining surfactant homeostasis in the lung. These results suggest that the activation of $P2X_7R$ increases surfactant secretion by releasing ATP from AEC I and subsequently stimulating $P2Y_2$ receptors in AEC II.

Key words: $P2X_7$ receptor, Exocytosis, Cell-cell communication, alveolar epithelial cells.

2.2 Introduction

Pulmonary surfactant, consisting of lipids and surfactant proteins, is synthesized and secreted by alveolar epithelial type II cells (AEC II). Surfactant secretion occurs through the fusion of the limiting membrane of lamellar bodies with the apical plasma membrane, followed by the extrusion of the lamellar body contents into the alveolar space. Numerous surfactant secretagogues such as ATP, terbutaline, phorbol esters, 5'-(-N-ethylcarboxamido) adenosine (NECA), vasopressin, and Ca^{2+} ionophores A23187 augment surfactant secretion in cultured AEC II (Andreeva *et al.*, 2007). These secretagogues initiate various signal transductions. For example, the stimulation of β_2-adrenergic receptors by terbutaline generates cAMP and activates protein kinase A (Dobbs and Mason, 1979), while the activation of purinergic $P2Y_2$ receptors ($P2Y_2R$) by ATP produces inositol triphosphate and diacylglycerol and activates protein kinase C (PKC) (Chander *et al.*, 1995;Linke *et al.*, 1997;Gobran and Rooney, 1999).

Pulmonary alveoli are lined by thin, flat squamous alveolar type I cells (AEC I) interspersed in the alveolar epithelium. These cells form a nexus with cuboidal AEC II. AEC I have traditionally been thought to play a role in effective gaseous exchange. However, several new functions of AEC I have recently been uncovered including their role in protecting the lung from injury (Chen *et al.*, 2006), and the regulation of alveolar fluid homeostasis (Johnson *et al.*, 2006).

Surfactant secretion alters with the spatiotemporal Ca^{2+} changes and signaling (Haller *et al.*, 2001). Intracellular Ca^{2+} perturbation in AEC I and AEC II bipartitely communicates with each other via Ca^{2+} wave propagation through gap junctional intercellular communication or paracrine ATP release (Isakson *et al.*, 2003;Patel *et al.*,

2005). *In situ* fluorescence imaging has shown that interalveolar Ca^{2+} conductance initiates in AEC I and stimulates lamellar body extrusion from AEC II (Ichimura *et al.*, 2006). Moreover, Ca^{2+} oscillations from AEC I communicate with AEC II during lung inflation, suggesting a role for AEC I in surfactant secretion (Ashino *et al.*, 2000). However, the mediators for AEC I and AEC II communication are unclear.

P2X7 receptor ($P2X_7R$) belongs to the P2XR family. $P2X_7R$ has a significantly longer intracellular C-terminus where the last 177 amino acids are critical for the formation of the non-selective pore (North, 2002). Unlike other P2XRs, $P2X_7R$ only forms homomultimers, is more potently inhibited by extracellular Ca^{2+} and/or Mg^{2+} (Baraldi *et al.*, 2004), and has a very low sensitivity to ATP (Young *et al.*, 2007). The activation of $P2X_7R$ leads to the opening of a cationic channel with significant permeability to Ca^{2+} and intracellular depolarization (Rassendren *et al.*, 1997;Virginio *et al.*, 1997). The cation channel can convert to a non-selective pore permeable to small molecules and ions in the continued presence of ATP and low levels of divalent cations (North, 2002). The activation of $P2X_7R$ also results in the release of various cytokines and signaling molecules. These include ATP from astrocytes with the propagation of Ca^{2+} transmission (Suadicani *et al.*, 2006a), interleukin-1 beta and matrix metalloproteinase-9 from immune cells as a pro-inflammatory response (Ferrari *et al.*, 2006;Gu and Wiley, 2006), prostaglandin from bone cells during osteogenesis (Li *et al.*, 2005) and neurotransmitters, GABA and glutamate from the hippocampus (Sperlagh *et al.*, 2002).

$P2X_7R$ is predominantly localized in immune cells, glial cells, hematopoietic cells and in various mammalian epithelial cells (Collo *et al.*, 1997). $P2X_7R$ has been

implicated in inflammation (Hughes *et al.*, 2007), periosteal and cancellous bone formation (Ke *et al.*, 2003), apoptosis (Placido *et al.*, 2006), Alzheimer Disease (Parvathenani *et al.*, 2003) and autoimmune encephalomyelitis (Chen and Brosnan, 2006). We have previously identified $P2X_7R$ as a specific marker of AEC I in the lung (Chen *et al.*, 2004b). However, the functional role of $P2X_7R$ in the lung remains unexplored. In this study, using *in vitro* cell culture and *in vivo* $P2X_7R$ knock-out ($P2X_7R^{-/-}$) mice, we demonstrate that upon the activation of $P2X_7R$, ATP is released from AEC I and modulates surfactant secretion in a paracrine manner via the $P2Y_2R$ and PKC-mediated pathway. Our findings reveal a novel function of $P2X_7R$ in alveolar epithelial cells and add a new layer to the complex regulation of lung surfactant secretion.

2.3 Materials and Methods

2.3.1 Materials

Reagents

3'-*O*-(4-benzoyl) benzoyl ATP (BzATP), Brilliant Blue G (BBG), adenosine deaminase (ADA), apyrase, suramin, staurosporine, ARL-67156, ATP bioluminescent assay kit (FLAA), polyclonal rabbit anti-$P2X_7$ purinergic receptor, anti-purinergic receptor $P2X_7$ (extracellular)-FITC and anti-podoplanin (anti-T1α) antibodies were obtained from Sigma (St. Louis, MO). Elastase was from Worthington Biochemical Corp. (Lakewood, NJ). Mouse anti-LB-180 (ABCA3) antibody was from Covance (Berkeley, CA). Alexa 546- and 488-conjugated anti-rabbit and anti-mouse secondary antibodies were from Molecular Probes (Eugene, OR). Cy3-conjugated Affini-pure goat anti-mouse and anti-hamster IgG was from Jackson ImmunoResearch Laboratories (West Grove, PA). The Dc protein assay kit was from Bio-Rad (Hercules, CA). The enhanced chemiluminescence detection system was from Amersham Biosciences (Piscataway, NJ). Anti-rat and anti-mouse IgG-conjugated magnetic beads were from Dynal Biotech (Lake Success, NY). Mouse anti-T1α antibody was a generous gift from Dr. Mary Williams (Boston University). Mouse anti-CD45 (anti-leukocyte common antigen or anti-LC) antibody was from BD Biosciences (Franklin Lakes, NJ). YOPRO-1 dye was from Invitrogen (Carlsbad, CA). Human embryonic kidney (HEK) 293 cells stably expressing rat $P2X_7R$ (HEK-$P2X_7R$), E10 cells and R3/1 cells were kindly provided by Dr. Annmarie Surprenant (University of Manchester), Dr. Mary Williams (Boston University) and Dr. Roland Koslowski (Dresden University of Technology).

2.3.2. Isolation of rat AEC I and AEC II

Rat AEC I and AEC II were isolated from the lungs of pathogen-free male Sprague-Dawley rats (150-200 gms) by modifying our previous method for isolating AEC I (Chen *et al.*, 2004a), in which the elastase concentration was increased from 4.5 U/ml to 8 U/ml. The Oklahoma State University Animal Care and Use Committee approved all the animal procedures used in this study. Rats were anesthetized with an intraperitoneal injection of ketamine (40 mg/kg) and xylazine (8 mg/kg). A tracheotomy was performed and rats were ventilated with a rodent ventilator throughout the process of perfusion. The rats were exsanguinated via abdominal aorta and heart transection. A catheter was placed in the pulmonary artery and the lungs were perfused with solution II (0.9% NaCl, 0.1% glucose, 10 mM HEPES, pH 7.4, 5 mM KCl, 1.3 mM $MgSO_4$, 1.7 mM $CaCl_2$, 0.1 mg/ml streptomycin sulfate, 0.06 mg/ml penicillin G, 3 mM Na_2HPO_4 and 3 mM NaH_2PO_4), followed by instilling solution I (solution II plus 0.06 mg/ml EGTA) through the trachea. Lungs were removed and lavaged with solution I. The lungs were then digested by instilling warm elastase three times (8 U/ml in solution II, 7 ml) for 20 min each at 37ºC to release AEC I and AEC II. The lung tissue was chopped and the cell suspension was mixed with 100 µg/ml DNase I and incubated for 5 min at 37ºC with gentle rotation. The cell suspension was then filtered through 160- and 37-µm nylon meshes once, followed by a 15-µm nylon mesh twice. The cells were incubated in rat IgG-coated 100 mm polystyrene bacteriological Petri dishes (3 mg IgG/dish for each rat) at 37ºC for 45 min. The unattached cells were centrifuged at 250 x*g* for 10 min and resuspended with 1 ml of solution III (RPMI 1640 medium containing 25 mM HEPES and 1% FBS).

To further remove the remaining leukocytes, the cells were resuspended in 0.5 ml Solution III and incubated with rat IgG (1 mg/ml) and anti-LC (16 μg/ml) at 4°C for 20 min with gentle rotation. After being washed with solution III twice, the cells were incubated with sheep anti-rat IgG (150 μl/rat) and goat anti-mouse IgG (150 μl/rat) Dynabeads at 4°C for 15 min. A magnetic field was applied to remove the cells attached to the magnetic beads. Finally, the cells were harvested and resuspended in DMEM containing 10% FBS, 0.1 mM nonessential amino acids, 1000 units/ml penicillin G and 100 μg/ml streptomycin and cultured overnight for further experiments. The viabilities of the cell preparations were determined by the Trypan blue dye exclusion method.

2.3.3. Isolation of mouse AEC I and AEC II

Mouse AEC I and AEC II were isolated from male C57BL/6 mice (6-8 wks of age) according to the previously reported procedure with some modification (Bortnick *et al.*, 2003). Mice were anesthetized with ketamine (80 mg/kg) and xylazine (10 mg/kg). The abdominal cavity was opened, exsanguinated and cannulated with a 20 gauge luer stub adapter through intratracheal route. Lungs were perfused with solution II, followed by instilling 1 ml of the digestion cocktail (dispase, 2500 caseinolytic units/ml and elastase, 4 U/ml in solution II) directly through the trachea. Three lungs were isolated, pooled into a beaker containing ~17 ml of the digestion cocktail and incubated at 37^{o}C for 15 min. After incubation, the lungs were chopped. Lung tissues were further digested with the addition of DNase I (100 μg/ml) for 45 min at 37^{o}C with intermittent shaking. The digested lungs were filtered through 160-, 37- and 15-μm nylon mesh sequentially. The filtrate was centrifuged at 250 x*g* for 10 min. The cell pellet was resuspended in DMEM media and incubated in a 100 mm petridish coated

with mouse IgG (75 μg/dish) for 1 hr. The cells were spun down at 250 x*g* for 10 min and resuspended in DMEM containing 10% FBS. The cell yield was ~8 x10^6 per mouse and the cell viability was >95%.

2.3.4. Immunocytochemistry

Freshly isolated AEC I and AEC II were fixed with 4% paraformaldehyde for 30 min, followed by cytospining them onto glass slides at 600 x*g* for 10 min. For overnight-cultured cells, the cells were cultured on coverslips overnight and washed 3 times with phosphate-buffered saline (pH 7.4) prior to fixation with 4% paraformaldehyde for 30 min. Cells were permeablized with 0.1% Triton X-100 for 15 min and blocked with 5% FBS for 1 hr. Cells were incubated with mouse monoclonal anti-ABCA3 (1:200), anti-T1α (E11, 1:100), and anti-CD45 (1:100) antibodies, and rabbit polyclonal anti-$P2X_7R$ (1:100) antibodies overnight at 4ºC. Cells were then washed and incubated with Alexa 546-conjugated anti-rabbit and Alexa 488-conjugated anti-mouse secondary antibodies or Cy-3-conjugated Affini-Pure anti-mouse IgG (1:250). 4'-6-Diamidino-2-phenylindole (DAPI, 2.5 mg/ml) staining was used for counting cells. Cells were viewed on a Nikon Eclipse E600 fluorescence microscope or Nikon Eclipse TE 2000 U inverted fluorescence microscope.

2.3.5. Cytometry

Cytometry of isolated AEC I and AEC II was done by resuspending cells in the staining buffer (Hank's balanced salt solution without phenol red plus 1% bovine serum albumin and 0.1% sodium azide) containing 10 μl $P2X_7R$ (ecto)-FITC antibody per 10^6 cells and incubated for 20 min at 4ºC with constant rotation. The cells were then washed

twice with the staining buffer and gated for $P2X_7R$ (ecto)-FITC-positive cells in a single argon laser cytofluorometer FACSCalibur (BD Biosciences).

2.3.6. FM1-43 staining

Fusion pore formation was monitored by FM1-43 staining as previously described (Chintagari *et al.*, 2006). Overnight-cultured AEC I and AEC II were pre-incubated with 100 nM BBG for 30 min and then stimulated for 1 hr with 25 μM BzATP. FM1-43 dye (4 μM final concentration) was added along with BzATP. Cells were washed, fixed with 4% ice-cold paraformaldehyde and examined with a fluorescence microscopy.

2.3.7. YOPRO-1 Dye uptake

Accumulation of the monomeric cyanine nucleic acid chelating dye, YOPRO-1 (MW 375 Da) was used as an indicator of the $P2X_7R$ activation (Stokes *et al.*, 2006). Freshly isolated AEC I and AEC II or cell lines (E10, R3/1 and HEK-$P2X_7R$ cells) (1 x 10^6/ml) were incubated with the assay buffer containing 15 mM HEPES, pH 7.4, 135 mM NaCl, 5 mM KCl, 1.8 mM $CaCl_2$ and 0.8 mM $MgCl_2$ in the presence or absence of 100 nM BBG for 20 min. YOPRO-1 at a 5 μM final concentration was added and incubated for additional 5 min. The cells were transferred to a cuvette under continuous stirring, and YO-PRO-1 fluorescence was measured by a FluoroMax-3 spectrofluorimeter (HORIBA Jobin Yvon, Edison, NJ) using an excitation and emission wavelength of 491 nm and 509 nm, respectively. BzATP (200 μM) was added after recording the baseline for 3-4 min. Fluorescence intensity was corrected with the cells without dye. In some cases, baselines were adjusted for comparisons between the different cells.

Dye uptake was also monitored directly by a fluorescence microscopy in order to assess the $P2X_7R$ activation in a specific type of cells of the AEC I and AEC II

heterocellular culture. Overnight-cultured cells were washed twice and incubated with the assay buffer for 15 min. BzATP (200 μM) was added and incubated with YOPRO-1 (5 μM) for 20 min. Cells were then incubated with Nile red (10 μM) for an additional 2 min, washed twice with PBS, fixed with 4% ice-cold paraformaldehyde and examined with a fluorescence microscopy.

2.3.8. Surfactant secretion assay

Surfactant secretion was performed as previously described (Chintagari *et al.*, 2006). The freshly isolated AEC I and AEC II (1 X 10^6 in a 35 cm dish for rat and 0.8 x 10^6 in each well of a 12-well plate for mouse) were cultured overnight in the presence of [^{3}H]choline (0.6 μCi/10^6 cells). The heterocellular culture was incubated with or without various inhibitors or antagonists for 30 min. One set of the dishes were removed at this time point for analyzing the *time zero* value. The cells were then incubated with BzATP or other secretagogues for 2 hrs. At the end of incubation, lipids in the medium and cells were extracted using a one-step phosphotidylcholine extraction method (Vassar *et al.*, 2007). The radioactivities were counted. Surfactant secretion (%) was expressed as (dpm in medium/dpm in medium and cells) x100. All of the secretion data was corrected by substracting the *time zero* value. A stimulation index was defined as a ratio of stimulated secretion to basal secretion.

2.3.9. MTT assay

Cell viability was assessed using a 3-(4, 5-dimethylthiazol-2-yl)-2, 5-diphenyl tetrazolium bromide (MTT) dye conversion or Trypan blue exclusion assays as described (Chintagari *et al.*, 2006).

2.3.10. Western blot

Cells were lysed in lysis buffer (10 mM Tris-HCl, pH 7.5, 1% Triton X-100, 1 mM EDTA, 1 mM phenylmethylsulfonyl fluoride, 10 μg/ml aprotonin and 10 μg/ml leupeptin). The protein concentration was determined by the Dc protein assay kit. Protein was separated on a 10% SDS-polyacrylamide gel and transferred to a nitrocellulose membrane. The membrane was stained with Ponceau S to ensure proper transfer and blocked overnight with 5% dry skim milk in 100 mM Tris-buffered saline plus 0.1% Tween 20 (TBST). The membranes were incubated with anti-$P2X_7R$ antibodies at a 1:1000 dilution or anti-β actin antibodies at a 1:2000 dilution overnight at 4°C. After being washed with TBST three times, the membranes were incubated with horseradish peroxidase-conjugated anti-rabbit IgG (1:2000) for 1 hr. The blots were washed again and individual target proteins were visualized using the enhanced chemiluminescence detection system.

2.3.11. Co-culture

HEK 293 cells stably expressing rat $P2X_7R$ (HEK $P2X_7R$) and HEK 293 cells were cultured in a DMEM and F12 (1:1) medium containing 10% FBS, 2 mM glutamine, 1000 units/ml penicillin G, and 100 μg/ml streptomycin. E10 and R3/1 cells were cultured in CMRL and F12-HAM's media containing 10% FBS, 2 mM glutamine, 1000 units/ml penicillin G and 100 μg/ml streptomycin, respectively. All the cells were grown to confluence, released and co-cultured with freshly isolated AEC II in a 1:2 ratio in DMEM media for 16-18 hrs. Cells were labeled and assayed for surfactant secretion as described above. The radioactive counts in E10, R3/1, HEK-$P2X_7R$ and HEK 293 cells were less than 10% of that in AEC II.

To determine the effects of conditioned media on surfactant secretion, E10 cells, HEK-P2X$_7$R and HEK 293 cells were grown to confluence in the respective culture media as described above. Freshly isolated AEC II was cultured for 16 -18 hrs in DMEM complete media. These cells were washed three times with DMEM and incubated with 100 μM ARL-67156 and 25 μM BzATP for 2 hrs. The conditioned media was removed and centrifuged at 250 x*g* for 5 min. The supernatant was transferred to recipient [^{3}H]choline-labeled AEC II. Cells were further incubated for 2 hrs and surfactant secretion was assayed.

2.3.12. Measurement of ATP concentration

The cells were washed three times with 1 ml of DMEM and pre-incubated with or without 100 nM BBG for 15 min. BzATP (25 μM) was added to stimulate the cells for 10 min. The media were removed to avoid the interference of BzATP for ATP assay. The fresh medium containing 100 μM ARL-67156 was added and incubated for 20 min. Media were centrifuged at 600 x*g* for 10 min. Supernatant was collected and frozen in aliquots at -20ºC for subsequent ATP assay.

ATP concentration was measured using the chemiluminescent luciferin-luciferase assay kit. Media (25 μl) were placed in a white opaque 96 well plate. An equal volume of luciferin-luciferase assay solution was added to each well. Luminescence was recorded using a FLUOSTAR microplate reader (BMG, Labtech, Germany). Luminescence measurements were taken for 5 min with an integration time of 60 ms/well. A stardand curve was generated for each experiment with ATP standards up to 1 μM. The results were expressed as nM ATP in bulk media per 10 μg of total cellular protein.

2.3.13. Knock-down of $P2X_7R$

Adenoviral shRNA vectors were construced as prevously described (Gou *et al.*, 2007).Two shRNA sequences targting to 574-592 and 669-689 of mouse $P2X_7R$ were chosen (Jun *et al.*, 2007;Lu *et al.*, 2007) and was named as si-X_7 (1) and si-X_7 (2). E10 cells were transduced with virus control, si-X_7 (1) and si-X_7 (2) for 4 days at a MOI of 0-100.

2.3.14. Preloading assay for dye transfer

This was done according to the methodology described by Koval M *et al.* (Abraham *et al.*, 2001). E10 cells cultured in 35 mm tissue culture dishes were incubated with DMEM containing 1 mg /ml of Texas Red Dextran (10,000 mw) and 10 µM calcein-AM for 30 min at 37ºC. Freshly isolated unlabeled acceptor AEC II were co-cultured with the double-labeled E10 cells for 5 hrs and fluorescence images were taken.

2.3.15. Real-time PCR

Real-time PCR analysis was performed as previously described (Jin *et al.*, 2006). The primers used were listed in Table 3. Data were normalized to 18S rRNA.

2.3.16. Surfactant secertion in mice

Surfactant secretion in wild-type and $P2X_7R^{-/-}$ mice was measured according to the method of Ikegmai et al. (Ikegami *et al.*, 2000). $P2X_7R^{-/-}$ mice on a C57BL/6 background were purchased from the Jackson Laboratory (strain: B6.129P2-*P2rx7*^{tm1Gab}/J) and bred in the Laboratory Animal Resources Unit at Oklahoma State University. The wild-type (C57BL/6) and $P2X_7R^{-/-}$ mice were given intraperitoneally 0.5 µCi[^{3}H] choline/g body weight and housed for 16 hrs. The mice were hyperventilated for

30 min with a tidal volume (Vt) of 30 ml/kg and a positive end-expiratory pressure (PEEP) of 5 cm H_2O as described (Wyszogrodski *et al.*, 1975). Under these conditions, surfactant secretion was increased and the inactivation of surfactant did not occur because of the use of positive end-expiratory pressure (Wyszogrodski *et al.*, 1975). The mice were killed. The lavage and lung tissue were collected. Lipids were extracted and saturated phosphatidylcholine isolated according to the method of Mason et al. (Mason *et al.*, 1976). Secretion was expressed as (dpm in lavage)/(dpm in lavage and lung tissue) x 100%.

2.3.17. Statistical Analysis

Data was expressed as means ± SE. Statistical analysis was performed by one-way analysis of variance, followed by Tukey's Analysis or student's *t* test using Graphpad prism version 4. A p value of <0.05 was considered significant.

2.4 Results

2.4.1 Characterization of a heterocellular culture of AEC I and AEC II

To study the communication of AEC I and AEC II, we first developed a new heterocellular culture of AEC I and AEC II. A mixed preparation of AEC I and AEC II was isolated from rat lungs based on the method modified from the AEC I isolation (Chen *et al.*, 2004a). The cell viability was ~97% and the cell yield was ~54 x 10^6/rat. Immunophenotyping using specific cell markers revealed that the freshly isolated cells contained ~31% AEC I and ~64% AEC II (Table 2.1). This ratio is similar to the AEC I and AEC II numbers *in vivo*. FACS analysis confirmed that 34% of AEC I existed in the mixed cell preparation. Macrophage contamination was ~3%. Overnight-cultured cells also showed a positive staining of T1α (AEC I marker) and ABCA3 (AEC II marker) (Figure 2.1A). AEC I displayed the characteristic squamous morphology with the retracted accordion-like appearance of long cytoplasmic extensions (Figure 2.1C). The ratio of AEC I and AEC II was essentially the same as that of the freshly isolated cells (Table 2.1). These results suggest that AEC I and AEC II maintain their phenotypes after overnight culture. Double-labeling demonstrated that $P2X_7R$ was only present in AEC I, but not in AEC II (Figure 2.1B), confirming the specific localization of $P2X_7R$ in AEC I of the lung (Chen *et al.*, 2004b).

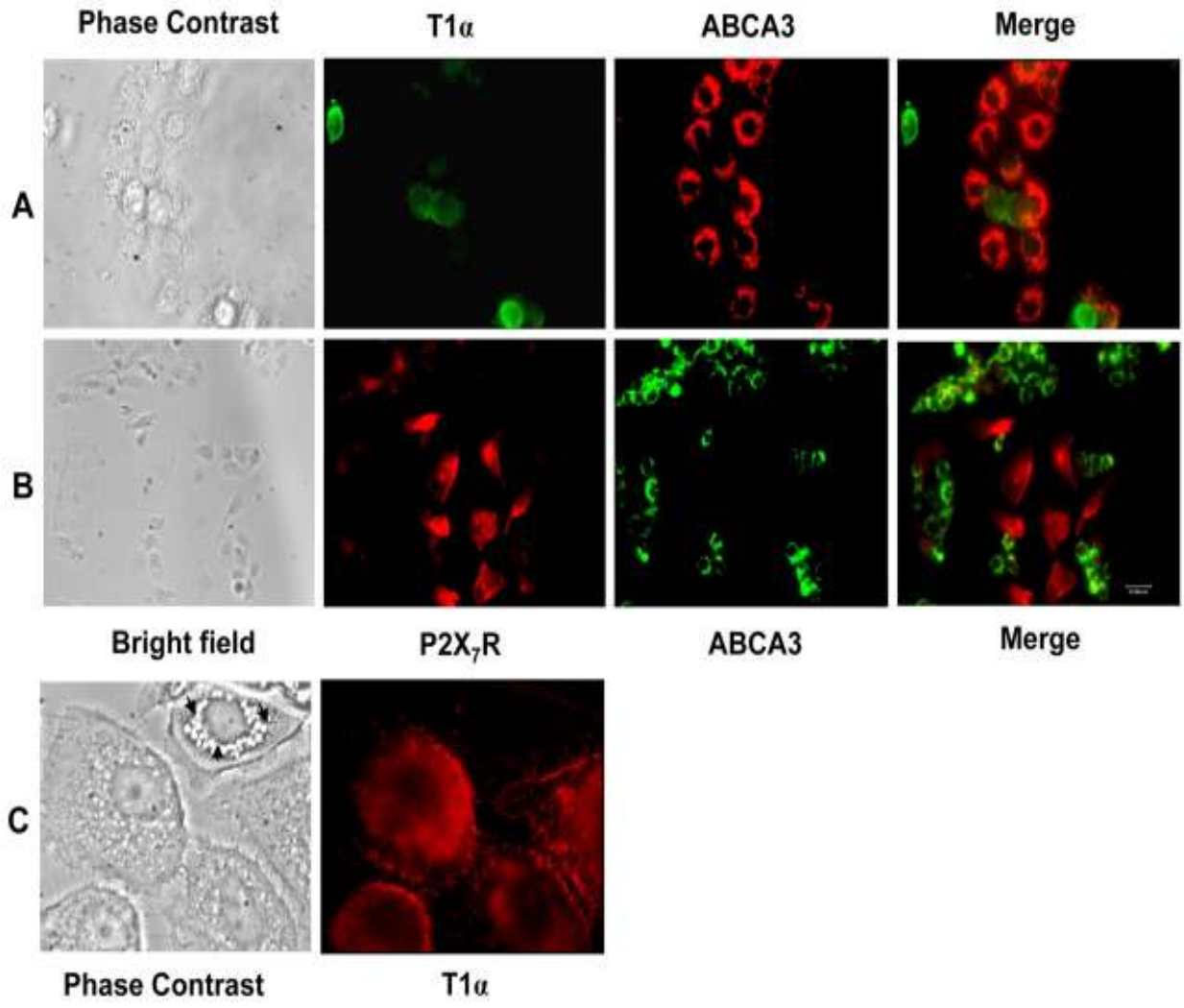

Figure 2.1: Identification of AEC I and AEC II in heterocellular culture.

(A) Overnight cultured cells were double-labeled with polyclonal rabbit anti-T1α (AEC I marker, green) and monoclonal mouse anti-ABCA3 (AEC II marker, red). (B) Overnight cultured cells were double-labeled with polyclonal rabbit anti-$P2X_7R$ (red) and monoclonal mouse anti-ABCA3 (green) antibodies. (C) Enlarged images showing AEC I characteristics labeled with AEC I specific monoclonal mouse anti-T1α. Arrows indicate characteristic lamellar bodies of AEC II. Scale bars: 40 μm.

Table 2.1 Characterization of AEC I and AEC II preparations

	AEC I (%)	AEC II (%)	Macrophages (%)	Others (%)	Yield (10^6/rat)	Viability (%)
D0	31.4 ± 1.9 *34.1 ±0.3	63.6 ± 2.2	2.9 ± 0.5	1.9 ± 0.3	54 ± 2	97 ± 3
D1	28.6 ± 1.9	63.6 ± 1.1	4.4 ± 0.9	3.9 ± 1.1		

Freshly isolated (D0) or overnight-cultured (D1) AEC I and AEC II were identified with anti-T1α and anti-ABCA3 antibodies, respectively. Macrophages were determined using mouse anti-CD 45. The cells were counted from 10 randomly selected fields of each cell preparation. The percentages of cell populations were calculated (means ± SE, n=5 independent cell preparations). *Data were obtained from flow cytometry analysis of AEC I labeled with FITC-$P2X_7R$ (n=2). Cell viability was determined by the trypan blue dye exclusion method.

2.4.2 The activation of P2X7R in AEC I

We next determined whether $P2X_7R$ can be activated in AEC I of the heterocellular culture of AEC I and AEC II. The activation of $P2X_7R$ leads to the opening of non-selective pores that are permeable to small molecules (<900 Da) including YO-PRO-1. The accumulation of the monomeric cyanine nucleic acid chelating dye, YO-PRO-1 has been used as an indicator of the $P2X_7R$ activation (Stokes *et al.*, 2006). The overnight cultured cells were incubated with YO-PRO-1 in the presence of 2', 3'-O-(4-benzoyl-benzoyl) ATP (BzATP), a specific agonist of $P2X_7R$. Nile red was used to identify AEC II (Chen *et al.*, 2004a). As shown in Figure 2.2A, the cells that did not have the Nile red staining took up the dye, indicating the activation of $P2X_7R$ in AEC I. To quantitate the dye uptake, the cells were incubated with YO-PRO-1 for 5 min and YO-PRO-1 fluorescence was measured by spectrofluorimeter. BzATP caused a rapid increase of the intensity in heterocellular AEC I and AEC II preparation, but had no effects on AEC II alone (Figure 2.2B). Brilliant Blue G (BBG) inhibits rat $P2X_7R$ at 100 nM and does not affect other P2X receptors even at >10 μM (Jiang *et al.*, 2000). The BzATP-mediated increase of the dye uptake was blocked by 100 nM BBG.

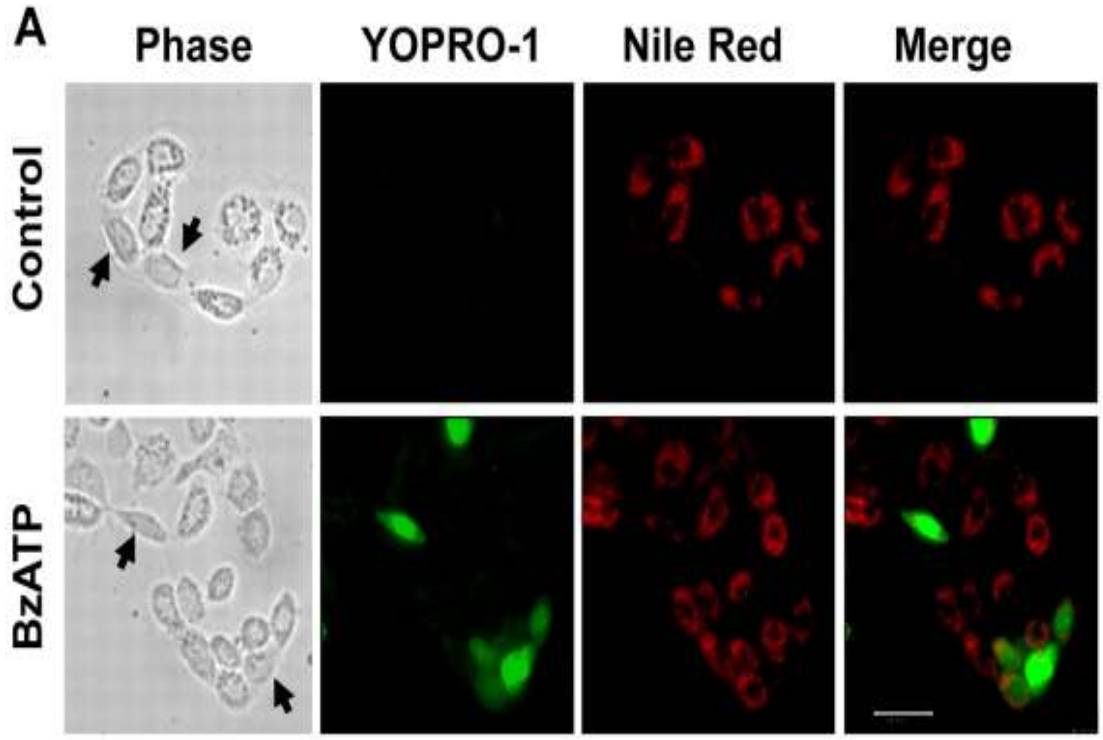
A
Phase
YOPRO-1
Nile Red
Merge
Control
BzATP

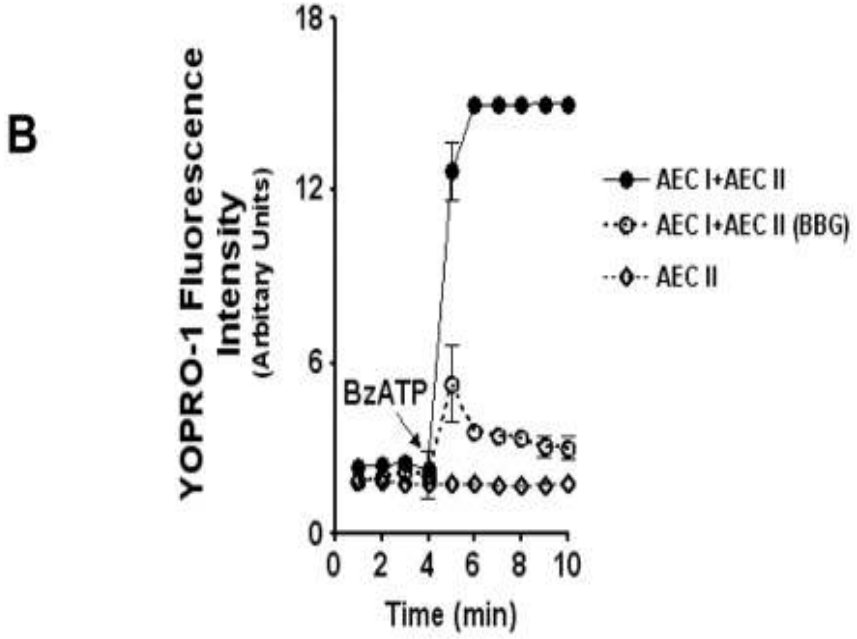
B
YOPRO-1 Fluorescence Intensity
(Arbitary Units)
18
12
6
0
BzATP
0 2 4 6 8 10
Time (min)
AEC I+AEC II
AEC I+AEC II (BBG)
AEC II

Figure 2.2: BzATP specifically increased YO-PRO-1 uptake in AEC I.

(A) Overnight-cultured AEC I and AEC II were incubated with 5 μM YO-PRO-1 in the absence (control) or the presence of 200 μM BzATP for 20 min, followed by incubation with 10 μM Nile red. The cells were fixed and examined with a fluorescence microscope. Arrows point to AEC I. Scale bar: 40 μm. (B) AEC I and AEC II mixture or AEC II alone were incubated with 5 μM YO-PRO-1 for 5 min in the absence or presence of 100 nM BBG. The basal line was recorded with Ex=491 nm and Em=509 nm and 100 μM BzATP was added at 4 min. The fluorescence intensities were corrected with the cells without the dye. Data are Means ± SE from three independent cell preparations.

2.4.3 BzATP stimulates surfactant secretion in a heterocellular culture of AEC I and AEC II

To determine the functional role of $P2X_7R$ in surfactant secretion, we stimulated the heterocellular culture of AEC I and AEC II with BzATP and assessed the changes in surfactant secretion. BzATP increased surfactant secretion in a dose-dependent manner with an EC_{50} of 4.5 ± 0.3 μM. However, BzATP had little effect when AEC II were seeded alone (Figure 2.3A). BBG abolished the BzATP-mediated surfactant secretion (Figure 2.3B). BBG was specific to $P2X_7R$ since BBG did not affect surfactant secretion induced by other lung surfactant secretagogues including ATP, terbutaline and PMA (Figure 2.3C). The cell viability was unchanged by BzATP or BBG as seen by MTT assay (data not shown). BzATP also increased the fusion pore formation as determined by FM1-43 staining (Chintagari *et al.*, 2006), which was blocked by BBG (Figure 2.4). Our results suggests that the activation of $P2X_7R$ in AEC I stimulates AEC II to release lung surfactant.

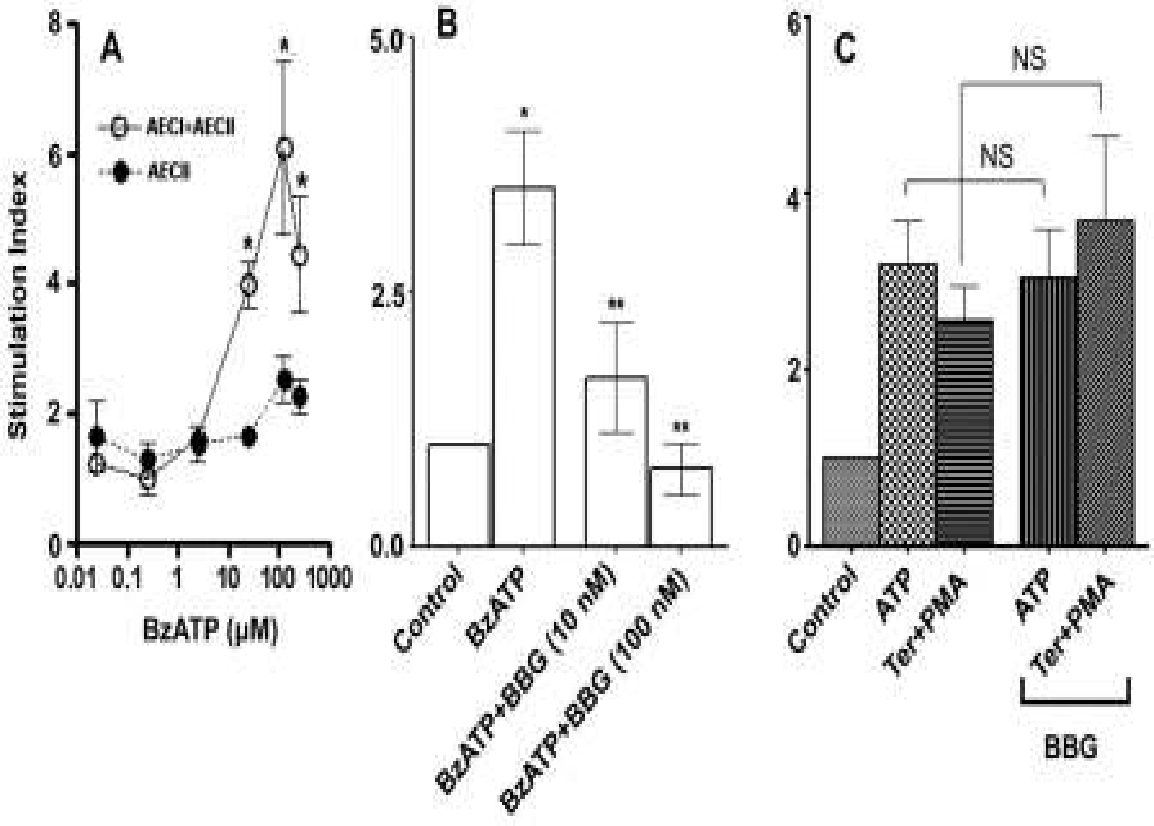

Figure 2.3: Effect of BzATP on surfactant secretion in a heterocellular culture.

Freshly isolated AEC I and AEC II or AEC II alone were incubated with [^{3}H] choline overnight. (A) The cells were stimulated with various concentrations of BzATP for 2 hrs. (B) AEC I and AEC II were pre-treated for 0.5 hr with 10 nM or 100 nM BBG and then incubated with 25 μM BzATP for 2 hrs. (C) AEC I and AEC II were pre-treated with 100 nM BBG for 30 min and then stimulated with 1 mM ATP or 0.1 μM terbutaline plus 1 μM PMA for 2 hrs. Surfactant secretion was measured by monitoring the release of [^{3}H]-labeled PC. The results were expressed as a stimulation index (a ratio of surfactant secretion in stimulated cells over those in unstimulated cells). Data shown are means ± SE. In (A), *P < 0.01 *v.s.* unstimulated cells (n=3-7, One way ANOVA and Tukey's multiple comparison). In (B), *P<0.0001 *v.s.* control; **P<0.0001 *v.s.* BzATP, n=5, student's *t* test). In (C), NS: not significant, P>0.05. n=3-5.

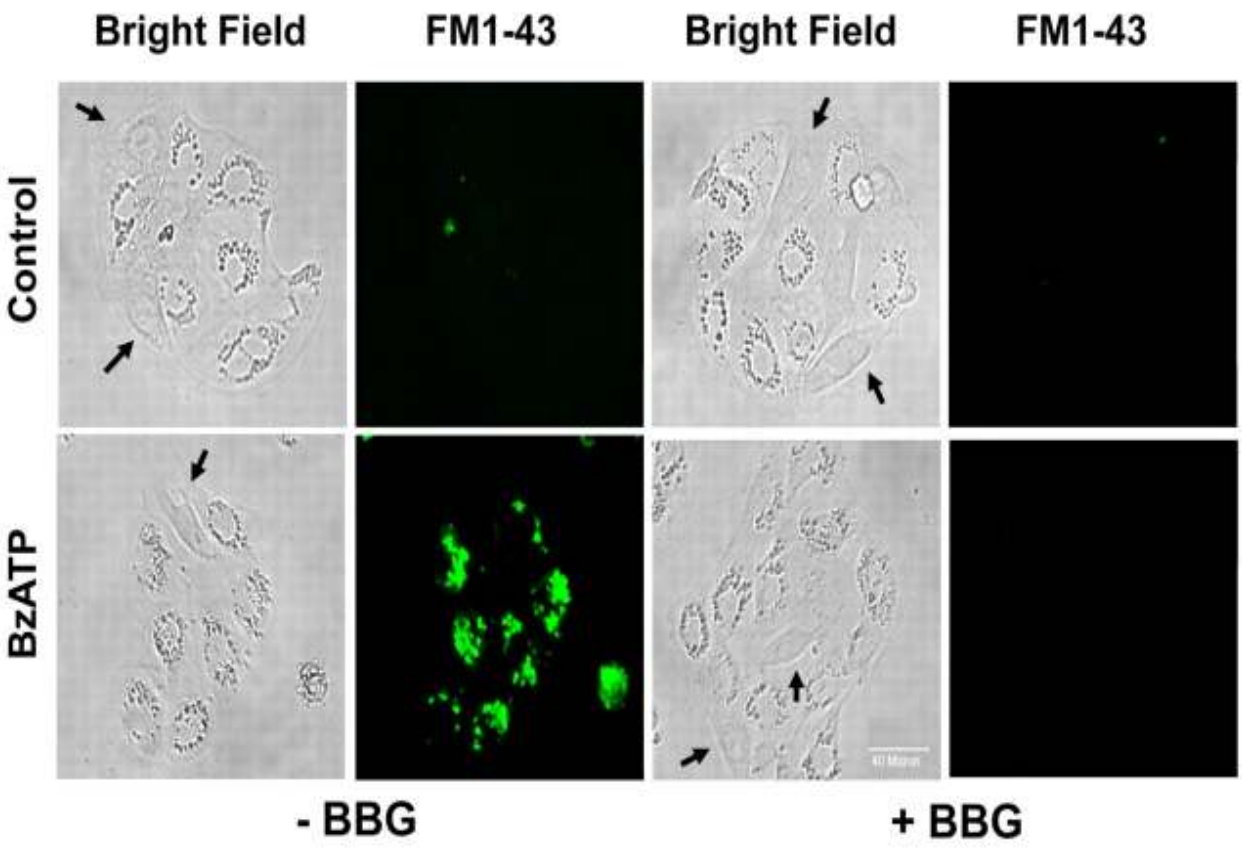

Figure 2.4: BzATP increases fusion pore formation.

AEC I and AEC II were pre-treated with 100 nM BBG for 30 min and then stimulated with 25 μM BzATP in the presence of 4 μM FM1-43 dye for 1 hr. Cells were washed twice with PBS and fixed for fluorescence microscopy. Arrows point to AEC I. *Scale bar*: 40 μm.

2.4.4 Co-culture of AEC I-like cell line containing P2X7R with AEC II increases surfactant secretion

$P2X_7R$ is highly expressed in the lung epithelial cell line, E10, but not in the R3/1 cell line (Barth *et al.*, 2007). Both cell lines have the properties similar to AEC I (Koslowski *et al.*, 2004;Kathuria *et al.*, 2007). We confirmed that E10 cells had very high expression of $P2X_7R$ and R3/1 cells expressed little $P2X_7R$ (Figure 2.5A). BzATP increased YOPRO-1 dye uptake in E10 cells, but not in R3/1 cells, indicating that $P2X_7R$ in E10 cells is functional (Figure 2.5B). We then co-cultured isolated AEC II with E10 or R3/1 cells in a ratio of 2:1 and examined the effects of the activation of $P2X_7R$ on surfactant secretion in this co-culture system. Upon BzATP stimulation, a significant increase in surfactant secretion from AEC II co-cultured with E10 cells was observed (Figure 2.5C). This increase in secretion was blocked when the cells were pre-treated with BBG. There was only a slight increase of surfactant secretion in the BzATP-stimulated AECII-R3/1 co-culture.

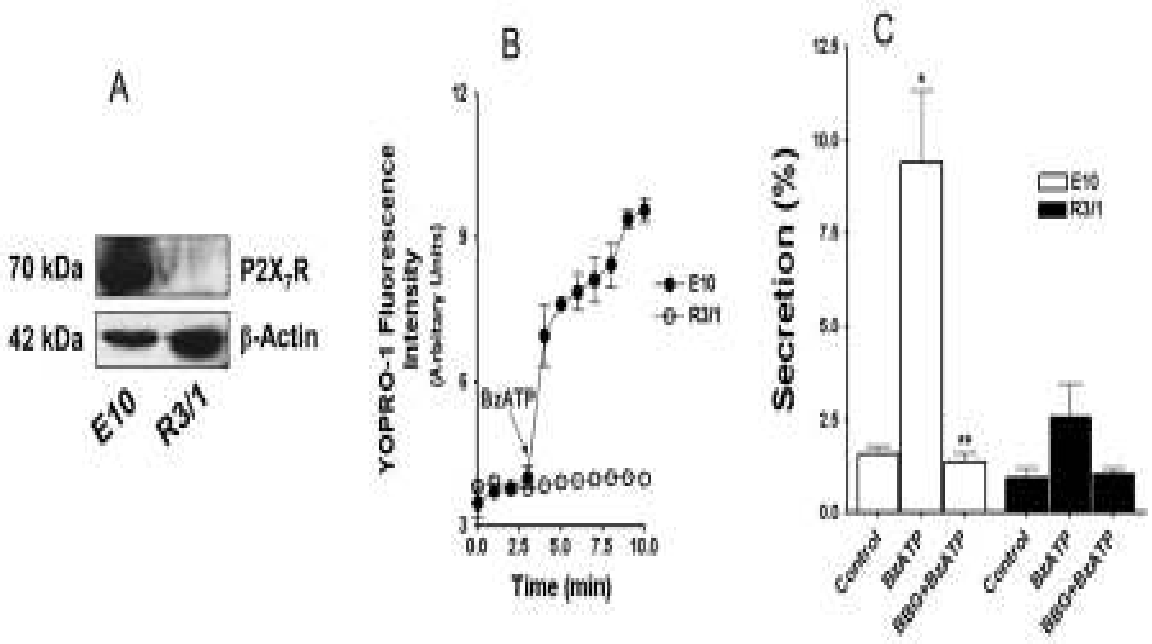

Figure 2.5: E10 cells expressing endogenous P2X7R increase surfactant secretion upon BzATP stimulation.

(A) Expression of endogenous $P2X_7R$ in E10 and R3/1 cells. 30 μg of total cell lysates were probed with anti-$P2X_7R$ and anti-β-actin antibodies. (B) Accumulation of YOPRO-1 dye. E10 and R3/1 cells were incubated with YOPRO-1 for 5 min and fluorescence was monitored. BzATP (200 μM) was added to initiate the reaction. Data are means ± SE (n=2). (C) AEC II were co-cultured with E10 or R3/1 cells overnight. The cells were then pre-treated with 100 nM BBG for 30 min and stimulated with 25 μM BzATP for 2 hrs. PC secretion was measured. The results were corrected by substracting that from E10 or R3/1 cells. Data are means ± SE (n=3 independent cell preparations). *P<0.001 *v.s.* control; **p<0.01 *v.s.* BzATP.

2.4.5 Co-culture of HEK293 cells stably expressing P2X7R with AEC II increases surfactant secretion

If $P2X_7R$ is the mediator for the communication between AEC I and AEC II, any cells that express a functional $P2X_7R$ should be able to replace AEC I. We thus utilized the HEK293 cells stably expressing rat $P2X_7R$ (HEK-$P2X_7R$) (Jiang *et al.*, 2000) for the co-culture experiment. HEK293 cells were used as a control. Western blot analysis showed that HEK-$P2X_7R$ expressed much higher $P2X_7R$ than HEK control cells (Figure 2.6A). The ectopically expressed $P2X_7R$ was functional since BzATP markedly increased YOPRO-1 uptake in HEK-$P2X_7R$ in comparison with HEK (Figure 2.6B). In the co-culture of HEK-$P2X_7R$ and AEC II, BzATP dramatically increased surfactant secretion (Figure 2.6C). This effect was abolished by BBG. No significant stimulation of surfactant secretion was observed in the co-culture of HEK293 and AEC II.

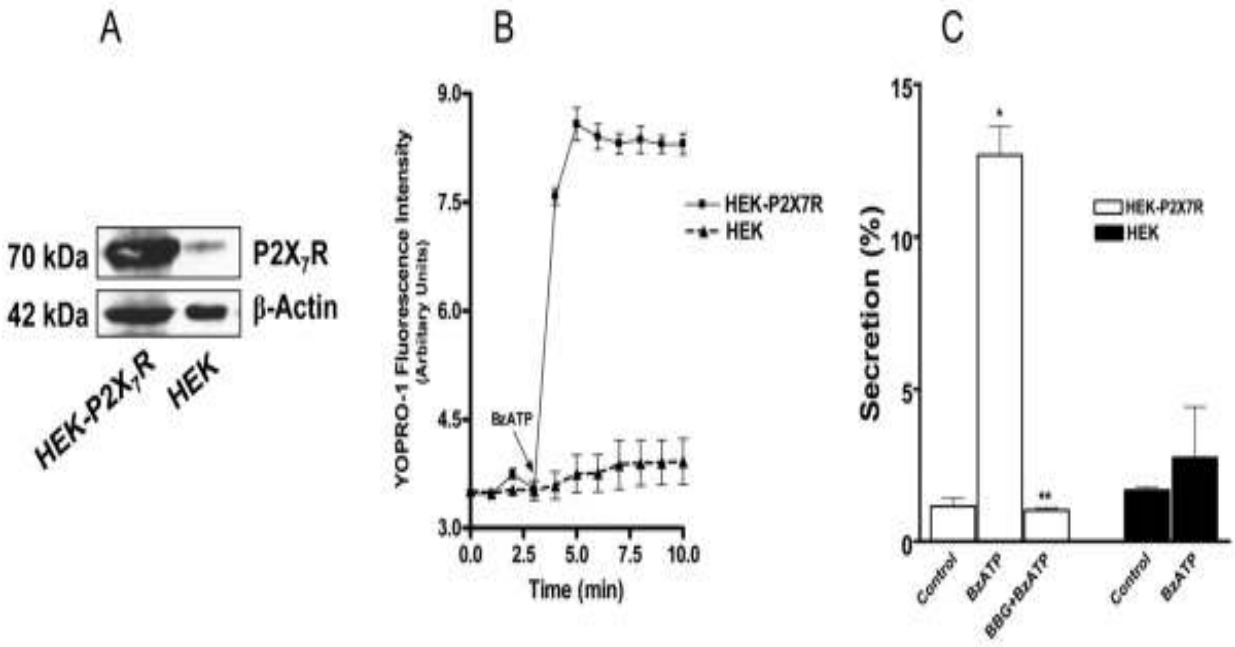

Figure 2.6: HEK293 cells stably expressing rat P2X7R increase surfactant secretion upon BzATP stimulation.

(A) Expression of recombinant rat $P2X_7R$ in HEK-$P2X_7R$ and HEK cells. Cell lysates (5 μg) were probed with anti-$P2X_7R$ and anti-β-actin antibodies. (B) YOPRO-1 accumulation. HEK-$P2X_7R$ and HEK cells were incubated with YOPRO-1 for 5 min and YOPRO-1 fluorescence was monitored. BzATP (200 μM) was added after 200 Sec. Data are means ± SE (n=2). (C) Surfactant secretion. AEC II were co-cultured with HEK-$P2X_7R$ or HEK cells (2:1) overnight. The cells were pre-treated with 100 nM BBG for 30 min and stimulated with 25 μM BzATP for 2 hrs. PC secretion was measured and corrected by substracting that from HEK-$P2X_7R$ or HEK alone. Data are means ± SE (n=3 independent cell preparations). *P<0.001 *v.s*. control; **P<0.001 *v.s*. BzATP.

2.4.6 P2X7R-evoked AEC communication is a paracrine phenomenon

To determine whether $P2X_7R$-mediated increase in surfactant secretion is via a paracrine stimulation or direct cell-cell contact, we examined the effects of conditioned media from the BzATP-stimulated E10 or HEK-$P2X_7R$ cells on surfactant secretion in AEC II. E10 or HEK-$P2X_7R$ cells were incubated with BzATP and ecto-ATPase inhibitor, ARL-67156 for 2 hrs. The conditioned media were then transferred to the recipient AEC II. The conditioned media from both E10 and HEK-$P2X_7R$ dramatically increased surfactant secretion by 9.5- and 7.2-fold, respectively (Figure 2.7A). Under the same conditions, AEC II and HEK293 conditioned media showed no significant increases in surfactant secretion from AEC II.

To further demonstrate that the observed effects are due to $P2X_7R$ receptors, we determined the effects of the conditioned media from the $P2X_7R$ knocked-down E10 cells on surfactant secretion from AEC II. E10 cells were transduced with an adenovirus carrying shRNA targeting to mouse $P2X_7R$ gene, 574-592 [si-X_7 (1)] and 669-689 [si-X_7 (2)]. Both shRNAs resulted in reduction of $P2X_7R$ protein after a 4-day transduction (Figure 2.7B). The stimulatory effects on surfactant secretion by the conditioned media from the $P2X_7R$ knocked-down E10 cells decreased significantly in comparison with that from control virus-treated cells (Figure 2.7C).

To further address the possible gap junction contribution to $P2X_7R$-mediated surfactant secretion, we co-cultured freshly isolated type II cells and E10 cells in a ratio of 2:1. Using a preloading assay (Abraham *et al.*, 2001), we observed gap junction formation between E10 cells and type II cells (Figure 2.7D). BzATP stimulated surfactant

secretion in this co-culture system. However, the gap junction blocker, β-glycyrrhetinic acid had no effect on the BzATP-stimulated secretion (Figure 2.7E).

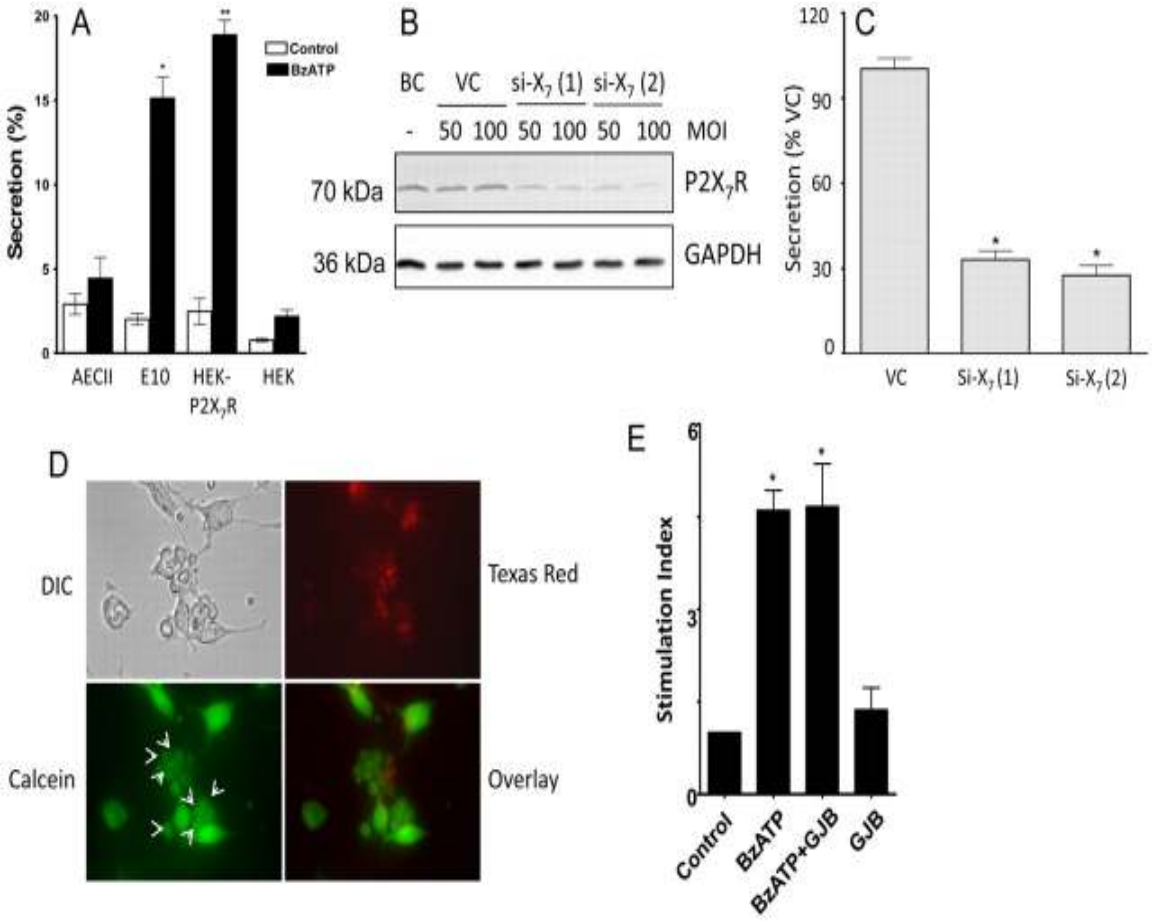

Figure 2.7: Effects of conditioned media from P2X7R-containing cells on surfactant secretion.

(A) AEC II, E10 cells, HEK-P2X$_7$R or HEK were incubated in the presence or absence of 25 μM BzATP for 2 hrs. The conditioned media were collected and transferred to the recipient AEC II and incubated for additional 3 hrs. PC secretion was measured. Data are means ± SE of 3 independent experiments. *$p<0.001$ *v.s.* unstimulated E10 control cells, **$p<0.01$ *v.s.* HEK-P2X$_7$R unstimulated control cells. (B) E10 cells were transduced with an adenovirus carrying irrelevant shRNA (VC), shRNA targeting to 574-592 [si-X$_7$ (1)] or 669-680 [si-X$_7$ (2)] of mouse P2X$_7$R at a MOI of 50 or 100. Un-treated cells were used as a blank control (BC). After 4 days, the cells were collected for Western blot analysis. (C) VC, si-X7 (1) or si-X7 (2)-treated E10 cells (4 days, MOI, 100) were incubated with 25 μM BzATP for 2 hrs. The conditioned media were added to type II cells. After 3 hrs, surfactant secretion was measured. *$P<0.001$ v.s. VC (n=3). (D) Preloading assay for dye transfer. E10 cells were preloaded with Texas Red Dextran and calcein-AM and then co-cultured with freshly isolated AEC II for 5 hrs. The donor E10 cells showed fluorescence in both Texas Red and Calcein. Arrows indicates the acceptor AEC II had only calcein fluorescence, indicating the formation of functional gap junction between E10 cells and type II cells. (E) AEC II and E10 cells were co-cultured (2:1 ratio) for 16 hrs and incubated with the gap junction blocker (GJB), 18-α-glycerrhitinic acid (40 μM) for 30 min. Cells were further stimulated with 25 μM BzATP for additional 2 hrs. Surfactant secretion was measured by monitoring the release of [^{3}H]-labeled PC. The results were expressed as a stimulation index (a ratio of surfactant

secretion in stimulated cells over those in unstimulated cells). *P<0.001 *v.s.* control (n=3).

2.4.7 ATP is responsible for the P2X7R-mediated surfactant secretion

The activation of $P2X_7R$ results in ATP release from rat astrocytes (Suadicani *et al.*, 2006a). We therefore examined whether ATP is released from AEC I upon $P2X_7R$ activation of AEC I and AEC II culture. BzATP was able to evoke a robust induction of ATP release (74 ± 17 nmole/10 μg of total protein) in the heterocellular culture of AEC I and AEC II (Figure 2.8A). This release was blocked by pre-incubating the cells with BBG. BzATP did not cause any changes in ATP levels in bulk media of the AEC II monoculture. To determine whether ATP released from AEC I is responsible for the BzATP-mediated surfactant secretion, we used the nucleotide scavengers, apyrase and adenosine deaminase to remove ATP and measured surfactant secretion in the AEC I and AEC II heterocellular culture. Surfactant secretion caused by BzATP was reduced by apyrase and adenosine deaminase treatment (Figure 2.8B). These results collectively indicate that $P2X_7R$ activation releases ATP from AEC I, which in turn acts on AEC II to stimulate surfactant secretion.

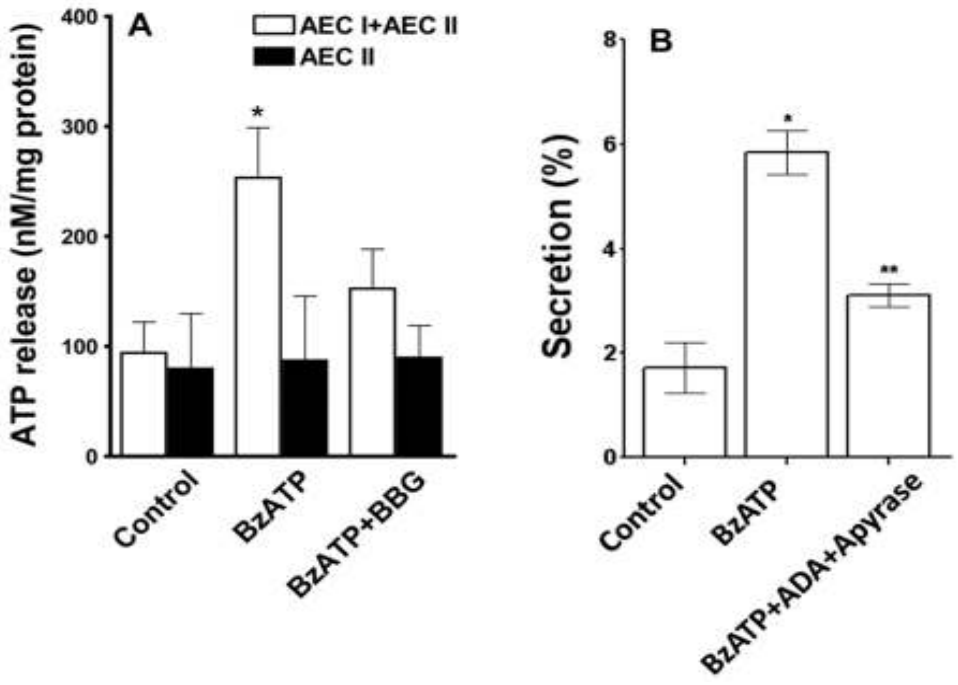

Figure 2.8: P2X7R evokes surfactant secretion through ATP release.

(A) Effect of $P2X_7R$ modulation on ATP release. AEC I and AEC II were pre-incubated with 100 nM BBG for 30 min and stimulated with 25 μM BzATP or 5 min. The BzATP was removed and fresh medium was added and incubated for additional 10 min. At the end of incubation, media were collected and ATP was measured. The results were expressed as nmole ATP secreted into media over 10 min normalized to 10 μg of total protein. Data are means ± SE from 3 independent cell preparations. *P<0.05 *v.s.* control; **P<0.05 *v.s.* BzATP. (B) Effect of removal of ATP on surfactant secretion. AEC I and AEC II were incubated with adenosine deaminase (ADA, 5 U/ml) and apyrase (10 U/ml) for 30 min, followed by stimulation with 25 μM ATP for 2 hrs. Surfactant secretion was measured by monitoring the release of [^{3}H]-labeled PC. Data are means ± SE. n=3-4. *P<0.001 *v.s*. control; **p<0.01 *v.s*. BzATP (Student's *t* test).

2.4.8 P2X7R-mediated surfactant secretion is via the P2Y2R signaling

Since the activation of $P2X_7R$ releases ATP, we determined whether BzATP-mediated surfactant secretion is due to the activation of the $P2Y_2R$ signaling. We measured surfactant secretion after blocking the $P2Y_2R$ signaling in the AEC I and AEC II heterocellular culture with suramin (an $P2Y_2R$ antagonist), BAPTA-AM (an intracellular Ca^{2+} chelator), and staurosporine (an PKC inhibitor). As shown in Figure 2.9, the BzATP-evoked surfactant secretion was significantly inhibited by all of the agents. However, no significant decrease in secretion was observed in the presence of the PKA inhibitor, H89. Taken together, these observations suggest that released ATP from AEC I acts through $P2Y_2R$ and PKC-dependent pathway to promote surfactant secretion in AEC

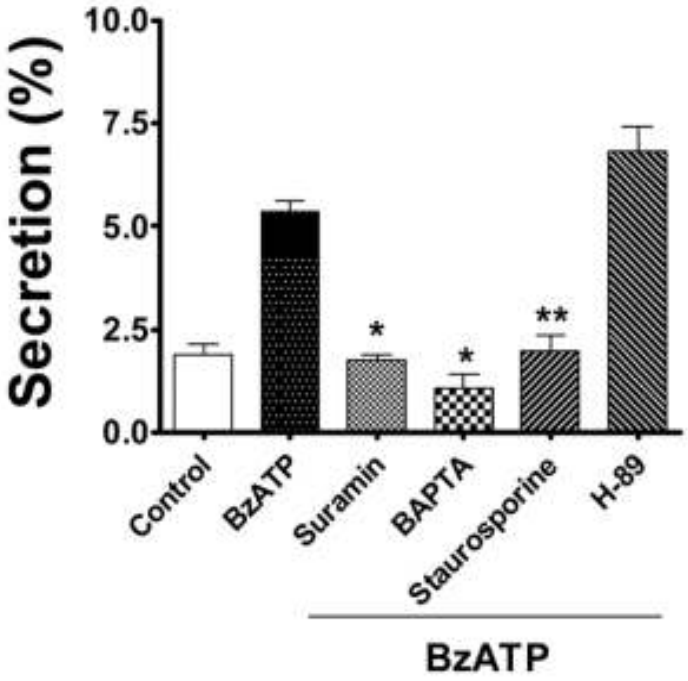

Figure 2.9: Paracrine control of surfactant secretion is mediated via P2Y2R and PKC signaling pathway

Overnight cultured AECI and AECII were pre-treated with suramin (100 μM), BAPTA-AM (50 μM), staurosporine (100 nM) or H89 (50 nM) for 30 min, followed by stimulation with BzATP (25 μM). PC secretion was measured. Data are means ± SE of 3-4 independent experiments. **P<0.001 *v.s*. control; *P<0.001 *v.s*. BzATP.

2.4.9 BzATP was not able to stimulate surfactant secretion in a heterocellular culture of AEC I and AEC II from P2X7R-/- mice.

We isolated mouse AEC I and AEC II from C57BL/6 mice. The cell yield was 8.2 ± 1.3 x 10^6 per mouse. Double labeling with anti-SP-C and T1α antibodies (Fig. 2.10A) revealed 57 ± 1% AEC II and 29 ± 1% AEC I (n=5). Yield, Purity and AECI-AECII ratio were not significantly different between wild-type and $P2X_7R^{-/-}$ mice. The known lung surfactant secretagogues (ATP, PMA and terbutaline) increased surfactant secretion by ~3-fold in the AEC I and AEC II from wild-type mice (Figure 2.10B), which is higher than the isolated mouse AEC II alone (Rice *et al.*, 2002;Gobran and Rooney, 2004;Guttentag *et al.*, 2005). BzATP also stimulated surfactant secretion and BBG blocked the BzATP effects in the wild-type mouse cells. Lung surfactant secretagogues markedly increased surfactant secretion from the $P2X_7R^{-/-}$ AEC I and AEC II heteroculture, indicating that AEC II respond to lung surfactant secretagogues normally. However, the AEC I and AEC II from $P2X_7R^{-/-}$ mice failed to respond to BzATP in surfactant secretion. These results further support our hypothesis that $P2X_7R$ is a mediator for AEC I and AEC II communication in the regulation of surfactant secretion.

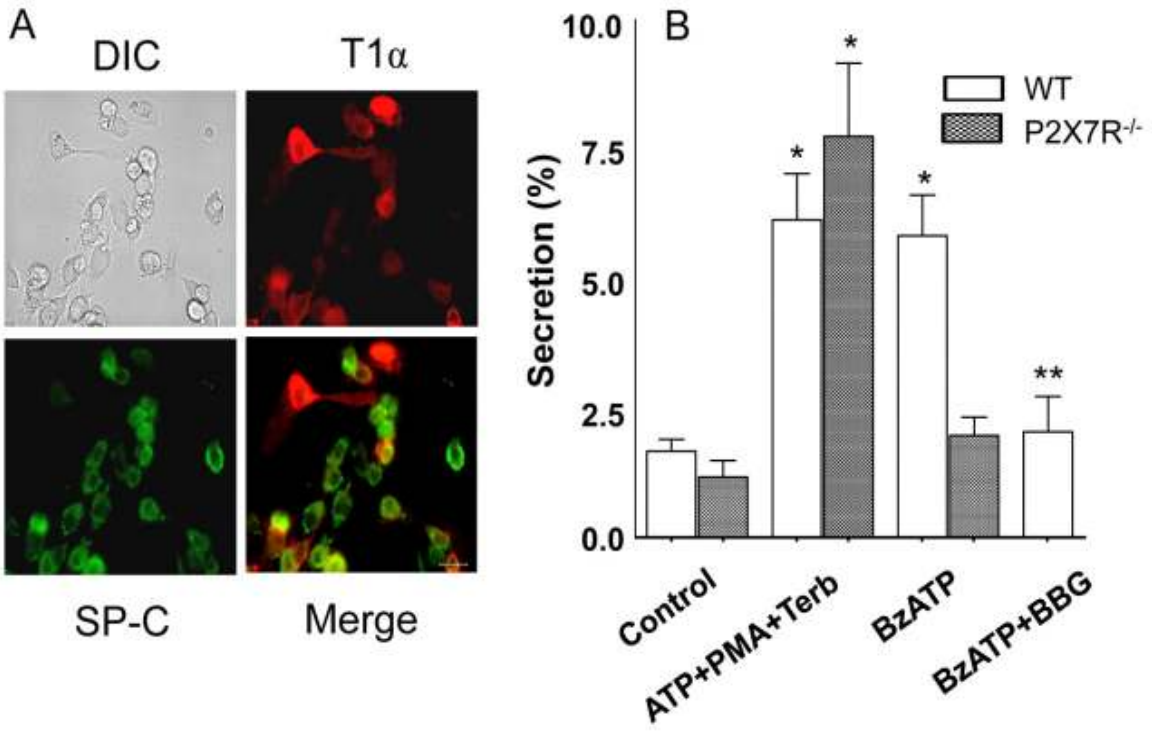

Fig. 2.10: Effect of BzATP on surfactant secretion in type I and type II cell heteroculture from wild-type and P2X7R-/- mice.

(A) Wild-type mouse type I and type II cells were double-labeled with mouse anti-ABCA3 (type II cell, green) and hamster anti-T1α (type I cells, red). Scale bar, 40 μm. (B) The cells were cultured overnight and stimulated for 2 hrs with lung surfactant secretagogues (100 μM ATP, 0.1 μM PMA and 10 μM Terbutaline) or 25 μM BzATP plus or minus 100 nM BBG. Secretion was measured. Data shown are means ± SE (n=3 independent cell preparations). *P<0.001 v.s. control; **P<0.001 v.s. BzATP. WT: wild-type; P2X7R-/-: P2X7R-/- knock-out.

2.4.10 Hyperventilation increases surfactant secretion in wild-type mice, but not in P2X7R-/- mice.

Hyperventilation has been shown to increase surfactant secretion (Oyarzun and Clements, 1978;Hildebran *et al.*, 1981;Nicholas and Barr, 1983), possibly through mechanical stretch (Wirtz and Dobbs, 1990). Since $P2X_7R$ interacts with the proteins that are associated with mechanotransduction (Pavalko *et al.*, 1998;Kim *et al.*, 2001;von *et al.*, 2003), we investigated potential defects in $P2X_7R^{-/-}$ mice in responses to hyperventilation. Western blot analysis confirmed the absence of $P2X_7R$ in the lungs of $P2X_7R^{-/-}$ mice (Figure 2.11A). Real-time PCR analysis revealed that P2X receptors, $P2X_2$ and $P2X_4$ were increased several folds in $P2X_7R^{-/-}$ mice in comparison with wild-type mice (Figure 2.11B). $P2X_1$, $P2X_3$ and $P2X_6$ receptors had a modest increase in the $P2X_7R^{-/-}$ mice. No changes were observed for $P2X_5$ receptors. P2Y receptors were not significantly affected by $P2X_7R$ knock-out (Figure 2.11C). While SP-B increased about 1-fold in the $P2X_7R^{-/-}$ mice, SP-A and SP-C were not changed (Figure 2.11D). T1 α, a type I cell marker was not different between wild-type and $P2X_7R^{-/-}$ mice.

We also compared surfactant lipid secretion in whole animal between wild-type and $P2X_7R^{-/-}$ mice according to the method of Ikegami et al. (Ikegami *et al.*, 2000). There was no significant difference in basal surfactant secretion between wild-type and $P2X_7R^{-/-}$ mice. However, hyperventilation increased surfactant secretion in wild-type mice, but not in $P2X_7R^{-/-}$ mice (Figure 2.11E). No significant changes were observed in total cell counts and total proteins in lavage under all of the conditions (data not shown), indicating that no lung injury occurred

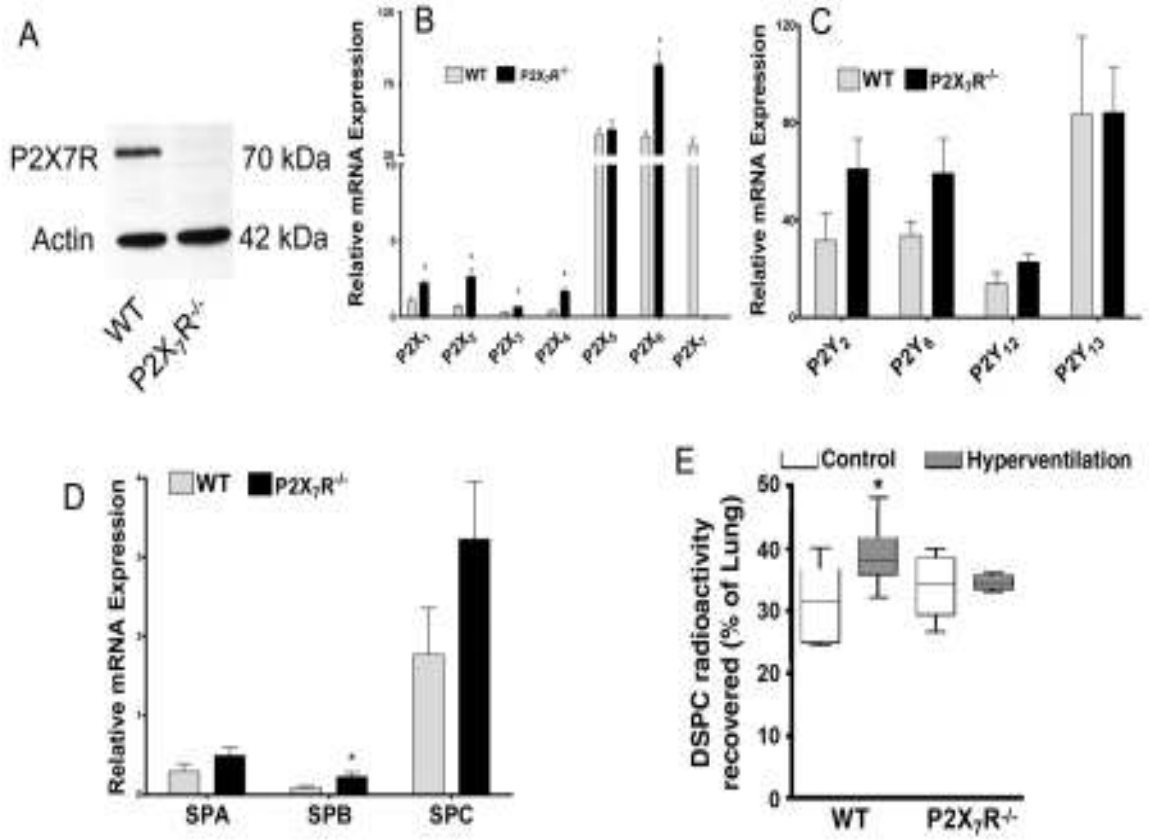

Fig. 2.11 Comparison of Surfactant secretion in P2X7R-/- and wild-type mice.

(A) Western blot of lung tissues from wild-type and $P2X_7R^{-/-}$ mice. (B-D) Real-time PCR analysis of P2X receptors (B), P2Y receptors (C) and Surfactant protein (D). Data were normalized to 18S rRNA. *P<0.05 (n=3 animals, assayed in duplicate). (E) Surfactant secretion. Mice were intraperitoneally injected 0.5 μCi/gm [^{3}H] choline and hyperventilated for 30 min. Lipids in lavage and lung tissue were extracted and saturated PC isolated. Surfactant secretion was calculated as a percentage of dpm in larvage over dpm in lavage and tissue. *P<0.05. Animal number; wild-type 10; wild-type hyperventilation 8; $P2X_7R^{-/-}$ 5; $P2X_7R^{-/-}$ hyperventilation 4.

Table 2. 2 Real-time PCR primers

Gene	Forward primer sequence	Reverse primer sequence
$P2X_1$	TCAAGGACATTGTGCAGAGAAC	CAGTTGCCTGTGCGAATACCT
$P2X_2$	GCGTTCTGGGACTACGAGAC	ACGTACCACACGAAGTAAAGC
$P2X_3$	AAAGCTGGACCATTGGGATCA	CGTGTCCCGCACTTGGTAG
$P2X_4$	CTCGGGTCCTTCCTGTTCG	GTTTCCTGGTAGCCCTTTTCC
$P2X_5$	AGGGGGTGGCCTATACCAAC	GGTTAGGAGTCACGATCAGGTT
$P2X_6$	GTTAAGGAGCTGGAGAACCG	AGGATGCTCTGGACATCTGC
$P2X_7$	TGCATCACCACCTCCAAGCTCTTCCAT	CACCAGCAAGGGATCCTGGTAAAGC
$P2Y_2$	TGTGGCCAATCCTATTTCAATTT	CCACGAGCCCAGAAAAAAGA
$P2Y_6$	TGACCCGTTCCGCTGTGTAC	GCGCTGGAAGCTAATGCAGG
$P2Y_{12}$	ATGGATATGCCTGGTGTCAACA	AGCAATGGGAAGAGAACCTGG
$P2Y_{13}$	TGGGTGTTCGTCCACATCC	GCAAGGTGTGAGTCGGAAAG
SP-A	GAGGAGCTTCAGACTGCACTC	AGACTTTATCCCCCACTGACAG
SP-B	CTGCTTCCTACCCTCTGCTG	CTTGGCACAGGTCATTAGCTC
SP-C	ATGGACATGAGTAGCAAAGAGGT	CACGATGAGAAGGCGTTTGAG
18S	ATTGCTCAATCTCGGGTGGCTG	CGTTCTTAGTTGGTGGAGCGATTTG

Hyperventilation causes mechanical stretch and alkalosis. To determine whether there is a difference in alkalosis between wild-type and $P2X_7R^{-/-}$ mice, we performed blood gas analysis. As shown in Table 2.3, hyperventilation did not causes significant changes in arterial blood oxygen (PaO_2) level in wild-type and $P2X_7R^{-/-}$ mice. However, hyperventilation increased arterial blood pH and decreased arterial blood CO_2 ($PaCO_2$) in both wild-type and $P2X_7R^{-/-}$ mice. These results indicate that there were no significant differences in hyperventilation-induced alkalosis between wild-type and $P2X_7R^{-/-}$ mice. Data are Means ± S.E. (n=3 animals), *$p < 0.05$ *v.s.* corresponding non-ventilated control, One way ANOVA , followed by Tukey's multiple comparison.

Table 2.3 Arterial blood gas analysis

	Wild-type		**$P2X_7R^{-/-}$**	
	Non-ventilated	Hyperventilated	Non-ventilated	Hyperventilated
P^H	7.46 ± 0.02	7.65 ± 0.16*	7.44 ± 0.05	7.65 ± 0.02*
$PaCO_2$	33.56 ± 4.71	19.97 ± 1.53*	32.96 ± 3.45	15.45 ± 1.60
PaO_2	146.82 ± 1.07	155.78 ± 1.53	153.08 ± 3.70	158.14 ± 0.88

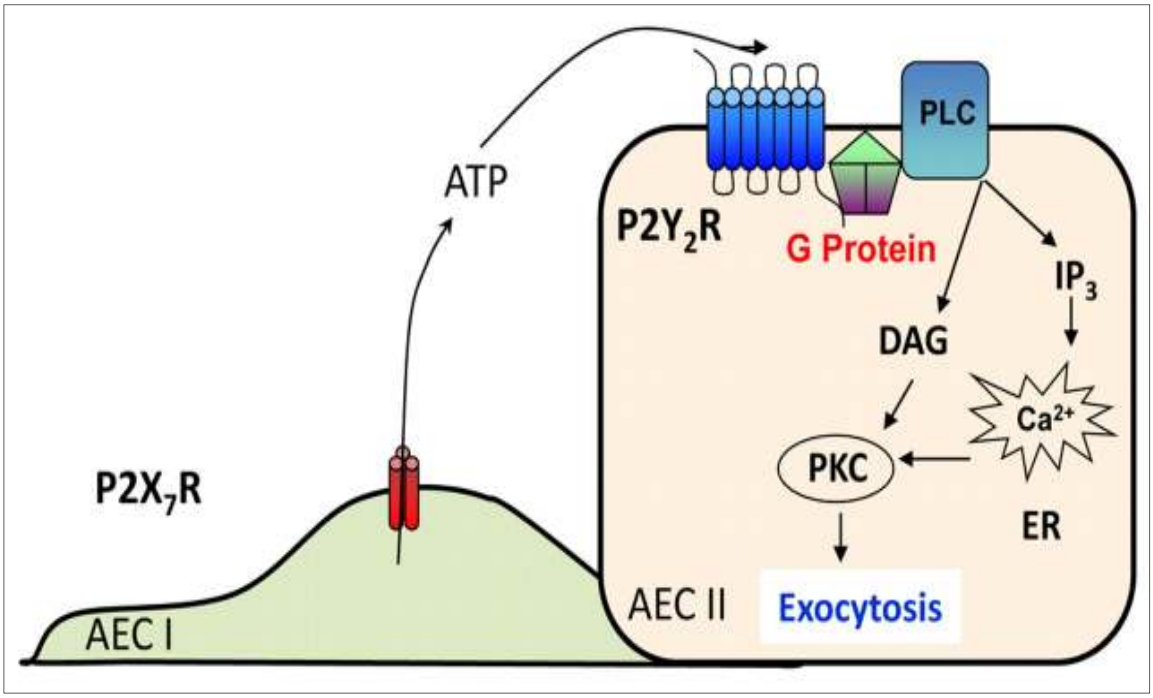

Figure 2.12: A proposed model for $P2X_7R$-mdiated surfactant secretion.

2.5 Discussion

Over the past few decades, substantial insights into mechanisms of surfactant synthesis and its release have been gained. However, the steps that control the regulation of this multifaceted event under physiological circumstances remain poorly understood. AEC I has been suggested as a potential contributor to the regulation of surfactant secretion in AEC II (Ashino *et al.*, 2000;Isakson *et al.*, 2003;Patel *et al.*, 2005). However, what factors in AEC I mediate AEC I and AEC II communication are unknown. In the present study, we report that $P2X_7R$ in AEC I is responsible for the communication between AEC I and AEC II in the regulation of surfactant secretion. The results from this work shows that upon $P2X_7R$ activation, AEC I releases ATP, which acts on AEC II in a paracrine manner to trigger surfactant release via the $P2Y_2R$ and PKC pathway.

The ensuing effort to understand the function of AEC I as a possible partner of AEC II largely depends upon the cell culture models. Due to the difficulty in isolating AEC I in high purity and yield, AEC I-like cells trans-differentiated from freshly isolated AEC II have been used to study the communication between AEC I and AEC II (Isakson *et al.*, 2003;Patel *et al.*, 2005). These AEC I-like cells may not represent the *in vivo* AEC I phenotype since DNA microarray analysis reveals a different set of gene expression between isolated AEC I and the AEC I-like cells (Gonzalez *et al.*, 2005). In this study, we developed a heterocellular culture of AEC I and AEC II directly isolated from rat lungs. This system has a 1:2 ratio of AEC I and AEC II numbers that is similar to that of the *in vivo* lungs. Furthermore, the model maintains AEC I and AEC II phenotypes including cell marker expression, functional receptors ($P2X_7R$ and $P2Y_2R$) and lung surfactant secretion.

Several lines of evidence support that the activation of $P2X_7R$ couples AEC I–AEC II for the regulation of surfactant secretion. First of all, BzATP, an agonist of $P2X_7R$, increased surfactant secretion and fusion pore formation in a hetercellular culture of AEC I and AEC II. The increase in surfactant secretion is due to specific activation of $P2X_7R$ in AEC I: (i) $P2X_7R$ is specifically expressed in AEC I, but not AEC II in intact lung tissue (Chen *et al.*, 2004b) and in our heterocellular culture of AEC I and AEC II; (ii) BzATP specifically activated $P2X_7R$ in AEC I as determined by the YOPRO-1 dye uptake; (iii) BzATP did not affect surfactant secretion in AEC II alone, indicating that BzATP does not activate other receptors in AEC II; (iv) BBG, an antagonist of $P2X_7R$ blocked the BzATP-induced surfactant secretion. The specificity of BBG was demonstrated by its failure to inhibit other lung surfactant secretagogue-stimulated surfactant secretion including ATP, terbutaline and PMA in the hetercellular culture of AEC I and AEC II; (v) BzATP had no effects on surfactant secretion from AEC I and AEC II isolated from $P2X_7R^{-/-}$ mice.

Another evidence for $P2X_7R$ as a mediator for the increase in surfactant secretion comes from co-culture of $P2X_7R$-expressing cells with AEC II. Two lung cell lines, E10 and R3/1 cells have AEC I properties (Koslowski *et al.*, 2004;Kathuria *et al.*, 2007). However, E10 cells express a high level of $P2X_7R$, while R3/1 cells have little $P2X_7R$ (Barth *et al.*, 2007). Thus, these cell lines provide a tool to investigate the effect of $P2X_7R$ on surfactant secretion in AEC II. Co-culture of E10 cells with AEC II results in a robust increase in surfactant secretion in response to BzATP stimulation, which was abolished in the presence of BBG. This increase in surfactant secretion was not observed when R3/1 cells were co-cultured with AEC II. E10 and R3/1 cells were established by a

clonal outgrowth of adult mouse lung tissue and explant-replica of the E20 fetal lungs of Han-Wistar rats, respectively. It is possible that the observed differences between E10 and R3/1 cells are due to other properties of the cell lines rather than $P2X_7R$. To eliminate this possibility, rat $P2X_7R$ was overepxressed in HEK 293 cells that do not express endogenous $P2X_7R$ and are not related to AEC I. The HEK 293 cells stably expressing $P2X_7R$, but not the control HEK 293 cells, when co-cultured with AEC II, elicited a marked increase in surfactant secretion upon BzATP stimulation. Furthermore, knock-down of $P2X_7R$ in E10 cells abolished its stimulatory effects on surfactant secretion. These results suggest that $P2X_7R$ is one of the key components in AEC I that regulates surfactant secretion.

The communication between AEC I and AEC II can be accomplished via two major routes: gap junction and paracrine communication (Koval, 2002). Gap junction channels are formed by the assembly of two hemichannels on two cells. Each hemichannel is composed of six connexins, a large family of transmembrane proteins. A gap junction channel allows the direct transmission of small signaling molecules and metabolites from one cell to another. AEC I and AEC II express different sets of connexins (Lee *et al.*, 1997;Abraham *et al.*, 1999;Isakson *et al.*, 2003). Functional and heterotypic gap junction channels have been demonstrated between AEC I and AEC II, which involves at least one of the connexin, Cx43 (Abraham *et al.*, 2001;Isakson *et al.*, 2003). In a heterocellular culture of AEC I-like and AEC II-like cells, mechanical stimulation of AEC I leads to Ca^{2+} wave propagation to AEC II via gap junctions (Isakson *et al.*, 2001;Isakson *et al.*, 2003). *In situ* fluorescence microscopic analysis of isolated perfused lungs reveals that a brief lung expansion evokes Ca^{2+} oscillations

initiated on AEC I which are transmitted to AEC II by gap junctions (Ashino *et al.*, 2000). Paracrine cell-to-cell communication involves the release of soluble factors from one type of cells and the action on another. Stretch triggers ATP release from AEC I-like cells, which stimulate surfactant secretion when co-cultured with freshly isolated type II cells (Patel *et al.*, 2005). However, in a heterocellular culture of AEC I-like and AEC II-like cells, AEC II-like cells transmit Ca^{2+} signal to other cells via ATP release (Isakson *et al.*, 2003).

What are the mechanisms for $P2X_7R$-mediated AEC I and AEC II communication? We can rule out cell-to-cell contact and/or gap junction as a major mechanism since the gap junction blocker, β-glycyrrhetinic acid did not block BzATP-stimulated surfactant secretion. Furthermore, the conditioned media from the BzATP-stimulated E10 or HEK-$P2X_7R$ cells had comparable stimulation of surfactant secretion as that in the co-culture of these cells with AEC II. Thus, the release of soluble factors from AEC I upon the activation of $P2X_7R$ is likely responsible for AEC I and AEC II communication. One such factor is ATP. Indeed, $P2X_7R$ activation in the heterocellular culture of AEC I and AEC II released ATP in the bulk milieu, which was blocked by BBG. This effect was completely absent in AEC II monoculture. There is evidence showing that $P2X_7R$ mediates ATP release in other cell systems (Arcuino *et al.*, 2002;Pellegatti *et al.*, 2005;Suadicani *et al.*, 2006b). The removal of ATP from the media nucleotide scavengers significantly inhibited the BzATP-stimulated surfactant secretion, further supporting that ATP released from AEC I upon the activation of $P2X_7R$ functions as a soluble mediator to enhance surfactant secretion.

Regulated surfactant secretion in AEC II responds to extracellular ATP stimulation through $P2Y_2R$ (Linke *et al.*, 1997). The activation of $P2Y_2R$ in AEC II stimulates G-protein coupled phospholipase C, resulting in the generation of diacylglycerol and IP_3 and the activation of PKC in a Ca^{2+}-dependent manner (Chander *et al.*, 1995). AEC II express several PKC isoforms (PKC- α, β1, β2, η, δ, μ and ξ) that potentiate protein phosphorylation and final fusion events (Gobran and Rooney, 1999). The blocking of $P2Y_2R$ by suramin, chelation of intracellular Ca^{2+} by BAPTA, and inhibition of PKC by staurosporine all abolished the BzATP-evoked increase in surfactant secretion in heterocellular culture of AEC I and AEC II. ATP can be degraded into adenosine (Fields and Burnstock, 2006), which can stimulate adenosine A2 receptors, activate PKA and increase surfactant secretion (Griese *et al.*, 1991). However, the increase in surfactant secretion caused by BzATP was unaffected by the PKA inhibitor, H89, indicating that the PKA pathway is not involved in the $P2X_7R$-mediated surfactant secretion. These results suggest that ATP released from AEC I upon the stimulation of $P2X_7R$ activates $P2Y_2R$ signaling in AEC II and thus increases surfactant secretion. Our results demonstrate for the first time purinergic signaling coupling between AEC I and AEC II for surfactant secretion regulation.

The $P2X_7R^{-/-}$ mice are viable and fertile (Solle *et al.*, 2001). However, some defects were observed. For example, although peritoneal macrophages from $P2X_7R^{-/-}$ and wild-type mice produce similar amounts of pro-IL-1β after LPS challenge, the macrophages from $P2X_7R^{-/-}$mice do not generate mature IL-1β in response to ATP (Solle *et al.*, 2001). These mice also have a decreased periosteal bone formation and an increased resorption in trabecular bone tissue (Ke *et al.*, 2003). The lack of $P2X_7R$ results

in a reduction of mechanical loading-stimulated bone growth (Li *et al.*, 2005). However, no information on the lung phenotype is available in these mice. Our present studies showed that BzATP did not stimulate surfactant secretion in AEC I and AEC II isolated from $P2X_7R^{-/-}$ mice. Furthermore, when they were challenged with hyperventilation, wild-type mice showed an enhanced surfactant secretion, but $P2X_7R^{-/-}$ mice did not. Hyperventilation is known to increase surfactant secretion (Oyarzun and Clements, 1978;Hildebran *et al.*, 1981;Nicholas and Barr, 1983), likely via mechanical stretch (Wirtz and Dobbs, 1990). $P2X_7R$ is involved in mechanotransduction (Pavalko *et al.*, 1998;Kim *et al.*, 2001;von *et al.*, 2003). Thus, the lack of response to hyperventilation in $P2X_7R^{-/-}$ mice may be due to a defect in sensing mechanical stretch in type I cells via $P2X_7R$.

It has been suggested that ATP may play a role in asthma and chronic obstructive pulmonary diseases (COPD) (Adriaensen and Timmermans, 2004). Adenosine, a metabolite of ATP in alveolar lining fluid increases 2-3 fold in asthmatics and non-symptomatic smokers in comparison with control subjects (60-70 μM). There is dys-regulation of surfactant homeostasis in infant and acute respiratory distress syndrome (Gunther *et al.*, 2001). Therefore, our finding of $P2X_7R$-mediated ATP signaling transduction and surfactant secretion regulation adds a novel and attractive therapeutic intervention to control alveolar surfactant pool by modulating the endogenous surfactant system, eventually resulting in the treatment of pulmonary diseases with surfactant defects.

In conclusion, our results demonstrate that the activation of $P2X_7R$ possibly by mechanical stress releases ATP from AEC I and paracrinacally stimulates surfactant

secretion from AEC II via the $P2Y_2R$ and PKC-mediated signaling pathway (Figure 2.12). This finding reveals a novel function of $P2X_7R$ in the lung by which AEC I communicates with AEC II via $P2X_7R$, contributing to fine tuning of surfactant balance. The current studies also reinforce the idea that AEC I is not a simple barrier for gas exchange, but functional cells in the lung. Thus, it is imperative to further study $P2X_7R$ biology in alveolar epithelial cells in order to gain a better understanding of the cellular and molecular events of surfactant homeostasis, cell-cell communication and the progression of lung diseases.

2.6. References

1. Abraham,V., Chou,M.L., DeBolt,K.M., and Koval,M. (1999). Phenotypic control of gap junctional communication by cultured alveolar epithelial cells. Am J Physiol *276*, L825-L834.

2. Abraham,V., Chou,M.L., George,P., Pooler,P., Zaman,A., Savani,R.C., and Koval,M. (2001). Heterocellular gap junctional communication between alveolar epithelial cells. Am. J. Physiol Lung Cell Mol. Physiol *280*, L1085-L1093.

3. Adriaensen,D. and Timmermans,J.P. (2004). Purinergic signalling in the lung: important in asthma and COPD? Curr. Opin. Pharmacol *4*, 207-214.

4. Andreeva,A.V., Kutuzov,M.A., and Voyno-Yasenetskaya,T.A. (2007). Regulation of Surfactant Secretion in Alveolar Type II cells. Am. J Physiol Lung Cell Mol. Physiol *293*, L259-L271.

5. Arcuino,G., Lin,J.H., Takano,T., Liu,C., Jiang,L., Gao,Q., Kang,J., and Nedergaard,M. (2002). Intercellular calcium signaling mediated by point-source burst release of ATP. Proc Natl Acad Sci U S A. *99*, 9840-9845.

6. Ashino,Y., Ying,X., Dobbs,L.G., and Bhattacharya,J. (2000). [Ca(2+)](i) oscillations regulate type II cell exocytosis in the pulmonary alveolus. Am. J. Physiol Lung Cell Mol. Physiol *279*, L5-13.

7. Baraldi,P.G., Di,V.F., and Romagnoli,R. (2004). Agonists and antagonists acting at P2X7 receptor. Curr. Top. Med. Chem. *4*, 1707-1717.

8. Barth,K., Weinhold,K., Guenther,A., Young,M.T., Schnittler,H., and Kasper,M. (2007). Caveolin-1 influences P2X7 receptor expression and localization in mouse lung alveolar epithelial cells. FEBS J. *274*, 3021-3033.

9. Bortnick,A.E., Favari,E., Tao,J.Q., Francone,O.L., Reilly,M., Zhang,Y., Rothblat,G.H., and Bates,S.R. (2003). Identification and characterization of rodent ABCA1 in isolated type II pneumocytes. Am. J. Physiol Lung Cell Mol. Physiol *285*, L869-L878.
10. Chander,A., Sen,N., Wu,A.M., and Spitzer,A.R. (1995). Protein kinase C in ATP regulation of lung surfactant secretion in type II cells. Am. J. Physiol. *268*, L108-L116.

11. Chen,J., Chen,Z., Chintagari,N.R., Bhaskaran,M., Jin,N., Narasaraju,T., and Liu,L. (2006). Alveolar type I cells protect rat lung epithelium from oxidative injury. J Physiol *572*, 625-638.

12. Chen,J., Chen,Z., Narasaraju,T., Jin,N., and Liu,L. (2004a). Isolation of highly pure alveolar epithelial type I and type II cells from rat lungs. Lab Invest. *84*, 727-735.

13. Chen,L. and Brosnan,C.F. (2006). Exacerbation of experimental autoimmune encephalomyelitis in P2X7R-/- mice: evidence for loss of apoptotic activity in lymphocytes. J. Immunol. *176*, 3115-3126.

14. Chen,Z., Jin,N., Narasaraju,T., Chen,J., McFarland,L.R., Scott,M., and Liu,L. (2004b). Identification of two novel markers for alveolar epithelial type I and II cells. Biochem. Biophys. Res. Commun. *319*, 774-780.

15. Chintagari,N.R., Jin,N., Wang,P., Narasaraju,T.A., Chen,J., and Liu,L. (2006). Effect of cholesterol depletion on exocytosis of alveolar type II cells. Am J Respir. Cell Mol Biol. *34*, 677-687.

16. Collo,G., Neidhart,S., Kawashima,E., Kosco-Vilbois,M., North,R.A., and Buell,G. (1997). Tissue distribution of the P2X7 receptor. Neuropharmacology. *36*, 1277-1283.

17. Dobbs,L.G. and Mason,R.J. (1979). Pulmonary alveolar type II cells isolated from rats. Release of phosphatidylcholine in response to beta-adrenergic stimulation. J Clin Invest *63*, 378-387.

18. Ferrari,D., Pizzirani,C., Adinolfi,E., Lemoli,R.M., Curti,A., Idzko,M., Panther,E., and Di Virgilio,F. (2006). The P2X7 receptor: a key player in IL-1 processing and release. J. Immunol. *176*, 3877-3883.

19. Fields,R.D. and Burnstock,G. (2006). Purinergic signalling in neuron-glia interactions. Nat. Rev. Neurosci. *7*, 423-436.

20. Gobran,L.I. and Rooney,S.A. (1999). Surfactant secretagogue activation of protein kinase C isoforms in cultured rat type II cells. Am J Physiol *277*, L251-L256.

21. Gobran,L.I. and Rooney,S.A. (2004). Pulmonary surfactant secretion in briefly cultured mouse type II cells. Am. J. Physiol Lung Cell Mol. Physiol *286*, L331-L336.

22. Gonzalez,R., Yang,Y.H., Griffin,C., Allen,L., Tigue,Z., and Dobbs,L. (2005). Freshly-isolated rat alveolar type I cells, type II cells, and cultured type II cells have distinct molecular phenotypes. Am J Physiol Lung Cell Mol Physiol *288*, L179-L189.

23. Gou,D., Weng,T., Wang,Y., Wang,Z., Zhang,H., Gao,L., Chen,Z., Wang,P., and Liu,L. (2007). A novel approach for the construction of multiple shRNA expression vectors. J Gene Med. *9*, 751-763.

24. Griese,M., Gobran,L.I., and Rooney,S.A. (1991). A2 and P2 purine receptor interactions and surfactant secretion in primary cultures of type II cells. Am. J. Physiol. *261*, L140-7.

25. Gu,B.J. and Wiley,J.S. (2006). Rapid ATP-induced release of matrix metalloproteinase 9 is mediated by the P2X7 receptor. Blood *107*, 4946-4953.

26. Gunther,A., Ruppert,C., Schmidt,R., Markart,P., Grimminger,F., Walmrath,D., and Seeger,W. (2001). Surfactant alteration and replacement in acute respiratory distress syndrome. Respir. Res. *2*, 353-364.

27. Guttentag,S.H., Akhtar,A., Tao,J.Q., Atochina,E., Rusiniak,M.E., Swank,R.T., and Bates,S.R. (2005). Defective surfactant secretion in a mouse model of Hermansky-Pudlak syndrome. Am. J. Respir. Cell Mol. Biol. *33*, 14-21.

28. Haller,T., Dietl,P., Pfaller,K., Frick,M., Mair,N., Paulmichl,M., Hess,M.W., Furst,J., and Maly,K. (2001). Fusion pore expansion is a slow, discontinuous, and Ca2+-dependent process regulating secretion from alveolar type II cells. J Cell Biol *155*, 279-289.

29. Hildebran,J.N., Goerke,J., and Clements,J.A. (1981). Surfactant release in excised rat lung is stimulated by air inflation. J. Appl. Physiol. *51*, 905-910.

30. Hughes,J.P., Hatcher,J.P., and Chessell,I.P. (2007). The role of P2X(7) in pain and inflammation. Purinergic. Signal. *3*, 163-169.

31. Ichimura,H., Parthasarathi,K., Lindert,J., and Bhattacharya,J. (2006). Lung surfactant secretion by interalveolar Ca2+ signaling. Am J Physiol Lung Cell Mol Physiol *291*, L596-L601.

32. Ikegami,M., Whitsett,J.A., Jobe,A., Ross,G., Fisher,J., and Korfhagen,T. (2000). Surfactant metabolism in SP-D gene-targeted mice. Am. J. Physiol Lung Cell Mol. Physiol *279*, L468-L476.

33. Isakson,B.E., Evans,W.H., and Boitano,S. (2001). Intercellular Ca2+ signaling in alveolar epithelial cells through gap junctions and by extracellular ATP. Am. J. Physiol Lung Cell Mol. Physiol. *280*, L221-L228.

34. Isakson,B.E., Seedorf,G.J., Lubman,R.L., Evans,W.H., and Boitano,S. (2003). Cell-cell communication in heterocellular cultures of alveolar epithelial cells. Am. J. Respir. Cell Mol. Biol. *29*, 552-561.

35. Jiang,L.H., Mackenzie,A.B., North,R.A., and Surprenant,A. (2000). Brilliant blue G selectively blocks ATP-gated rat P2X(7) receptors. Mol. Pharmacol. *58*, 82-88.

36. Jin,N., Kolliputi,N., Gou,D., Weng,T., and Liu,L. (2006). A novel function of ionotropic gamma -aminobutyric acid receptors involving alveolar fluid homeostasis. J Biol. Chem. *281*, 36012-36020.

37. Johnson,M.D., Bao,H.F., Helms,M.N., Chen,X.J., Tigue,Z., Jain,L., Dobbs,L.G., and Eaton,D.C. (2006). Functional ion channels in pulmonary alveolar type I cells support a role for type I cells in lung ion transport. Proc. Natl. Acad. Sci. U. S. A. *103*, 4964-4969.

38. Jun,D.J. *et al.* (2007). Extracellular ATP mediates necrotic cell swelling in SN4741 dopaminergic neurons through P2X7 receptors. J Biol. Chem. *282*, 37350-37358.

39. Kathuria,H., Cao,Y., Hinds,A., Ramirez,M.I., and Williams,M.C. (2007). ERM is expressed by alveolar epithelial cells in adult mouse lung and regulates caveolin-1 transcription in mouse lung epithelial cell lines. J. Cell Biochem. *102*, 13-27.

40. Ke,H.Z. *et al.* (2003). Deletion of the P2X7 nucleotide receptor reveals its regulatory roles in bone formation and resorption. Mol. Endocrinol. *17*, 1356-1367.

41. Kim,M., Jiang,L.H., Wilson,H.L., North,R.A., and Surprenant,A. (2001). Proteomic and functional evidence for a P2X7 receptor signalling complex. EMBO J. *20*, 6347-6358.

42. Koslowski,R., Barth,K., Augstein,A., Tschernig,T., Bargsten,G., Aufderheide,M., and Kasper,M. (2004). A new rat type I-like alveolar epithelial cell line R3/1: bleomycin effects on caveolin expression. Histochem. Cell Biol. *121*, 509-519.

43. Koval,M. (2002). Sharing signals: connecting lung epithelial cells with gap junction channels. Am. J. Physiol Lung Cell Mol. Physiol *283*, L875-L893.

44. Lee,Y.C., Yellowley,C.E., Li,Z., Donahue,H.J., and Rannels,D.E. (1997). Expression of functional gap junctions in cultured pulmonary alveolar epithelial cells. Am. J. Physiol. *272*, L1105-L1114.

45. Li,J., Liu,D., Ke,H.Z., Duncan,R.L., and Turner,C.H. (2005). The P2X7 nucleotide receptor mediates skeletal mechanotransduction. J. Biol. Chem. *280*, 42952-42959.

46. Linke,M.J., Burton,F.M., Fiedeldey,D.T., and Rice,W.R. (1997). Surfactant phospholipid secretion from rat alveolar type II cells: possible role of PKC isozymes. Am J Physiol *272*, L171-L177.

47. Lu,H., Burns,D., Garnier,P., Wei,G., Zhu,K., and Ying,W. (2007). P2X7 receptors mediate NADH transport across the plasma membranes of astrocytes. Biochem. Biophys. Res. Commun. *362*, 946-950.

48. Mason,R.J., Nellenbogen,J., and Clements,J.A. (1976). Isolation of disaturated phosphatidylcholine with osmium tetroxide. J. Lipid Res. *17*, 281-284.

49. Nicholas,T.E. and Barr,H.A. (1983). The release of surfactant in rat lung by brief periods of hyperventilation. Respir. Physiol. *52*, 69-83.

50. North,R.A. (2002). Molecular physiology of P2X receptors. Physiol Rev. *82*, 1013-1067.

51. Oyarzun,M.J. and Clements,J.A. (1978). Control of lung surfactant by ventilation, adrenergic mediators, and prostaglandins in the rabbit. Am. Rev. Respir. Dis. *117*, 879-891.

52. Parvathenani,L.K., Tertyshnikova,S., Greco,C.R., Roberts,S.B., Robertson,B., and Posmantur,R. (2003). P2X7 mediates superoxide production in primary microglia and is up-regulated in a transgenic mouse model of Alzheimer's disease. J Biol. Chem. *278*, 13309-13317.

53. Patel,A.S., Reigada,D., Mitchell,C.H., Bates,S.R., Margulies,S.S., and Koval,M. (2005). Paracrine stimulation of surfactant secretion by extracellular ATP in response to mechanical deformation. Am. J. Physiol Lung Cell Mol. Physiol. *289*, L489-L496.

54. Pavalko,F.M., Chen,N.X., Turner,C.H., Burr,D.B., Atkinson,S., Hsieh,Y.F., Qiu,J., and Duncan,R.L. (1998). Fluid shear-induced mechanical signaling in MC3T3-E1 osteoblasts requires cytoskeleton-integrin interactions. Am. J. Physiol *275*, C1591-C1601.

55. Pellegatti,P., Falzoni,S., Pinton,P., Rizzuto,R., and Di Virgilio,F. (2005). A novel recombinant plasma membrane-targeted luciferase reveals a new pathway for ATP secretion. Mol. Biol. Cell. *16*, 3659-3665.

56. Placido,R., Auricchio,G., Falzoni,S., Battistini,L., Colizzi,V., Brunetti,E., Di Virgilio,F., and Mancino,G. (2006). P2X(7) purinergic receptors and extracellular ATP mediate apoptosis of human monocytes/macrophages infected with Mycobacterium tuberculosis reducing the intracellular bacterial viability. Cell Immunol. *244*, 10-18.

57. Rassendren,F., Buell,G.N., Virginio,C., Collo,G., North,R.A., and Surprenant,A. (1997). The permeabilizing ATP receptor, P2X7. Cloning and expression of a human cDNA. J. Biol. Chem. *272*, 5482-5486.

58. Rice,W.R., Conkright,J.J., Na,C.L., Ikegami,M., Shannon,J.M., and Weaver,T.E. (2002). Maintenance of the mouse type II cell phenotype in vitro. Am J Physiol Lung Cell Mol Physiol *283*, L256-L264.

59. Seminario-Vidal L, Kreda S, Jones L, O'Neal W, Trejo J, Boucher RC, Lazarowski ER (2009) Thrombin promotes release of ATP from lung epithelial cells through coordinated activation of rho- and Ca2+-dependent signaling pathways. J Biol Chem.;284 (31):20638-48

60. Solle,M., Labasi,J., Perregaux,D.G., Stam,E., Petrushova,N., Koller,B.H., Griffiths,R.J., and Gabel,C.A. (2001). Altered cytokine production in mice lacking P2X(7) receptors. J. Biol. Chem. *276*, 125-132.

61. Sperlagh,B., Kofalvi,A., Deuchars,J., Atkinson,L., Milligan,C.J., Buckley,N.J., and Vizi,E.S. (2002). Involvement of P2X7 receptors in the regulation of neurotransmitter release in the rat hippocampus. J Neurochem. *81*, 1196-1211.

62. Stokes,L. *et al.* (2006). Characterization of a selective and potent antagonist of human P2X(7) receptors, AZ11645373. Br. J. Pharmacol. *149*, 880-887.

63. Suadicani,S.O., Brosnan,C.F., and Scemes,E. (2006a). P2X7 receptors mediate ATP release and amplification of astrocytic intercellular Ca2+ signaling. J. Neurosci. *26*, 1378-1385.

64. Suadicani,S.O., Brosnan,C.F., and Scemes,E. (2006b). P2X7 receptors mediate ATP release and amplification of astrocytic intercellular Ca2+ signaling. J. Neurosci. *26*, 1378-1385.

65. Tatur S, Groulx N, Orlov SN, Grygorczyk R. (2007). Ca2+-dependent ATP release from A549 cells involves synergistic autocrine stimulation by coreleased uridine nucleotides. J Physiol. 15 ;584: 419-35.

66. Vassar,V., Hagen,C., Ludwig,J., Thomas,R., and Zhou,J. (2007). One-step method of phosphatidylcholine extraction and separation. Biotechniques *42*, 442, 444.

67. Virginio,C., Church,D., North,R.A., and Surprenant,A. (1997). Effects of divalent cations, protons and calmidazolium at the rat P2X7 receptor. Neuropharmacology *36*, 1285-1294.

68. Von,W.G., Jiang,G., Kostic,A., De,V.K., Sap,J., and Sheetz,M.P. (2003). RPTP-alpha acts as a transducer of mechanical force on alphav/beta3-integrin-cytoskeleton linkages. J. Cell Biol. *161*, 143-153.

69. Wirtz,H.R. and Dobbs,L.G. (1990). Calcium mobilization and exocytosis after one mechanical stretch of lung epithelial cells. Science. *250*, 1266-1269.

70. Wyszogrodski,I., Kyei-Aboagye,K., Taeusch,H.W., Jr., and Avery,M.E. (1975). Surfactant inactivation by hyperventilation: conservation by end-expiratory pressure. J Appl. Physiol *38*, 461-466.

71. Young,M.T., Pelegrin,P., and Surprenant,A. (2007). Amino acid residues in the P2X7 receptor that mediate differential sensitivity to ATP and BzATP. Mol. Pharmacol. *71*, 92-100.

CHAPTER III

A CRITICAL ROLE OF P2X7 RECEPTOR-INDUCED VCAM-1 SHEDDING AND NEUTROPHIL INFILTRATION DURING ACUTE LUNG INJURY

3.1 Abstract

The trafficking of neutrophil to sites of injury is largely directed by signals from the epithelium, but how chemotactic gradients are formed is not known. Here we have demonstrated a novel mechanism by which $P2X_7$ receptor ($P2X_7R$) on type I alveolar epithelial cells (AEC I) regulates soluble VCAM-1 shedding that functions as a potent chemoattractant for neutrophil. Employing a clinically relevant two-hit model of mechanical ventilation (MV) and lipopolysachharide (LPS) we demonstrate that in the mice with $P2X_7R$ deficiency ($P2X_7R^{-/-}$) or selective inhibition of pulmonary $P2X_7R$, infiltration of neutrophils in the bronchoalveolar lavage (BAL) was abrogated. This was accompanied by a reduction of sVCAM-1, IL-1β and IL-6 in BAL. Neutrophil infiltrations and pro-inflammatory cytokine release was also significantly reduced by functional antibody blocking of alveolar VCAM-1 activity. In contrast, recombinant VCAM-1 rescued the $P2X_7R^{-/-}$ phenotype. ADAM-17 from the AEC I surface cleaved IL-1β-stimulated VCAM-1 in a $P2X_7R$-dependent manner. Neutrophil chemotaxis is directed predominantly towards soluble VCAM-1. Together, these findings suggest that soluble VCAM-1 shed from AEC I in injured alveoli functions as a competent chemoattractant for neutrophils. This is the first description of a new function of soluble VCAM-1 in the lung. Therapeutic interventions targeting $P2X_7R$ and VCAM-1

may provide a novel strategy to reduce neutrophil sequestration without altering yet critical mediators in lung injury.

Key words: AEC I, $P2X_7R$, VCAM-1, Shedding, Neutrophil, acute lung injury.

3.2 Introduction

Acute lung injury is a progressive syndrome that develops directly from pneumonia, gastric acid aspiration, inhalation of toxic gases or indirectly from extra pulmonary sepsis or trauma. Among them sepsis-related clinical cases possess the highest risk of lung injury progression and associated mortality rates (Rubenfeld *et al.*, 2005). At present, mechanical ventilation (MV) with a low tidal volume is the life-saving supportive therapy adopted in clinical practices of these critically ill patients (Chiumello & Cressoni, 2009;Kallet *et al.*, 2005).

Alveolar epithelium provides the first line of defense against invading pathogens and produces a range of pro-inflammatory mediators including IL-1β, IL-6, TNF-α, KC, MIP-2 and soluble forms of adhesion molecules (Skerrett *et al.*, 2004a;Mendez *et al.*, 2006). The release of soluble proteins from alveolar epithelium acts in consort to recruit and confine inflammatory cells to sites of injury. The regulatory mediators are operational when the inflammatory process is most likely to be reversible (Pittet *et al.*, 1997). A well orchestrated series of events follow the rapid ingress of neutrophil in alveolar space with hemorrhage and protein–rich edema fluid accumulation, as an early consequence of capillary-alveolar barrier damage. Even though information has been accumulated in recent years on the sentinel events of neutrophil recruitment at the site of injury, therapy is limited because of incomplete understanding of the molecular mechanisms regulating these events.

Vascular cell adhesion molecule 1 (VCAM-1) is a member of the immunoglobin supergene family and was colligated originally as an cytokine-inducible adhesion molecule on human endothelial cells (Osborn *et al.*, 1989;Rice & Bevilacqua, 1989). The

membrane-bound form of VCAM-1 (a 110-kDa type-I transmembrane glycoprotein) is abundantly found on the surface of leukocytes (Walsh *et al.*, 1996;Ibbotson *et al.*, 2001;Elices *et al.*, 1990;Ruegg *et al.*, 1992) and act as a counter ligand for the α4β1 (very late antigen-4 [VLA-4, CD49d/CD29]) and α4β7 (lymphocyte-Peyer's patch adhesion molecule-1 [LPAM-1, CD49d/CD103]) integrins. The VCAM-1 expedites transmigration of α4 integrin–positive cells across the inflamed endothelium and epithelium in the lung (Chin *et al.*, 1997;Parmley *et al.*, 2007). VCAM-1 can be released into a soluble variant, sVCAM-1 by proteolytic cleavage (Garton *et al.*, 2003). sVCAM-1 binds with α4β1 integrins and mediates function ascribed to their transmembrane counterpart (Rose *et al.*, 2000;Nakao *et al.*, 2003a). sVCAM-1 levels are correlated with various diseases. sVCAM-1 is elevated in synovial fluids from patients with rheumatoid arthritis (Wellicome *et al.*, 1993), cerebrospinal fluid of patients with active multiple sclerosis (McDonnell *et al.*, 1998), serum of patients with advanced cancers (Velikova *et al.*, 1998;Velikova *et al.*, 1997), inflammatory bowel disease, and type I diabetes (Goke *et al.*, 1997;Clausen *et al.*, 2000), and alveolar lining fluid from pneumonia and asthma patients (Matsuno *et al.*, 2007;Hamzaoui *et al.*, 2001).

The margination of neutrophil into the lung primarily sieve through narrow capillaries. However, in other organs like liver, kidney neutrophils are sequestered via post-capillary venules of systemic circulation (Erzurum *et al.*, 1992;Downey *et al.*, 1993). The essential firm adhesion between heterodimeric β2 integrins (CD18/α_M) and/or CD11 (CD11a,-b, -c, -d) on circulating neutrophils and ICAM-1 (CD54) on activated endothelial cells permit effective egress of neutrophils (Hogg & Walker, 1995). However, functional blockade of CD11/CD18-dependent adhesion pathways only inhibits 60-80%

of neutrophil emigration in response to *E.coli* lipopolysachharide (LPS), *Pseudomonas aeruginosa* or IL-1β, alluding the importance of CD18-independent pathways (Doerschuk *et al.*, 2000). Neutrophil emigration become decisive on CD18-independent interactions in *Streptococcus* pneumonia, *Staphylococcus aureus* infection, hydrochloric acid, hyperoxia or complement-induced acute lung injury, where blockade of CD18-dependent components completely fails to alter neutrophil egress (Doerschuk *et al.*, 1999). The molecular mechanisms of CD18-independent pathways have not been identified. Emerging evidence has highlighted importance of functional α4-integrins on neutrophil and α4-integrin/VCAM-1 interaction to temper inflammation (Ibbotson *et al.*, 2001;Burns *et al.*, 2001).

Purinergic $P2X_7$ receptor ($P2X_7R$), an ATP-gated cation channel, is unique among all other family members because of its ability to respond to various stimuli and to modulate pro-inflammatory signaling. The activation of $P2X_7R$ has been shown to be an absolute requirement for mature IL-1β and IL-18 production and release from hematopoietic cells (Ferrari *et al.*, 2006;Mehta *et al.*, 2001). Loss of $P2X_7R$ exhibits resistance to collagen-induced arthritis and fails to release IL-1β and IL-6 from peritoneal macrophages in response to systemic LPS and ATP challenge (Solle *et al.*, 2001). $P2X_7R$ has been implicated in Alzheimer's disease, rheumatoid arthritis, chronic lymphocytic leukemia and cancers (Li *et al.*, 2006;Parvathenani *et al.*, 2003;Mitsiades & Mitsiades, 2003). Recent findings have suggested the involvement of $P2X_7R$ in the pathogenesis of pulmonary emphysema, chronic obstructive pulmonary disease (COPD) and lung fibrosis (Muller *et al.*, 2010;Cicko *et al.*, 2010). We have previously shown that $P2X_7R$ from alveolar type I cells (AEC I) are functional and release ATP to regulate surfactant

secretion from AEC II in a paracrine fashion. $P2X_7R^{-/-}$ mice fails to reverse the surfactant increase following hyperventilation (Mishra *et al.*, 2011a). However, functional studies exploring the role of $P2X_7R$ in acute lung injury *in vivo* are lacking.

In the present study, we tested the hypothesis that $P2X_7R$ regulates neutrophil trafficking in the injured lung by stimulated ectodomain shedding of VCAM-1 from AEC I surface. Employing an experimental strategy of clinically relevant two-hit injury model of moderate tidal volume MV and low dose LPS we tested this idea using $P2X_7R$-null mice and selective $P2X_7R$ inhibition. Furthermore, we determined the role of VCAM-1 on neutrophil recruitment into the alveolar space by functional blockade of VCAM-1 activity. Our findings identified a specific pathway of neutrophil recruitment *in vivo* through sVCAM-1 shed from AEC I, providing a novel function of AEC I. Pharmacological targeting of $P2X_7R$ or VCAM-1 may constitute a new strategy for the treatment of acute lung injury.

3.3 Materials and Methods

3.3.1 Mice

All animal procedures were approved by the Institutional Animal Care Committee of Oklahoma State University. Wild-type C57BL/6 and $P2X_7R^{-/-}$ (B6.129P2-P2rx7^{tm1}Gab/J) breeder mice were obtained from Jackson Laboratories (Bar Harbor, ME, USA) and bred in the Animal Resource Unit of Oklahoma State University. The animals between 6-8 weeks old were used for experiments.

3.3.2 Murine model of acute lung injury

We used a modification of the murine two-hit lung injury model with a low dose LPS pretreatment, followed by mechanical ventilation (Altemeier *et al.*, 2005). Mice were

randomly assigned one of four groups: 1) spontaneous breathing non ventilated control (CONT), 2) mechanical ventilation (MV), 3) LPS or 4) LPS with mechanical ventilation (LPS+MV). Mice were anesthetized with ketamine (80 mg/kg) and xylazine (10 mg/kg) intraperitoneally. Tracheotomy was performed through the anterior neck soft tissues to expose the trachea. A 22-gauge needle was inserted into the trachea. Mice were placed in a supine position on a warming device with a heating lamp to maintain the body temperature to 37°C throughout the experiment. Mice were instilled with pyrogen-free saline (1.5 µl/g) or LPS (*Escherichia coli* serotype 0111:B4, Sigma-Aldrich; 0.5 µg/g bodyweight, 1.5 µl/g), through the inserted needle. Sixty minutes after instillation, mice were ventilated on a small animal ventilator (SAR-830/AP; CWE Inc) with following settings: respiratory rate = 125 breaths per minute; inspiratory and expiratory ratio = 1:2; tidal volume (Vt) = 12 ml/kg bodyweight; PEEP = 3 cm of H_2O and an inspired oxygen fraction of 0.21 for 150 min. Mice were given xylazine and ketamine, both at half of the initial dosage intraperitoneally at every 1 hr interval throughout the experiment for adequate sedation.

In separate experiments, LPS was co-administered into the lung with AZ10606120-dihydrochloride ($P2X_7R$ antagonists, 100 µM, final volume 1.5 µl/g b.wt, Tocris Biosci, Ellisville, MO), functional blocking monoclonal antibody against VCAM-1 (88 µg/mouse, purified rat anti-mouse CD-106, Pharmingen, San Diego, CA) and isotype–matched control (purified rat IgG2a κ isotype control, Pharmingen) in wild-type mice or recombinant VCAM-1 (5 µg/mouse, recombinant mouse VCAM-1/CD106 Fc chimera, R&D Systems, Minneapolis, MN) in $P2X_7R^{-/-}$ mice. Mechanical ventilation with the same settings was started after 60 min and continued for additional 150 min as described

above. At the end of protocol, mice were euthanized and exasanguinated via abdominal aorta puncture.

3.3.3 Bronchoalveolar lavage

Bronchoalveolar lavage (BAL) was performed using 1 ml of 0.9% sterile saline for 3 times. BAL recovered were pooled and centrifuged at 250 *g* for 10 min. The BAL fluid was used for total protein and cytokine analyses. The harvested lung tissue samples were snap-frozen and stored in liquid nitrogen in aliquots at – 80°C for biochemical and gene expression analyses. Cell pellets were cytospun at 600 *g* for 10 min. Total cell numbers were counted with a standard hemocytometer. Differential cell counting was done using a modified Wright Giemsa stain. A total of 500 cells were counted from randomly chosen fields from each sample. The total protein concentration in the BAL fluid was determined by the bicinchoninic acid method (BCA protein assay kit; Pierce, Rockford, IL) with bovine serum albumin as standards.

3.3.4 Cytokine antibody array

BAL fluids from wild-type and $P2X_7R^{-/-}$ mice were assayed for cytokines using the RayBio Mouse Cytokine Antibody Array (C-series 2000, RayBiotech, Inc., Norcross, GA), according to the manufacturers' instruction. In brief, BAL fluids pooled from three mice in each group were added to pre-blocked protein array membranes overnight at 4ºC. Array membranes were washed three times with wash buffer and incubated with biotin-conjugated anti-cytokine antibodies for 2 hours at room temperature. After washing, streptavidin-horseradish peroxidase were added and incubated for 2 hours. Protein array membranes were incubated 1 min for detection and then exposed to Kodak films. The resulting membrane films were quantified using Quantity One software Tool (Bio-Rad,

Hercules, CA). To eliminate the loading difference the average optical densities (OD) of each cytokine was normalized to the average OD of biotin-conjugated positive control samples (upper left and lower right of each membrane). Fold change was then determined as the difference between CONT and LPS+MV treated conditions.

3.3.5 ELISA

sVCAM-1, IL-1β, IL-6, TNF-α, MCP-1 and IgM concentrations in BAL and/or serum were determined by ELISA, according to the manufacturers' recommendations (mouse IgM ELISA kit; Bethyl Labs, Inc., Quantikine mouse IL-1β and sVCAM-1 immunoassay; R&D Systems, Minneapolis, MN; and mouse IL-6, TNF-α, and MCP-1 ELISA Ready-SET-Go; eBiosciences, San Diego, CA). Undiluted samples were used to maximize detection level. The sensitivity were 1.37 ng/ml for IgM, 0.3 ng/ml for sVCAM-1, 4 pg/ml for IL-6 and 8 pg/ml for IL-1β, TNF-α, and MCP-1, respectively.

A cell based ELISA assay were developed in isolated rat alveolar macrophages from BAL for the sVCAM-1 binding experiments. Alveolar macrophages were cultured in 96-well micro titer plates (Costar, Cambridge, MA) in DMEM. Cells (0.2 X 10^6/well) were plated for 1 hour and incubated with different concentrations of sVCAM-1 (0, 100, 1000, 10000 ng/ml) in DMEM for 45 min at 37°C. After carefully washing with PBS, cells were incubated for 1 hour with rabbit anti-rat-VCAM-1 detector antibody (Abcam, Cambridge, MA) or a preimmune IgG fraction at a concentration of 50 μg/ml. This was followed by anti-rabbit horseradish peroxidase-conjugated antibody (1/5000 dilution, Amersham, Arlington Heights, IL) incubation for 45 min. The assay was developed by addition of o-phenylenediamine dihydrochloride substrate and the reaction was stopped by 50 μl of 3 M H_2SO4. Optical density (OD) was measured at 490 nm.

3.3.6 Nitrite/nitrate production

Rat alveolar macrophages were seeded at density of 1 X 10^6/ml in 12-well culture plates (Falcon Laboratories) in DMEM supplemented with 10% FBS, penicillin and streptomycin (GIBCO). Cells were incubated for 1 hour, to remove unattached cells, and incubated with LPS (1 μg/ml) or VCAM-1 (10 μg/ml) for 4 hours. Nitrite and nitrate concentrations in cell-free culture supernatants were determined using NADPH-dependent nitrate reductase assay (Green *et al.*, 1982). Briefly, samples were reacted with 1% sulfanilamide, 0.1 % naphthyl-ethelene diamine at room temperature for 10 min and the nitrite concentration was determined by absorbance at 540 nm with standard solutions of sodium nitrite run in parallel.

3.3.7 Lung tissue myeloperoxidase

Whole lung tissue was homogenized in 1 ml of 50 mM potassium phosphate, pH 6.0 and centrifuged at 14,000 *g* for 15 min at 4°C. The pellet was redissolved in the phosphate buffer containing 50 mM hexadecyltrimethylammonium bromide. The samples were sonicated on ice for 20 seconds, freeze-thawed twice and centrifuged at 14,000 *g* for 10 min at 4°C. One hundred μl of undiluted samples were added immediately to 2.9 ml of phosphate buffer containing 0.167 mg/ml O-danisidine dihydrochloride and 0.0005% hydrogen peroxide in cuvettes and absorbance at 460 nm was measured for 5 min. Myeloperoxidase (MPO) activities were expressed as absorbance per min per milligrams of total protein.

3.3.8 Lung microvascular permeability

Lung microvascular permeability in wild-type and $P2X_7R^{-/-}$ mice were assessed by a modified Evans blue (EB) dye extravasation method as previously described (Chen *et al.*,

2006). Extravasations of EB dye into the extravascular pulmonary tissue spaces were used as a quantitative measure of changes in lung microvascular permeability. In brief, EB dye (20 mg/kg body weight) was injected into the jugular vein of the animals after LPS instillation and ventilated for 3 hour. The lungs were perfused with 1 ml of 0.9% sterile saline via right ventricle to remove the remaining blood from pulmonary circulation. Lungs were harvested and weighed. EB dye was extracted from lung homogenates following incubation with formamide 8 ml/gm wet tissue for 48 hours at room temperature and centrifuged at 2,000 *g* for 30 min. EB dye concentrations in the lung tissue were quantified by measuring absorbance at 620 nm from a standard curve. The total amount of EB dye present in the pulmonary tissues were quantified and normalized to tissue weight.

3.3.9 Histopathology

Wild-type and $P2X_7R^{-/-}$ mouse lungs (n=6) were instilled with 4% paraformaldehyde in PBS at 20 cm H_2O pressure and fixed for 48 hours, embedded in paraffin and sectioned at 4 μm thickness. The sections were stained with hematoxylin and eosin and were examined under a light microscope.

3.3.10 Isolation and culture of mouse AEC II

Murine alveolar epithelial type II cells (AEC II) were isolated from wild-type and $P2X_7R^{-/-}$ mice (6-8 weeks of age) as described previously (Corti *et al.*, 1996). Lung was perfused free of blood with solution containing 0.9% NaCl, 0.1% glucose, 10 mM HEPES, pH 7.4, 5 mM KCl, 1.3 mM $MgSO_4$, 1.7 mM $CaCl_2$, 0.1 mg/ml streptomycin sulfate, 0.06 mg/ml penicillin G, 3 mM Na_2HPO_4 and 3 mM NaH_2PO_4. AEC II were released from the lung by enzymatic digestion with dispase (2500 caseinolytic units/ml,

BD Biosciences, Franklin Lakes, NJ) instilled (0.5 ml) via the trachea for 15 min. Three lungs were isolated, chopped and pooled into a beaker. The lung slices were further digested with DNase I (100 µg/ml) for 45 min at 37^{o}C in a 50 ml beaker (~17 ml digestion cocktail) with intermittent shaking. The digested lungs were filtered through 160-, 37- and 15-µm nylon mesh sequentially. The filtrate was centrifuged at 250 x*g* for 10 min. The cell pellet was resuspended in DMEM media (GIBCO, Grand Island, NY) and incubated in a 100 mm petridish coated with mouse IgG (75 µg/dish) for 1 hour. The cells were spun down at 250 x *g* for 10 min and resuspended in DMEM containing 10% FBS. The cell yield was ~10 x10^{6} per isolation and the cell viability was >97% by trypan blue exclusion. AEC II were then cultured in fibronectin coated 12-well tissue culture plates (corning) at 1x 10^{6} cells/well in DMEM supplemented with 10% FBS, penicillin and streptomycin (GIBCO). AEC II was cultured for three days to allow them trans-differentiate into AEC I. For dose–response experiments, *day 3* cultured cells were stimulated with IL-1β (0, 0.1, 1, 10 or 100 ng/ml, R&D Systems, Minneapolis, MN) for 24 and 48 hours. In separate experiments, *day 3* cultured AEC were stimulated with IL-1β (10 ng/ml) in the presence or absence of the MMP inhibitor, GM-60001 (50 µM, EMD Millipore, Billerica, MA) for 48 hours. ADAM-17 (5 ng/ml) (R&D Systems, Minneapolis, MN) was added at the last 3 hours of incubation, media were collected for determining sVCAM-1 by ELISA.

3.3.11 Isolation and culture of mouse AEC I and AEC II

Murine AEC I and AEC II were freshly isolated from C57BL/6 mice (6-8 wks of age) following LPS+MV injury (Mishra *et al.*, 2011b). Briefly, lungs were perfused with solution (containing 0.9% NaCl, 0.1% glucose, 10 mM HEPES, pH 7.4, 5 mM

KCl, 1.3 mM $MgSO_4$, 1.7 mM $CaCl_2$, 0.1 mg/ml streptomycin sulfate, 0.06 mg/ml penicillin G, 3 mM Na_2HPO_4 and 3 mM NaH_2PO_4) followed by instilling 1 ml of the digestion cocktail (dispase, 2500 caseinolytic units/ml and elastase, 4 U/ml in solution) directly through the trachea. Three lungs were isolated, pooled into a beaker containing ~17 ml of the digestion cocktail and incubated at 37°C for 15 min. After incubation, the lungs were chopped. Lung tissues were further digested with the addition of DNase I (100 μg/ml) for 45 min at 37°C with intermittent shaking. The digested lungs were filtered through 160-, 37- and 15-μm nylon mesh sequentially. The filtrate was centrifuged at 250 x*g* for 10 min. The cell pellet was resuspended in DMEM media and incubated in a 100 mm petridish coated with mouse IgG (75 μg/dish) for 1 hour. The cells were spun down at 250 x*g* for 10 min and resuspended in DMEM containing 10% FBS. The cell yield was ~8 $x10^6$ per mouse and the cell viability was >95%.

3.3.12 Flow Cytometry

The surface expression of integrins on neutrophils was determined using fluoroscein isothiocynate (FITC)-conjugated integrin α4, CD-11b and integrin β7 (rat IgG2b, κ; Pharmingen, San Diego, CA) and a phycoerythrin (PE)-conjugated mAb against the murine granulocyte marker Gr-1(RB6-8C5; Pharmingen) by fluorescence activated cell sorter (FACS). Blood neutrophils (10^6 cells in 100 μl staining buffer, PBS containing 1% bovine serum albumin and 0.1% sodium azide) or BAL cells (1 X 10^5 cells in 100 μl staining buffer) were incubated for 45 min at 4ºC with FITC- and PE-conjugated antibodies. Cells were also labeled with isotype control rat anti-mouse IgG antibodies. The cells were then washed twice with the staining buffer.

AEC I and AEC II were stained with PE-conjugated podoplanin (AEC I cell marker) (BioLegend, San Diego, CA) and FITC-conjugated monoclonal-VCAM-1(Abcam, Cambridge, MA). Fluorescence was determined on a single argon laser cytofluorometer FACSCalibur (BD Biosciences) and analyzed using CELLQuest software. Granulocyte, lymphocyte and monocyte (or macrophage) populations were delineated using forward- and side- scattering properties of the three cell populations. Mean fluorescence intensity (MFI) values were determined from the histograms of the gated populations, and each mean fluorescence was obtained by subtracting the measured control IgG fluorescence from the mean fluorescence for the population.

3.3.13 Chemotaxis assay

Peripheral rat blood neutrophils were isolated using OptiPrep ^{TM} density gradient (Sigma, St. Louis, MO). Circulating neutrophils were isolated from EDTA-anti-coagulated whole blood collected by abdominal aorta puncture. Briefly, red blood cells were removed by hypotonis lysis. Neutrophils were further purified by centrifugation through a Histopaque density gradient and resuspended in HBSS (2 X 10^7/ml).

Chemotaxis of neutrophils was conducted in duplicate using 3-μm polyvinylpyrrolidone-free polycarbonate membranes (Nuclepore Corp.,Pleasanton, CA) in Boyden-chambers . Mouse recombinant VCAM-1 (R&D Systems) was diluted in media and placed in the lower wells (200 μl) at a concentration of 10 μg/ml of the transwell. In some experiments BAL fluid or cultured AEC (50% conditioned media) from wild-type and $P2X_7^{-/-}$ mice were kept in lower chambers. Neutrophils were pre-activated with dihydrochalasin B (a known inducer of surface integrin expressions, 2.5 μM/ml) for 10 min. One hundred micro liters of neutrophils at $1X10^6$ cells/ml were

placed in the upper chambers. The loaded chambers were incubated at 37ºC in humidified air containing 5% CO_2 for 1 hour. The membrane was then removed, fixed and stained with Wright Giemsa stain. The cells that migrated and adhered to the lower surface of the membrane were counted from 10 microscope fields under the x 10 objectives (Olympus). Data are expressed as average number of neutrophils per field.

3.3.14 Western blot

Lung homogenate and cell lysates were separated on a 10% SDS-polyacrylamide gel and transferred to a nitrocellulose membrane. The membrane was stained with Ponceau S to ensure proper transfer and blocked overnight with 5% dry skim milk in 100 mM Tris-buffered saline plus 0.1% Tween 20 (TBST). The membranes were incubated with anti-pERK1/2, total ERK1/2 antibodies (Cell Signaling Technology, Danvers, MA) at a 1:1000 dilution or anti-β actin at a 1:2000 dilution overnight at 4°C. After being washed with TBST three times, the membranes were incubated with horseradish peroxidase-conjugated anti-rabbit IgG (1:2000) for 1 hour. The blots were washed again and individual target proteins were visualized using the enhanced chemiluminescence detection system (Amersham Biosciences, Piscataway, NJ).

3.3.15 Real-time PCR

Quantitative real-time PCR was performed to measure the relative levels of cytokine and chemokine transcripts. Total RNA was extracted using the TRI Reagent (Molecular Research Center Inc., Cincinnati, OH) and reverse-transcribed into cDNA using Moloney murine leukemia virus reverse transcriptase (Invitrogen) and gene-specific primers (Table 1). The quantitative real-time PCR was done using an ABI prism 7700 system (PE Applied Biosystems, Foster city, CA). The expression levels were normalized with 18S

rRNA and expressed as fold changes compared to the control wild-type and $P2X_7R^{-/-}$ mice, respectively.

3.3.16 ADAM-17 activity assay

Freshly isolated AEC I and AEC II from wild-type and $P2X_7R^{-/-}$ with or without LPS+MV or HEK cells stably expressing rat-$P2X_7$ receptor (HEK-$P2X_7R$) treated with BzATP (200 μM, Sigma) or the ERK1/2 inhibitor (10 μM, Promega, Madison, WI) for indicated time periods were lysed. The lysate (25 μg) were analyzed for ADAM 17 activity using a fluorogenic peptide based assay kit (R&D Systems, Minneapolis, MN) . The enzymatic activity was obtained from a serially diluted standard of recombinant ADAM17 run in parallel.

3.3.17 Zymography

Standard gelatin zymography was done to evaluate the activity of matrix metalloproteinase (MMP) 2 and 9 in BAL fluid from wild-type and $P2X_7R^{-/-}$ mice. Ten microgram proteins of BAL fluid were separated in an 8% SDS-polyacrylamide gel containing 0.2% gelatin. The gel was washed and stained with Commassie Blue and destained with a mixture of acetic acid and methanol. Gels were scanned and the band intensities were quantified (in arbitrary density units) using Image J software (National Institute of Health, USA). To eliminate the differences between gels, two samples of all experimental groups were loaded in the same gel.

3.3.18 Statistical analysis

The results were analyzed by one-way ANOVA with posthoc *Tukey's* test for multiple comparisons of control and treatment groups. A two-tailed Wilcoxon ranked test was used for non-parametric data, using Graph pad Prism software (version 4). All results

were reported as means ± SE (n=4-8). Difference was considered statistically significant when P value was less than 0.05.

3.4 Results

3.4.1 P2X7R-/- mice and P2X7R antagonism protects against acute lung injury

MV potentiates lung inflammation in the presence of LPS and increased cytokine levels, neutrophil transmigration, alveolar–capillary damage and protein leakage (Altemeier *et al.*, 2005). The two-hit LPS+MV injury model is reproducible and recapitulates the aspects of acute lung injury in humans (Kallet *et al.*, 2005). We examined whether $P2X_7R^{-/-}$ mice or pharmacological inhibition of $P2X_7R$ in wild-type mice would provide protection against LPS+MV-induced lung injury. The total cell counts in the BAL from wild-type mice were increased in the LPS+MV group in comparison with the control group. Neutrophil was the major recruited cell type in our experimental model of acute lung injury as revealed by differential cell count analysis (7.06 ± 1.01 in LPS+MV *vs.* 0.04 ± 0.007 X 10^4 neutrophils/ml in CONT, respectively). This recruitment of neutrophil was ~ 7-fold higher in wild-type compared to $P2X_7R^{-/-}$ mice. Intratracheal administration of the $P2X_7R$ inhibitor, AZ 10606120 dihydrochloride showed significantly less neutrophil in BAL (Figure 3.1A). Lung MPO activity was 4-fold increased by LPS+MV in wild-type mice. This increase was absent in $P2X_7R^{-/-}$ mice (Figure 3.1B).

Lung vascular permeability was assessed using the Evans blue dye extravasations method (Chen *et al.*, 2006). LPS+MV caused significant accumulation of dye in the lungs of wild-type, but not in $P2X_7R^{-/-}$ mice (Figure 3.1C). However, there was no significant difference in dye accumulation between wild-type and $P2X_7R^{-/-}$ mice without LPS+MV treatment. Importantly, BAL IgM concentration was ~ 5 fold increased by LPS+MV in

wild-type, which was significantly attenuated in $P2X_7R^{-/-}$ mice and following $P2X_7R$ inhibition (Figure 3.1D).

BAL IL-1β, IL-6, and MCP-1 levels were increased following LPS+MV in wild-type (Figure 3.1E-G). LPS+MV-induced increases in IL-1β, IL-6, and MCP-1 in BAL were less after pharmacological inhibition of $P2X_7R$ and in $P2X_7R^{-/-}$ mice. mRNA levels of IL-1β, IL-6 and MCP-1 were also increased by LPS+MV (Figure 3.2A-D). The mRNA induction of these cytokines was 30-50% less in $P2X_7R^{-/-}$ mice in comparison with that in wild-type mice. The result indicates that $P2X_7R$ also regulates cytokine expression. However, TNF-α expression from wild-type and $P2X_7R^{-/-}$ mice lung tissues had little differences (Figure 3.1H). Taken together, these results demonstrate that $P2X_7R$ contributes to alveolar-endothelial infringement and cytokine induction and release following acute lung injury. The results of $P2X_7R$ inhibition are consistent with those observed in $P2X_7R^{-/-}$ mice.

Histological examination of lung tissue from wild-type mice with LPS and MV showed evidence of diffuse lung injury with significant inflammatory cell infiltrate around the interstitial, peri-vascular and intra-alveolar spaces (Figure 3.1I). There were widespread infiltration of neutrophil within alveolar septa and lumens. In sharp contrast to the wild-type mice, the $P2X_7R^{-/-}$ mice instilled with LPS and MV exhibited less evidence of neutrophil infiltration. For example, the multiple foci of neutrophil infiltration occurred in the wild-type mouse lung, which were not detected in the $P2X_7R^{-/-}$ mice. Similarly, numerous scattered foci of alveolar septal necrosis seen in wild-type mice (Figure 3.1I, indicated by arrow) were not seen in sections from $P2X_7R^{-/-}$ mice lungs.

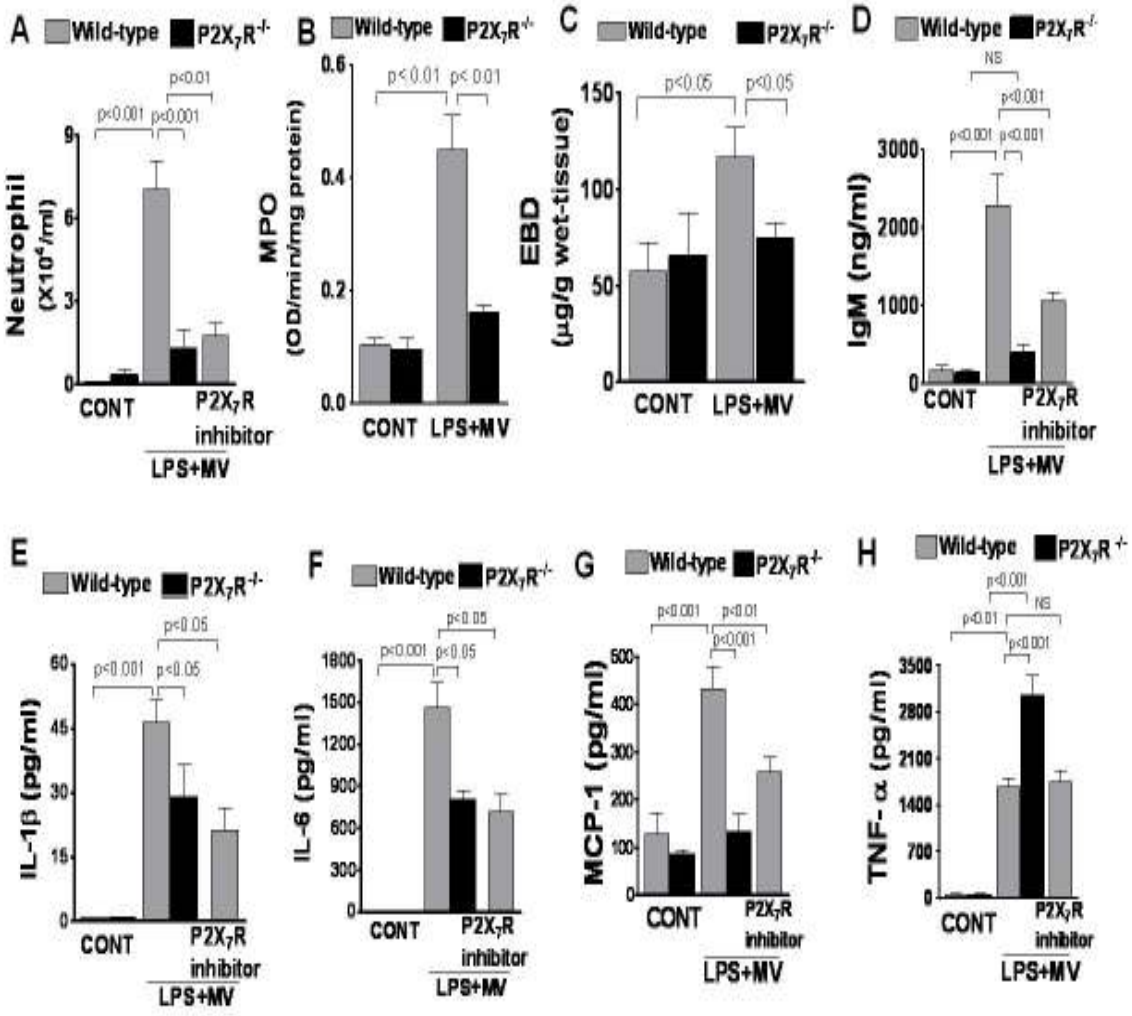
A
Wild-type
P2X7R-/-
Neutrophil (X10⁴/ml)
p<0.001
p<0.001
p<0.01
CONT
P2X7R inhibitor
LPS+MV
B
Wild-type
P2X7R-/-
MPO (OD/min/mg protein)
p< 0.01
p< 0.01
CONT
LPS+MV
C
Wild-type
P2X7R-/-
EBD (μg/g wet-tissue)
p<0.05
p<0.05
CONT
LPS+MV
D
Wild-type
P2X7R-/-
IgM (ng/ml)
NS
p<0.001
p<0.001
p<0.001
CONT
P2X7R inhibitor
LPS+MV
E
Wild-type
P2X7R-/-
IL-1β (pg/ml)
p<0.05
p<0.001
p<0.05
CONT
P2X7R inhibitor
LPS+MV
F
Wild-type
P2X7R-/-
IL-6 (pg/ml)
p<0.05
p<0.001
p<0.05
CONT
P2X7R inhibitor
LPS+MV
G
Wild-type
P2X7R-/-
MCP-1 (pg/ml)
p<0.001
p<0.01
p<0.001
CONT
P2X7R inhibitor
LPS+MV
H
Wild-type
P2X7R-/-
TNF-α (pg/ml)
p<0.001
NS
p<0.01
p<0.001
CONT
P2X7R inhibitor
LPS+MV

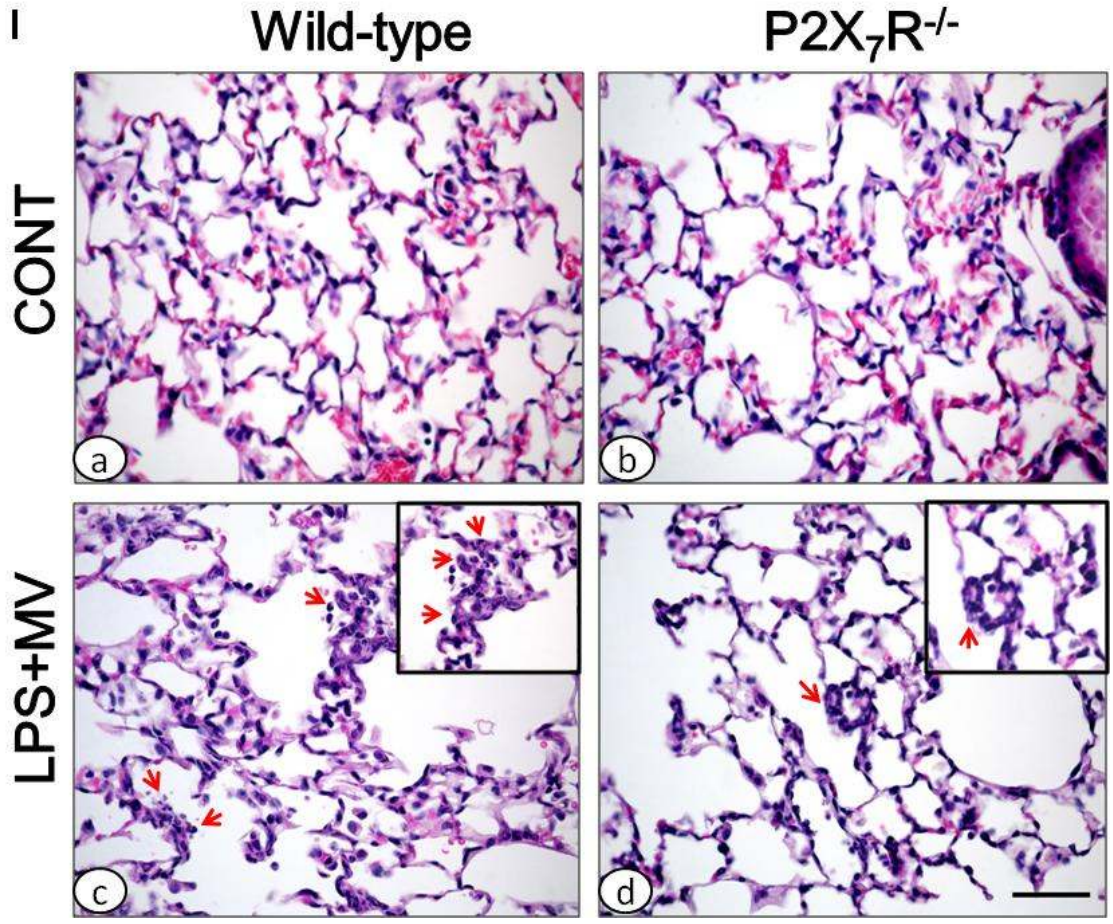
I
Wild-type
P2X7R-/-
CONT
LPS+MV
a
b
c
d

Figure 3.1: Reduced inflammation during acute lung injury in $P2X_7R^{-/-}$ or $P2X_7R$ antagonism.

(A) Neutrophil in the BAL of wild-type and $P2X_7R^{-/-}$ mice or following $P2X_7R$ inhibition from LPS+MV as described in Materials and Methods. Data are expressed as mean ± SE (n=6-8). *(B)* MPO activity *(C)* Evans blue dye extravasations in wild-type and $P2X_7R^{-/-}$ mice were quantified. Evans blue dye (20 mg/kg bodyweight) is injected intravenously to LPS+MV treated mice and extracted from lungs. Data are expressed as mean ± SE (n=4-8 animals). *(D)* IgM, *(E)* IL-1β and *(F)* IL-6 *(G)* MCP-1 and *(H)* TNF-α concentrations in BAL of control and LPS+MV in the presence or absence of $P2X_7R$ antagonist from wild-type and $P2X_7R^{-/-}$ mice. Data are expressed as mean ± SE (n= 4-6). *(I)* Histological analysis of inflamed lungs of wild-type and $P2X_7R^{-/-}$ mice. Parrafin sections (4 μm) of lungs were stained with H&E from *(a)* wild-type and *(b)* $P2X_7R^{-/-}$ control compared to LPS+MV (*c* and *d*, respectively). Red arrow indicates alveolar septal necrosis (Scale bar= 50 μm).

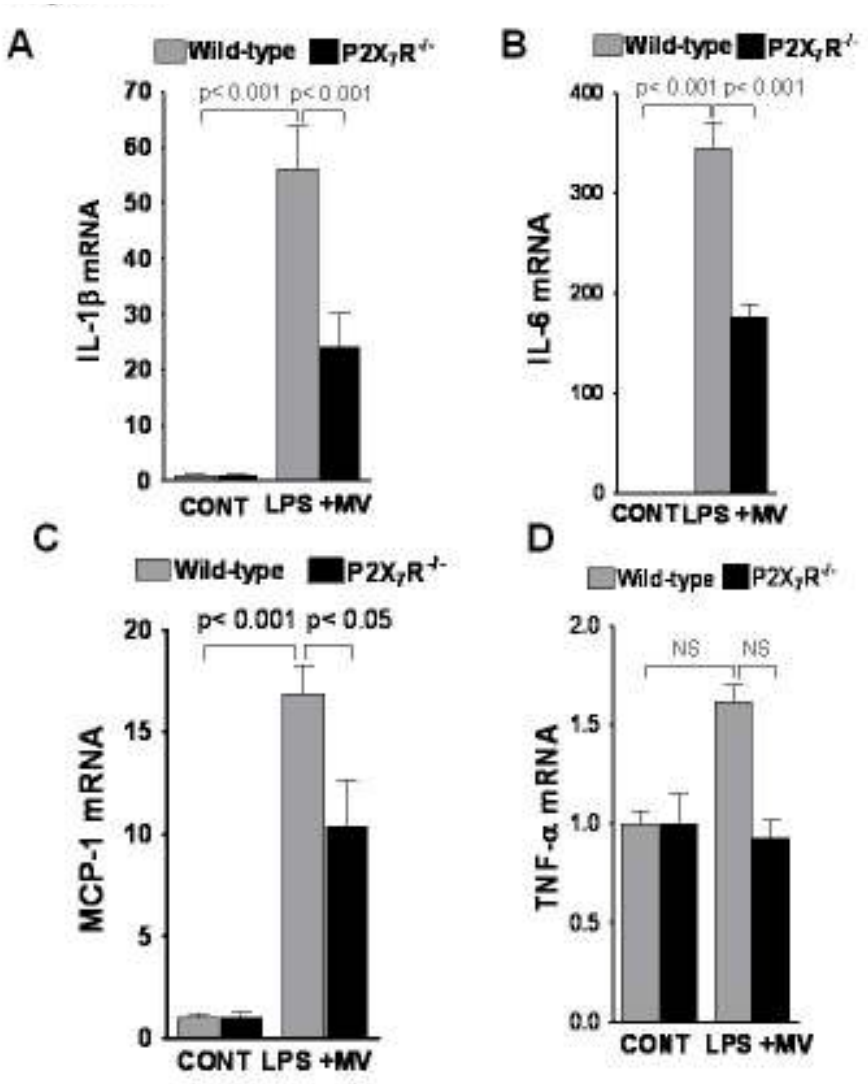

Figure 3.2: Pro-inflammatory cytokine expression in P2X7R-/- mice lung

(A) IL-1β, *(B)* IL-6, *(C)* MCP-1 and *(D)* TNF-α expressions were measured in lung homogenates from control (CONT) or LPS combined with mechanical ventilation (LPS+MV) mice. Data are expressed as means ± SE (n=3-4 animals/group) and compared with corresponding wild-type and $P2X_7R^{-/-}$ CONT, respectively.

Table.3.1 Real-time PCR primers

Gene	Forward primer sequences	Reverse primer sequences
mIL-1β	GCAACTGTTCCTGAACTCAACT	ATCTTTTGGGGTCCGTCAACT
mIL-6	TAGTCCTTCCTACCCCAATTTCC	TTGGTCCTTAGCCACTCCTTC
mTNF-α	CCGGGAGAAGAGGGATAGCTT	TCGGACAGTCACTCACCAAGT
mMCP-1	CTTCTGGGCCTGCTGTTCA	CCAGCCTACTCATTGGGATCA
rat IL-1β	TTGCTTCCAAGCCCTTGACT	TGAGTGACACTGCCTTCCTGAA
rat IL-6	CCACCAGGAACGAAAGTCAAC	TGTCAACAACATCAGTCCCAAGA
18 S	ATTGCTCAATCTCGGGTGGCTG	CGTTCTTAGTTGGTGGAGCGATTTG

3.4.2 P2X7R regulates soluble VCAM-1 (sVCAM-1) release in acute lung injury

$P2X_7R$ has previously been shown to be a prime regulator of mature IL-1β processing and release *in vitro* (Ferrari *et al.*, 2006;Mehta *et al.*, 2001) and *in vivo* (Solle *et al.*, 2001). To further elucidate the $P2X_7R$-mediated mechanisms of lung inflammatory response, we screened 144 cytokines in BAL from wild-type and $P2X_7R^{-/-}$ mice using cytokine array (Figure 3.3A). The array detects- acute phase cytokines, chemokines, and soluble mediators in biological fluids. 54 cytokines were detectable following LPS+MV. There was significant induction of 34 cytokines in both genotypes following lung injury. Among them 25 cytokines shows no difference in induction level between wild-type and $P2X_7R^{-/-}$ mice (Table 3.2). The cytokine array confirms the ELISA results which shows inadequate IL-6, MCP-1, and unaltered levels of TNF-α between wild-type and $P2X_7R^{-/-}$ mice in response to injury (Figure 3.1F-H). IL-1β was not detected due to the low expression level. Notably, soluble VCAM-1 and P-Selectin were induced by LPS+MV in wild-type, but not in $P2X_7R^{-/-}$ mice (Figure 3.3B).

To verify our array results, we next determine the levels of soluble VCAM-1 and P-Selectin in BAL. LPS+MV significantly induces sVCAM-1 release in wild-type mice. There was significant decrease in sVCAM-1 level in BAL following $P2X_7R$ antagonism or from $P2X_7R^{-/-}$ mice. (Figure 3.3C). However, there was no change observed in soluble P-Selectin level ensuing lung injury (Figure 3.3D).

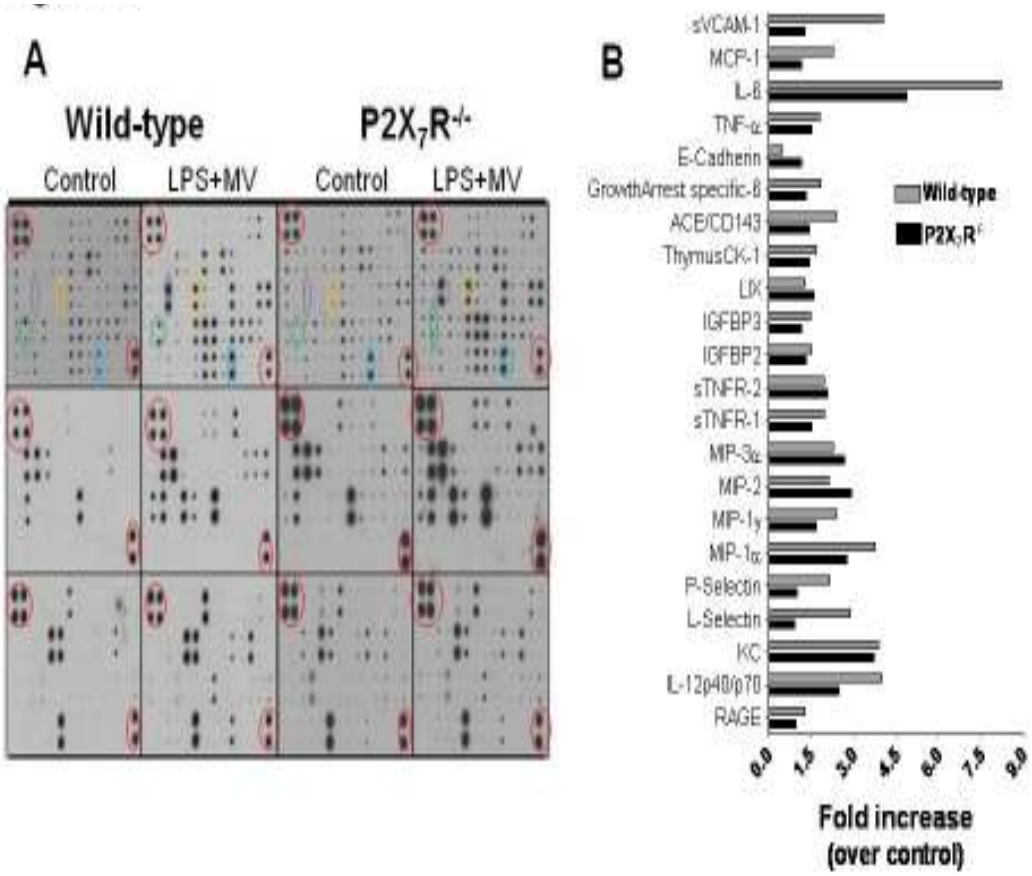
A
Wild-type
P2X7R-/-
Control
LPS+MV
Control
LPS+MV
B
sVCAM-1
MCP-1
IL-8
TNF-α
E-Cadherin
GrowthArrest specific-6
ACE/CD143
ThymusCK-1
LIX
IGFBP3
IGFBP2
sTNFR-2
sTNFR-1
MIP-3α
MIP-2
MIP-1γ
MIP-1α
P-Selectin
L-Selectin
KC
IL-12p40/p70
RAGE
Wild-type
P2X7R-/-
0.0
1.5
3.0
4.5
6.0
7.5
9.0
Fold increase
(over control)

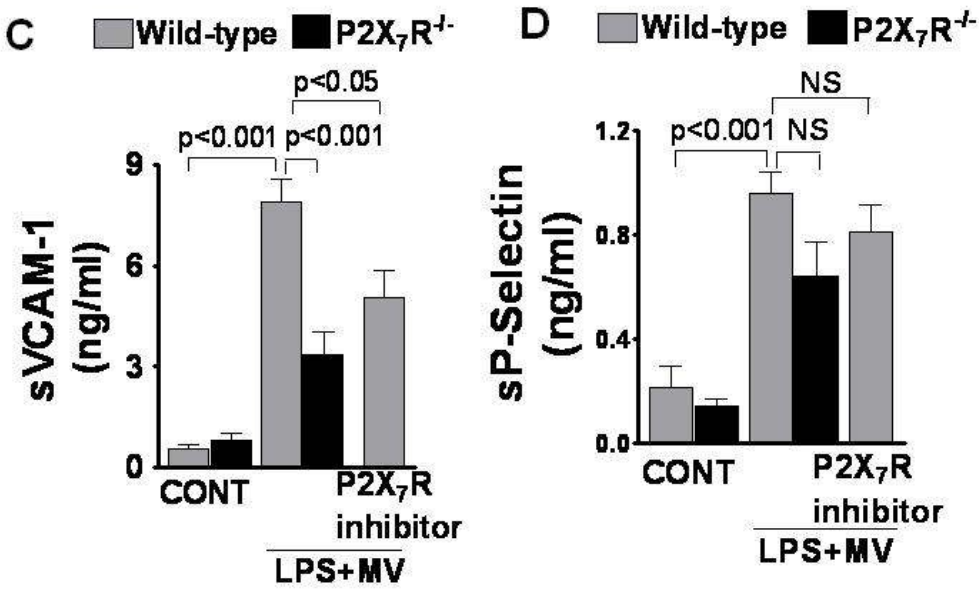
C
Wild-type
P2X7R-/-
p<0.05
p<0.001
p<0.001
sVCAM-1
(ng/ml)
9
6
3
0
CONT
P2X7R
inhibitor
LPS+MV
D
Wild-type
P2X7R-/-
NS
p<0.001
NS
sP-Selectin
(ng/ml)
1.2
0.8
0.4
0.0
CONT
P2X7R
inhibitor
LPS+MV

Figure 3.3: sVCAM-1 release is compromised in $P2X_7R^{-/-}$ mice following acute lung injury:

(A) A presentative protein-array membrane obtained from incubation with BAL fluid from control or LPS combined with mechanical ventilation (LPS+MV) as indicated. Positive controls are circled in red and were used for data normalisation. $P2X_7R^{-/-}$ mice shows altered IL-6 (purple), IL-12 (yellow), MCP-1 (green), and sVCAM-1 (blue) release following LPS+MV. *(B)* Comparison of changes in soluble mediator release induced by LPS+MV plotted as fold increase over respective control from BAL of wild-type and $P2X_7R^{-/-}$. *(C)* sVCAM-1 and *(D)* s-P-Selectin levels in the BAL of wild-type and $P2X_7R^{-/-}$ mice and following P2X7R inhibition after lung injury. sVCAM-1 and sP-Selectin were quantified by ELISA. Each data point from individual animals are measured in duplicates and expressed as means ± SE (n=5-8 animals in each group).

Table 3.2. Summary of cytokine antibody array

Induced by LPS+MV Significantly differs between WT & KO (> 25%)							Induced by LPS+MV No difference between WT & KO		Non-induced
	Wild-type			$P2X_7^{-/-}$			(> 50% Induction)		(< 50% Induction)
IL-6							KC	CXCL16	Axl, BLC, IL-12P70, IL13, IL4, IL3Rb, IL2, CTACK, MIP3B, MIG, MCSF, MCP5, Eotaxin2, PF4, IGF1, MDC, TCA3, RANTES, Leptin, Lymphotactin
IL12P40/P70							MIP2,MIP3a	IL-1a	
MCP-1							TNF-a,sTNFR1,sTNFR2	ICAM-1	
MIP-1*							IGFBP2,IGFBP3	MMP-2, MMP-3, pro-MMP9	
MIP-1γ							LIX	Lungkine	
VCAM-1							Osteopontin	E-selectin	
L-Selectin							Thymus-CK1	Bfgf	
P-Selectin							Growth –arrest specific 6	EGF	
ACE/CD143							RAGE	E-cadherin, TweakR	

3.4.3 Soluble VCAM-1 activates alveolar macrophages and potentiates neutrophil chemotaxis

To obtain information related to soluble VCAM-1 function in the lung, we first examined the binding of sVCAM-1 to rat alveolar macrophages by means of a cell-based ELISA. The cells were incubated with different concentrations of sVCAM-1 (0-10,000 ng/ml), and then anti-VCAM-1or preimmune IgG was added. The OD was directly proportional to the sVCAM-1 concentrations added to the wells, indicating binding and immobilization of the antibody to VCAM-1 present on the surfaces of alveolar macrophages (Figure 3.4A). No increase was observed in binding of preimmune IgG to cells, indicating the Fc receptor-independent binding of the antibody in alveolar macrophages. Furthermore, the binding of sVCAM-1 to alveolar macrophages increases nitrate/nitrite production (Figure 3.4B). In addition, VCAM-1 stimulation induces expressions of IL-1β and IL-6 mRNA (Figure 3.4C-D), indicating binding of sVCAM-1 to alveolar macrophages is able to activate and intensify inflammatory response through enhanced cytokine induction.

VCAM-1 in solution acts as a soluble agonist and adhere with higher avidity to α4β1 integrin expressing cells (Woodside *et al.*, 2006) and promotes cell migration and aggregation (Nakao *et al.*, 2003b). Our results show increases in BAL sVCAM-1 concentrations and neutrophilia in wild-type mice, but not in $P2X_7R^{-/-}$ mice following LPS+MV. To examine whether sVCAM-1 is a chemoattractant for neutrophils, a series of chemotaxis assay were performed. Peripheral rat neutrophils responded avidly to the known chemotactic stimulus fMLP (100 μM), (187.4±19.17 neutrophil/field). Neutrophil migration was also markedly increased by recombinant VCAM-1 (97±5.3 *vs.* 24±2.1

neutrophil/field) (Figure 3.4E). Next, the BAL samples from LPS+MV–treated wild-type and $P2X_7R^{-/-}$ mice were neutralized with blocking monoclonal antibody against VCAM-1. Neutrophil chemotaxis was significantly compromised in presence of VCAM-1 neutralization compared to the respective isotype control (160.4±8.9 in control *vs*.51.3±6.4 in anti-VCAM-1), indicating BAL VCAM-1 is the key mediator of increased neutrophil flux in acute lung injury. In presence of BAL from $P2X_7R^{-/-}$ mice, neutrophil migration was relatively less responsive (100.5±8.8 neutrophil/field). This implies sVCAM-1 as one of the important cues specifically for the neutrophil-deficient phenotype of $P2X_7R^{-/-}$mice.

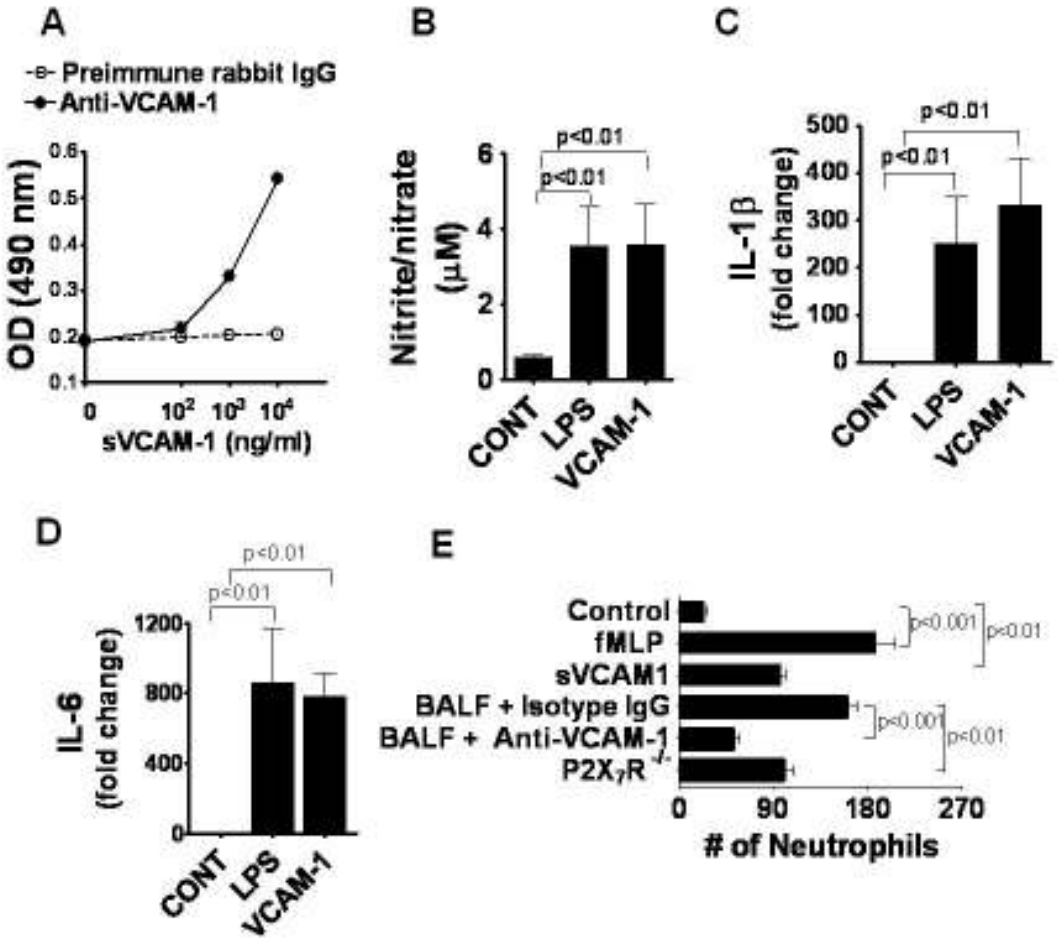

Figure 3.4: VCAM-1 activates macrophages and induces neutrophil chemotaxis.

(A) The binding of sVCAM-1 to alveolar macrophages. As described in *Materials and Methods* a cell-based ELISA has been developed using rat alveolar macrophages. Binding of sVCAM-1 with different concentrations were monitored following incubation with the detector anti-VCAM-antibody. Increase in OD was proportional to the sVCAM-1 concentrations. VCAM-1 activates alveolar macrophages and increases *(B)* nitrate/nitrite production *(C)* IL-1β and *(D)* IL-6 mRNA. *(E)* Chemotaxis assays on rat peripheral neutrophil. Briefly, neutrophils were pre-treated with dihydrochalasin B (2.5 μM) for 10 minutes and then placed on the upper chamber. Murine sVCAM-1 (10 μg/ml)

and fMLP (100 μM, a positive control), and control media was added in the bottom wells. LPS+MV treated-BAL from wild-type mice or $P2X_7R^{-/-}$ mice were incubated for 30 minutes with anti-VCAM-1 antibody or isotype control IgG (20 μg/ml) and placed at the lower chamber. The membrane was then removed, fixed and stained with Wright Giemsa stain. The cells that migrated and adhered to the lower surface of the membrane were counted from 10 microscopic fields under 40X objective. The data are expressed as means ± SE from 3 independent preparations in duplicates.

3.4.4 Anti-VCAM-1 antibody blocks LPS+MV-induced BAL neutrophilia and reverts lung injury in P2X7R-/- mice with recombinant-VCAM-1

To determine whether sVCAM-1 is responsible for neutrophil recruitment *in vivo* we neutralized VCAM-1 in alveoli with anti-VCAM-1 antibody. Intratracheal blockade of VCAM-1 yielded a striking decrease in lung neutrophil sequestration in wild-type compared to the corresponding isotype controls (6.5 ± 0.14 *vs*.0.87 ± 0.2 X 10^4/ml neutrophil) (Figure 3.5A). However, there was no significant difference observed in macrophage recruitment following treatment (Figure 3.5 B), indicating that neutrophils are the potent responders to VCAM-1 in the acute phase of inflammation. The release of IL-1β, IL-6, and MCP-1 (Figure 3.5C-E) into alveolar space was significantly reduced by VCAM-1 blockade.

Next, to demonstrate directly the less neutrophil infiltration phenotype in $P2X_7R^{-/-}$ mice challenged with LPS+MV is due to VCAM-1, we performed rescue experiments in $P2X_7R^{-/-}$ mice. $P2X_7R^{-/-}$ which develops less leukosequesterd-phenotype in response to LPS+MV shifted towards an amplified neutrophil recruitment in presence of recombinant VCAM-1 (4.8 ± 0.6 X 10^4/ml). Instillation of recombinant-VCAM-1 to the lung of $P2X_7R^{-/-}$ mice restored lung neutrophil infiltration following LPS+MV challenge (compare Figure 3.1A and 3.5A). BAL IL-1β, IL-6 and MCP-1 levels in BAL were also increased by VCAM-1 reconstitution. Our results suggest that the amplified neutrophil recruitment in the wild-type mice following LPS+MV is a consequence of increased VCAM-1 shedding in BAL and is $P2X_7R$-dependent. Together, these data demonstrate a critical role for VCAM-1-dependent neutrophil sequestration in injured lung tissue.

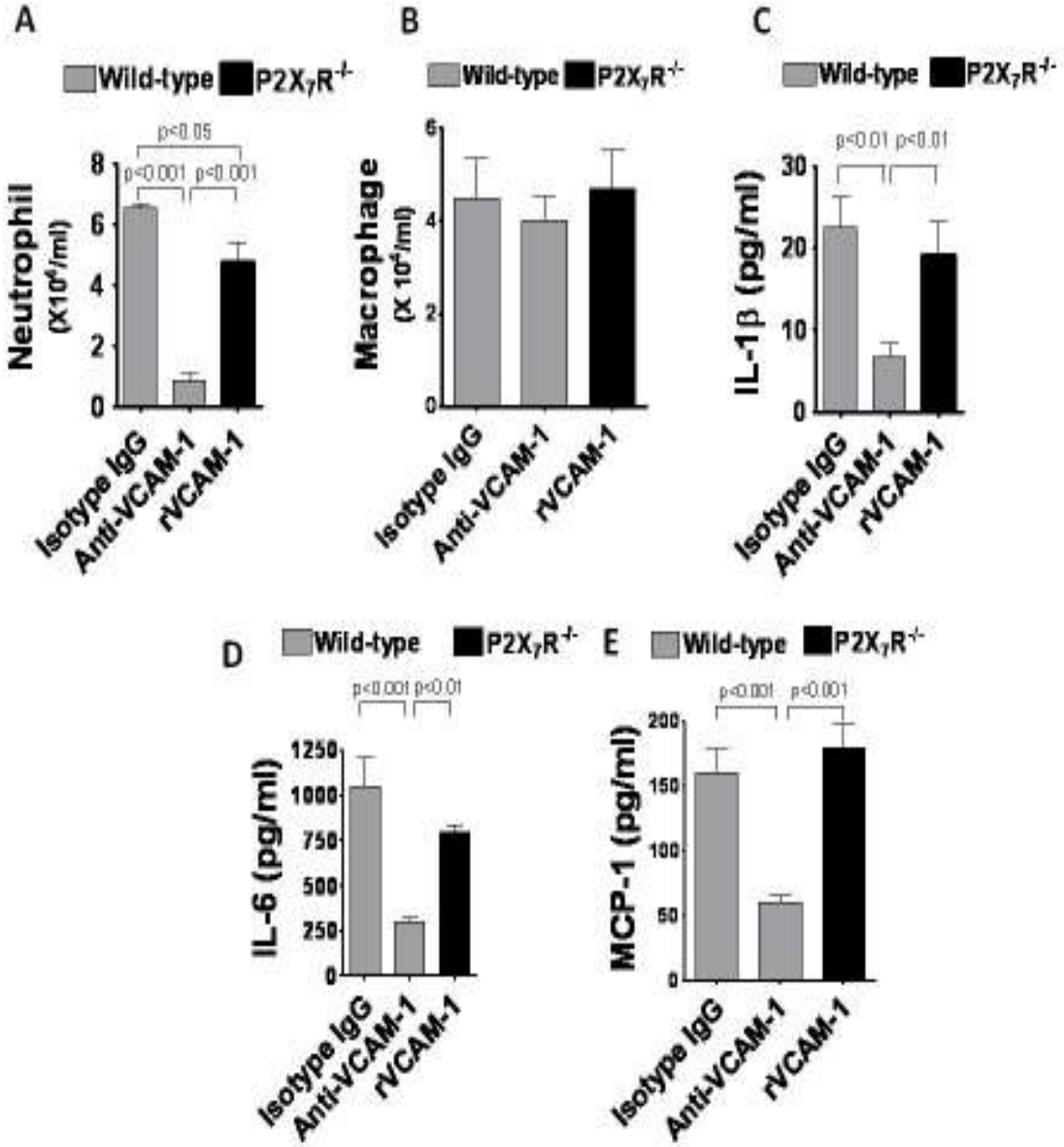
A
Wild-type
P2X7R-/-
p<0.05
p<0.001
p<0.001
Neutrophil
(X10⁶/ml)
8
6
4
2
0
Isotype IgG
Anti-VCAM-1
rVCAM-1
B
Wild-type
P2X7R-/-
Macrophage
(X 10⁶/ml)
6
4
2
0
Isotype IgG
Anti-VCAM-1
rVCAM-1
C
Wild-type
P2X7R-/-
p<0.01
p<0.01
IL-1β (pg/ml)
30
20
10
0
Isotype IgG
Anti-VCAM-1
rVCAM-1
D
Wild-type
P2X7R-/-
p<0.001
p<0.01
IL-6 (pg/ml)
1250
1000
750
500
250
0
Isotype IgG
Anti-VCAM-1
rVCAM-1
E
Wild-type
P2X7R-/-
p<0.001
p<0.001
MCP-1 (pg/ml)
200
150
100
50
0
Isotype IgG
Anti-VCAM-1
rVCAM-1

Figure 3.5: VCAM-1 neutralization in wild-type mice protects acute lung injury and is revert in P2X7R-/- mice in presence of recombinant VCAM-1 reconstitution.

Effect of function-blocking monoclonal antibody (mAb) against VCAM-1 in wild-type or reconstitution of recombinant-VCAM-1 in $P2X_7R^{-/-}$ mice on alveolar accumulation of *(A)* Neutrophil *(B)* Macrophage *(C)* IL-1β, *(D)* IL-6 and *(E)* MCP-1 following LPS+MV. Wild-type mice were intratracheally co-administered with isotype-matched control IgG or function-blocking mAb against VCAM-1 (88 μg/mouse) and $P2X_7R^{-/-}$ mice with murine recombinant VCAM-1 (5 μg/mouse) instilled along with LPS and ventilated as indicated in Materials and Methods. IL-1β, IL-6 and MCP-1 concentrations were evaluated using a murine ELISA. Values are given as mean ± SEM (n= 5-8 animals / group).

3.4.5 Systemic response to acute lung injury in $P2X_7R^{-/-}$ mice

Surface expression of β1 and β2-integrins on neutrophil is low in normal physiological conditions and is modulated in acute lung injury (Ridger *et al.*, 2001). We reasoned the sVCAM-1 mediated neutrophil sequestration in alveolar space requires up-regulation of integrins responsible for VCAM-1 binding. To determine whether the expression of α4β1 (VLA-4, CD49d/CD29), α4β7 (LPAM-1, CD49d/CD103) and $\alpha_M\beta2$ (CD11b/CD18) is modulated during lung injury, we performed flow cytometric analyses of these integrins on the neutrophils obtained from either peripheral blood or BAL from wild-type and $P2X_7R^{-/-}$ mice following LPS+MV. LPS+MV up-regulated α4 level but had a modest effect on β7 and α_M integrin levels on circulating blood neutrophils from wild-type mice (Figure 3.6A-C). In contrast, LPS+MV increased the levels of all three α4, β7 and α_M integrins. Isotype (rat IgG2b, κ) control antibody yielded minimal fluorescence intensity on BAL neutrophils as compared to anti-α4, anti-α_M and anti-β7 antibody (Data not shown). There was no significant difference in the expression of α4, β7 and α_M integrins on circulating and migrated neutrophils between wild-type and $P2X_7R^{-/-}$ mice. Cell surface expression of α4, β7 and α_M integrin was similar between the two genotypes in untreated control group.

We reasoned that the pulmonary origin of acute inflammation might propagate the effect systematically and could furthermore influence the neutrophil infiltrations to the lung. Serum sVCAM-1, IL-1β and IL-6 levels between wild-type and $P2X_7R^{-/-}$ mice following injury was compared. Serum sVCAM-1 concentrations were increased in wild-type mice following LPS+MV. This increase in $P2X_7R^{-/-}$ mice was modest (Figure 3.6D). Baseline levels of circulating sVCAM-1 were similar between control wild-type and

$P2X_7R^{-/-}$ mice. There was marked increased in serum IL-1β and IL-6 levels in wild-type mice which is less in $P2X_7R^{-/-}$ mice (Figure 3.6E-F). Collectively, these results suggest that β7 and α_M integrins on neutrophils play crucial role for the migration of neutrophil to alveolar space. Furthermore, the reduced neutrophil influx in $P2X_7R^{-/-}$ mice lung is due to abnormal VCAM-1 shedding in alveolar space, but not integrin expressions.

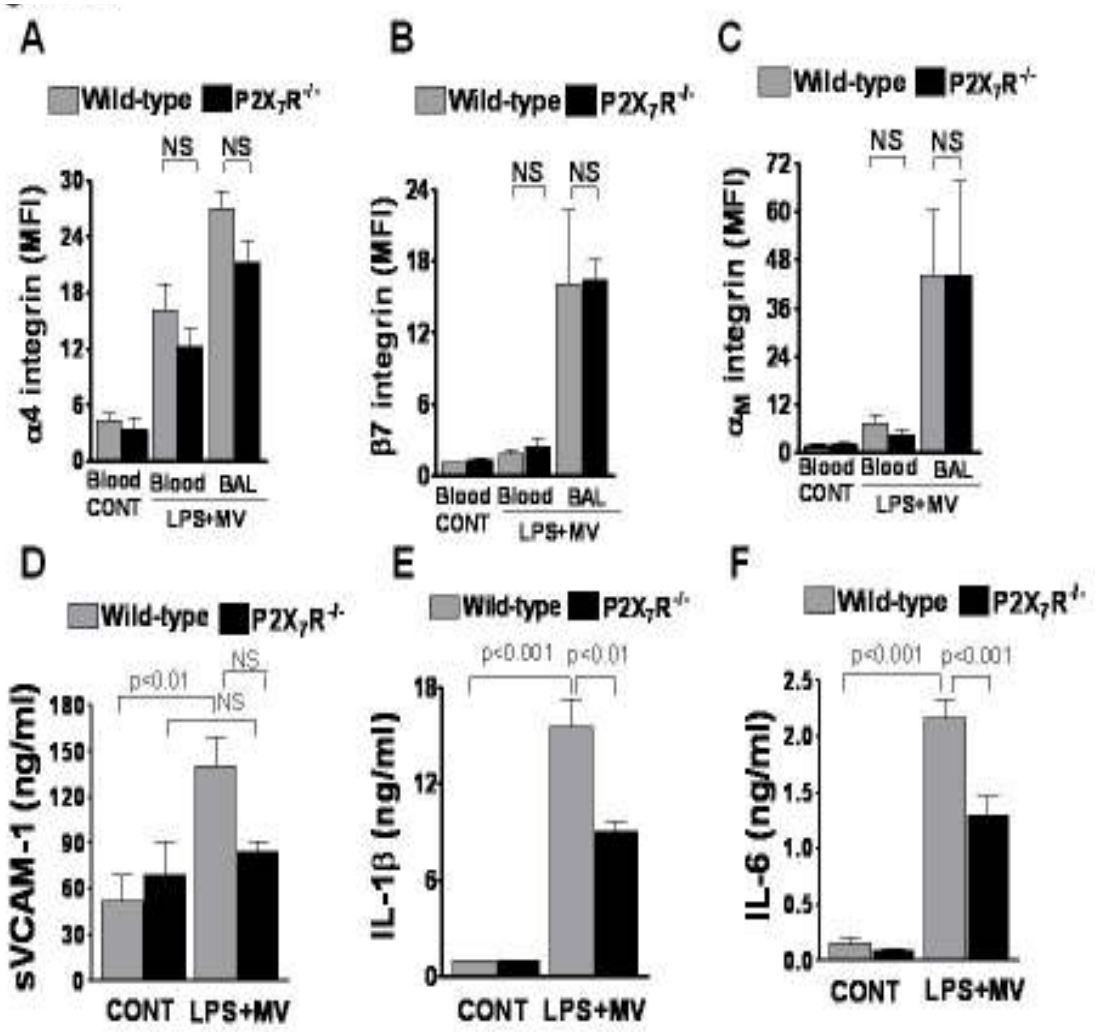

Figure3.6: The systemic effect of LPS+MV in P2X7R-/- mice

(A) α4 *(B)* β7 and *(C)* α_M –integrin expression in circulating or infiltrated BAL neutrophil from wild-type and $P2X_7R^{-/-}$ mice following LPS+MV. For flow cytometric analyses, EDTA-blood was taken from inferior venacava, and red blood cells were hypotonically lysed. Neutrophils were separated and stained as described in *Materials and Methods*. Neutrophils were gated on a two-dimensional forward and side scattergram of the single argon laser cytofluorometer FACSCalibur (BD Biosciences). Gr-1 positive cells had forward and side scatter characteristics consistent with granulocytes. The fluorescence

intensity was measured for each sample from 5,000 Gr-1 bright cells. The mean fluorescence intensities (MFI) obtained when neutrophils from either wild-type and $P2X_7R^{-/-}$ mice were labeled with the isotype (rat IgG 2b, κ) control antibody and was subtracted from the α4, β7 and α_M fluorescences. *(D)* sVCAM-1 *(E) IL-1β and (F) IL-6* in serum from LPS+MV or control wild-type and $P2X_7R^{-/-}$ mice as determined by ELISA. The data are expressed as means ± SE (n=4).

3.4.6 P2X7R in AEC I is functionally active for VCAM-1 shedding and neutrophil chemotaxis

The marked increase of sVCAM-1 in alveolar space suggests that alveolar epithelial cells are likely involved in VCAM-1 shedding in acute lung injury. We hypothesized that the reduced neutrophil flux seen in $P2X_7R^{-/-}$ mice were because of lack of $P2X_7R$ in AEC I due in part to less soluble VCAM-1 shedding. To test this, we assessed the trans-differentiated alveolar epithelial cells (AEC I-like cells) to shed soluble VCAM-1in the presence of pro-inflammatory IL-1β. VCAM-1 protein expression was increased during the trans-differentiation of AEC II to AEC I in culture (Figure 3.7A). Moreover, VCAM-1 was induced by IL-1β in wild-type AEC I, but not in $P2X_7R^{-/-}$ as determined by ELISA (Figure 3.7B). An elevated level of sVCAM-1 in the medium of the IL-1β–treated AEC I was observed. The IL-1β stimulated shedding of VCAM-1 was time-dependent. This stimulation was absent in AEC I from $P2X_7R^{-/-}$ mice (Figure 3.7C). Basal VCAM-1 shedding was comparable between wild-type and $P2X_7R^{-/-}$ from *day 3* and *day 5* AEC I (Figure 3.7D). A marked increase in soluble form of VCAM-1 was observed with IL-β stimulation at doses of 1 ng/ml and above which was completely absent in AEC I from $P2X_7R^{-/-}$. IL-1β-stimulated shedding was blocked by the broad spectrum metalloprotease inhibitor, GM-6001 (Figure 3.7E).

We sought to determine next the potency of shed sVCAM-1 from AEC I surface directly to neutrophil chemotaxis. Conditioned-media from IL-1β treated AEC I transferred to the lower-Boyden chamber amplifies the migration of neutrophil significantly in wild-type, but not from $P2X_7R^{-/-}$ (96.4±5.6 vs. 34.4±2.1) (Figure 3.7F), suggesting sVCAM-1 from AEC I is an efficient neutrophil chemoattractant and

differentially regulated in $P2X_7R^{-/-}$ mice. These data further indicate that AEC I is functionally active in VCAM-1shedding and $P2X_7R$ present in AEC I regulates the shedding process.

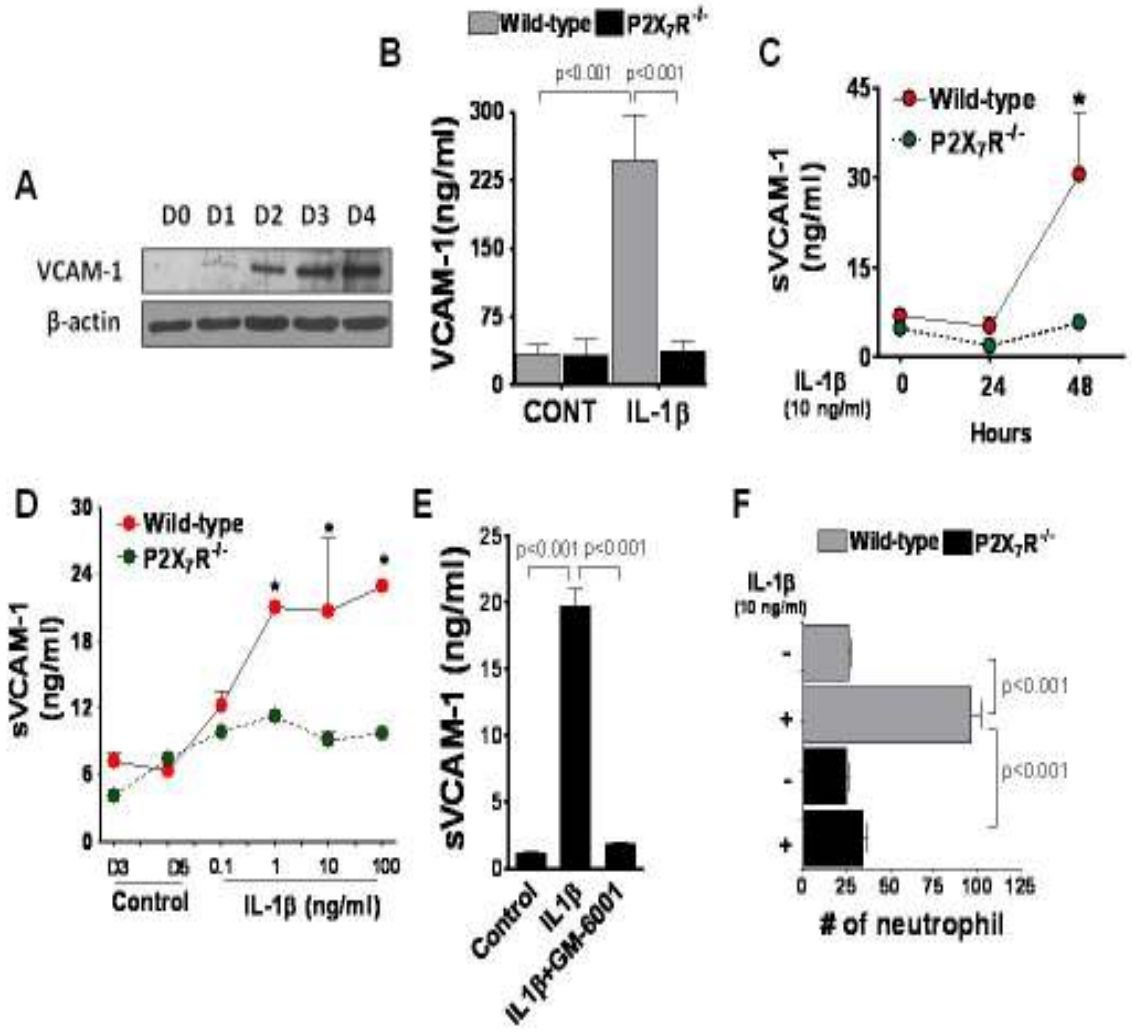

Figure 3.7: IL-1β induced VCAM-1 shedding from AEC I is P2X7R-dependent.

(A) Western blot analysis of VCAM-1 in AEC II (D0) and trans-differentiated AEC I (D1-D4) *(B)* Expression of VCAM-1 in trans-differentiated AEC I from wild-type and $P2X_7R^{-/-}$ mice as measured by ELISA. Cells were allowed to adhere for 48 h followed by gentle washing with replacement of media for *3 days*. AEC culture was stimulated with vehicle (Me_2SO) or IL-1β (10 ng/ml). *(C)* Time-dependent increase in sVCAM-1 shedding from wild-type AEC I by IL-1β stimulation on *day3* and *(D)* Dose-response of sVCAM-1 shedding in IL-1β stimulated and *(E)* GM-6001-treated AEC I culture. Supernatants were collected following stimulations with different dosage (0.1-100 ng/ml) of IL-1β and GM-6001 for 48 hours. Supernatants are subjected to centrifugation before measurement by ELISA. There were increased levels of sVCAM-1 in the culture supernatant as a result of IL-1β stimulation at higher doses after 48 hour in wild-type, but not in $P2X_7R^{-/-}$. Data are expressed as means ± SE from 3 independent preparations, *$p < 0.05$ vs. D5 wild-type control. *(F)* Migration of neutrophils towards conditioned-media collected from ± IL-1β-treated AEC I (10 ng/ml, 50% conditioned media were transferred to the lower chamber) from wild-type and $P2X_7^{-/-}$ mice and expressed as means ± SE from 3 independent preparations.

3.4.7 Soluble VCAM-1 shedding from AEC I surface is a $P2X_7R$-dependent ADAM-17 mediated phenomenon

To further characterize the mechanisms of induced VCAM-1 shedding from the AEC I, we adopted an *ex vivo* approach to measure ADAM-17 activity using freshly isolated AEC from wild-type and $P2X_7R^{-/-}$ mice following acute lung injury (Mishra *et al.*, 2011b). Surface expression of VCAM-1 in AEC I was significantly induced by LPS+MV in wild-type, and was modest in $P2X_7R^{-/-}$ mice as determined by flow cytometry (Figure 3.8A). ADAM-17 activity in AEC from wild-type was increased by LPS+MV and this increase was less in AEC I from $P2X_7R^{-/-}$ mice (321.8±53.4 *vs*. 193.4±19.6 ng/ml) (Figure 3.8B). In addition, the activation of $P2X_7R$ with BzATP increased ADAM-17 activity in a time dependent manner in HEK-$P2X_7R$ cells (HEK cells stably expressing rat-$P2X_7R$) (Figure 3.8C). The BzATP stimulated increase in ADAM17 activity was significantly blocked in presence of the ERK1/2 inhibitor (Figure 3.8D).Delving into the signaling pathway of $P2X_7R$ activation, we also examined the MAPK signaling pathway in AEC I-like E10 cells. BzATP stimulation increases phosphorylated pERK1/2 (Figure 3.8E), suggesting activation of $P2X_7R$ and engagement of MAPK signaling pathway in AEC I.

To examine the effect of other proteases in the process of VCAM-1 shedding from AEC I, we tested the MMP activities in BAL. Moreover, MMP2 and MMP9 activity in BAL from wild-type and $P2X_7R^{-/-}$ mice were similar following LPS+MV (Figure 3.8F-G), suggesting the stimulated shedding of VCAM-1 from AEC I is a $P2X_7R$-dependent phenomenon coupling ADAM-17. Collectively, these results supports

that VCAM-1 shedding from AEC I surface is mediated by $P2X_7R$ stimulation and MAPK signaling pathway and engage ADAM-17 activation.

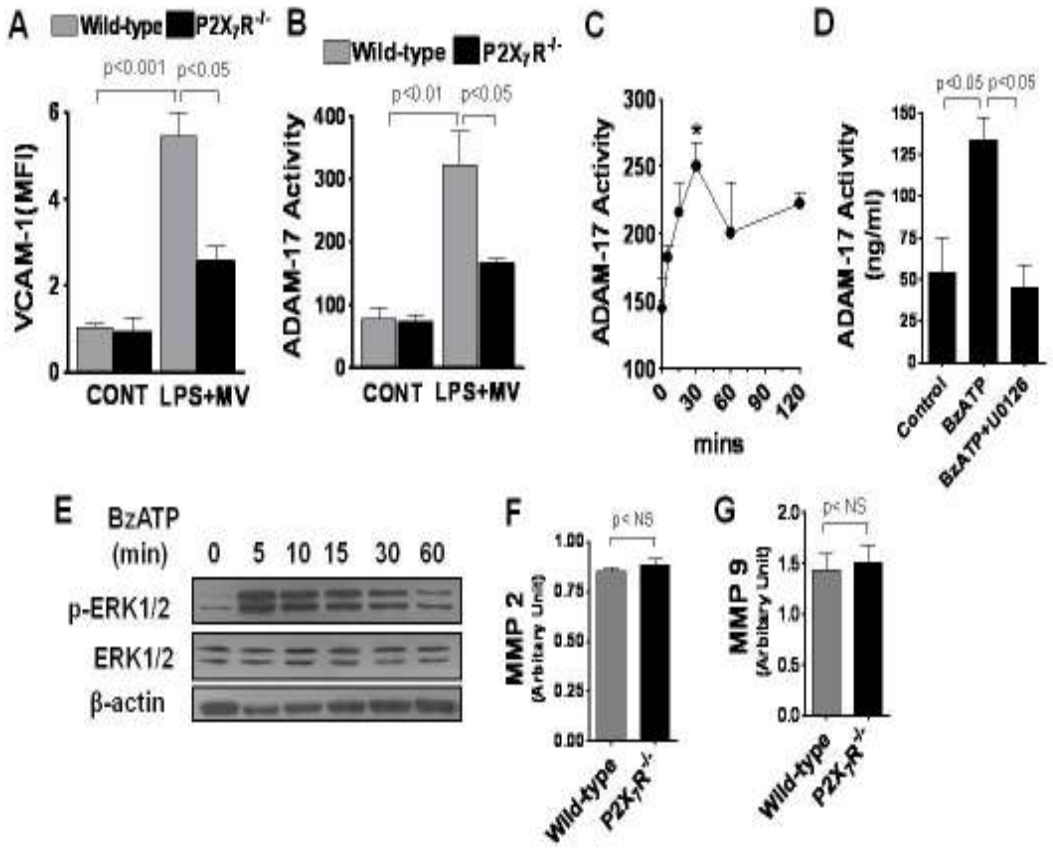

Figure 3.8: Shedding of VCAM-1 from AEC I is ADAM-17 mediated P2X7R-dependent phenomenon.

(A) FACS analysis of cell surface VCAM-1 expression in podoplanin (AEC I marker)-positive cells and *(B)* ADAM-17 activity in freshly isolated alveolar epithelial cells (AEC) following LPS+MV from wild-type and $P2X_7R^{-/-}$ mice as described in *Materials and Methods* (n=3). *(C)* ADAM-17 activity in HEK-$P2X_7R$ cells following BzATP stimulation with different time periods and *(D)* in presence of ERK1/2 inhibitor. *(E)* Time-dependent increase in phosphorylated ERK1/2 following BzATP stimulation in AEC-I like cells (E10). *(F-G)* Zelatin zymography of MMP 2 *and* MMP 9 activity in BAL from wild-type and $P2X_7R^{-/-}$ ensuing LPS and MV. MMP 9 and MMP2 activity were quantified from the zymogram using Image J software (n=8).

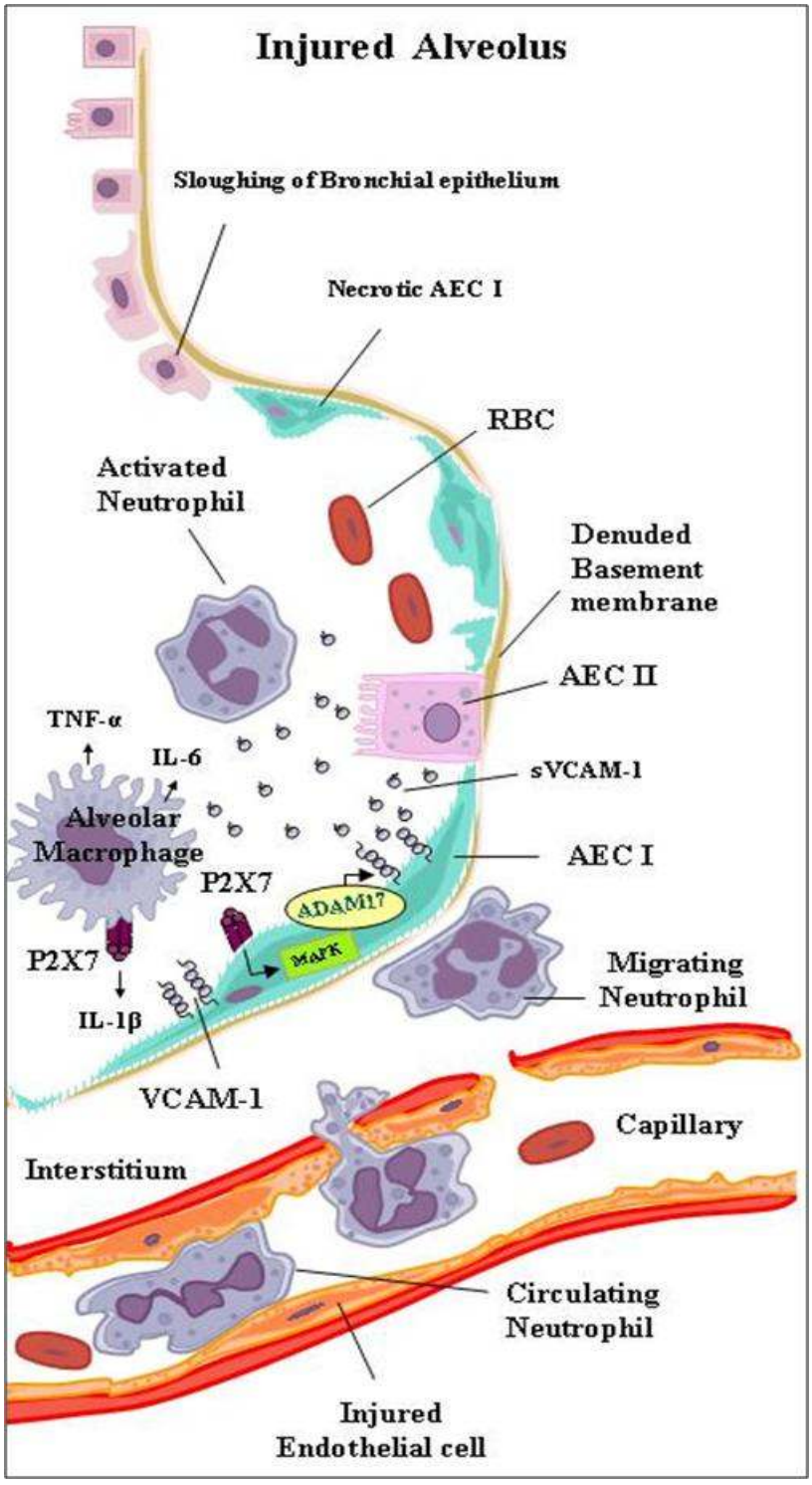

Figure 3.9: Pathophysiological role of $P2X_7R$ in acute lung injury

3.5 Discussion

The classic paradigm of inflammatory signaling in the lung has focused on neutrophil recruitment and activation of leukocytes, with concomitant release of soluble mediators that amplify and accelerate the process. Migration of neutrophil into the lungs is central to the pathogenesis of acute lung injury and requires an integrative signal. Our study describes a mechanism in which three epithelial components – a plasma membrane bound receptor ($P2X_7R$), a soluble adhesion molecule (sVCAM-1) and a metalloproteinase (ADAM-17) - act coordinately to direct neutrophils to injury sites. We identified $P2X_7R$, the predominant pro-inflammatory receptor on alveolar epithelia, as a regulator for soluble VCAM-1 shedding *in vivo* and *in vitro* through ADAM-17-dependent cleavage. Our data indicate that IL-1β rapidly induces VCAM-1 expression and cleaves the adhesion molecule from alveolar epithelial surface by activating ADAM-17 protease in a $P2X_7R$–dependent manner. The shed soluble VCAM-1 is then transported, either actively or passively, to the interstitial space creating a chemotactic gradient guiding neutrophils into the airspace. We propose that in response to injury, AEC I synthesize and shed VCAM-1 into the alveolar lining fluid. The $P2X_7R$ is a bona fide pro-inflammatory purinergic receptor and plays a crucial role in lung injury (Figure 3.1).

We used the two-hit moderate tidal volume MV and low dose LPS (LPS+MV)-induced lung injury model, because it recapitulates the aspects of acute lung injury in humans (Spragg *et al.*, 2010;Rubenfeld *et al.*, 2005). The model is reproducible and reliable and generates an early inflammatory response in the lung with neutrophil influx, proinflammatory cytokine release and alveolar-capillary damage (Altemeier *et al.*,

2004;Lopez-Aguilar *et al.*, 2010). Priming of lungs with LPS makes the lungs more susceptible to mechanical ventilation (Wosten-van Asperen *et al.*, 2010;Bregeon *et al.*, 2005). MV also potentiates lung inflammation and multi-organ dysfunction in the presence of whole bacteria like *staphylococcus aureus* and *Escherichia coli* (Dhanireddy *et al.*, 2006). In the current study, the potential involvement of $P2X_7R$ in the early inflammatory response was evaluated in using the two-hit model (Figure 3.1). Acute lung injury was more severe in wild-type mice than that in the mice treated with $P2X_7R$ antagonist or $P2X_7R$-deficient mice as evidenced by: (1) a greater accumulation of neutrophils in airway, alveolar and interstitial compartments, (2) an increased vascular permeability accompanied by increased exudation of plasma proteins, and (3) copious release of acute inflammatory cytokines and shedding of adhesion molecules in bronchoalveolar space (Figure 3.1 and 3.2).

The alveolar epithelium has the capacity not only to respond to microbial products but also to integrate the pro-inflammatory cascades in triggering or worsening acute lung injury. A number of regulatory molecules for examples IL-1β, IL-6, MCP-1, KC have been suggested as putative candidates to amplify these inflammatory events in the lung (Skerrett *et al.*, 2004b). The reduced levels of sVCAM-1 and concomitant less accumulation of neutrophil by LPS and MV in the lungs of $P2X_7R^{-/-}$ mice and following $P2X_7R$ antagonism provided an important clue to uncover the mechanism by which alveolar epithelium regulates neutrophil movement (Figure 3.2B). VCAM-1 is rapidly induced in epithelial cells in response to acute lung injury (Atsuta *et al.*, 1997). Shedding of VCAM-1 is a common phenomenon of inflamed epithelia (Vanderstocken *et al.*, 2010). Interestingly, intelligible shedding mechanisms of these adhesion molecules were

attributed to its location on endothelial cells from the opposite sides of the alveolar wall (Mendez *et al.*, 2008). VCAM-1 ectodomain shedding from the activated endothelial cells are the major source of the circulating VCAM-1. Cell and tissue specific disintegrin and metalloproteases family members have been shown to induce the release of the soluble form of VCAM-1 (Singh *et al.*, 2005;Rizzoni *et al.*, 2003). The current data suggests alveolar lining epithelium as a major source of soluble VCAM-1. Although cytokines are perceived to stimulate the induction of VCAM-1 on endothelial cells (Gerritsen & Bloor, 1993;Mchale *et al.*, 1999), the present investigation is the first to definitively attribute VCAM-1 shedding from alveolar epithelial cells. Furthermore, the less VCAM-1 shedding and ADAM-17 activity in $P2X_7R^{-/-}$ mice following acute lung injury, along with our *in vitro* studies showing that IL-1β-induced VCAM-1 ectodomain shedding from cultured alveolar epithelial cells, indicates that $P2X_7R$ is a physiologic component of the shedding process of this adhesion molecule.

The early emigration of circulating neutrophils into the airspaces results from interference with adhesion process of endothelial and epithelial membrane. The fact that neutrophils are normally in prolonged contact with capillary endothelium in the pulmonary vessels suggests that the mechanisms mediating migration of neutrophil into pulmonary capillary walls are different from other tissues (Downey *et al.*, 1993;Erzurum *et al.*, 1992;McDonald *et al.*, 2010). This “sieving” process causes a large population of neutrophils to form a marginated pool within the lung. Indeed the lower transmural pressure and close proximity of pulmonary circulation, gradient of soluble mediators in the alveolar and interstitial space plays a major role in the inflamed lung. This scheme of neutrophil infiltrations into the lung following acute lung injury is mediated by CD18-

dependent and –independent mechanism. Furthermore, in various models of lung injury, neutrophil influx is significantly reduced in mice treated with anti-ICAM-1, anti-CD18 or anti-CD11b antibodies (Kumasaka *et al.*, 1996b;Folkesson & Matthay, 1997;Gao *et al.*, 2005). Though CD11b/CD18 integrins are found to be up-regulated in neutrophils, blockade with saturating CD18 and ICAM-1 monoclonal antibodies could only block 40% of neutrophil influx to the lung (Gao *et al.*, 2001). Despite the recognized importance of CD11b/CD18 integrins and ICAM-1-mediated pathways in early migration of neutrophils, surrogate sequestration mechanisms are operational in the lung (Burns *et al.*, 2001;Doerschuk *et al.*, 2000). As there was no difference in neutrophil surface integrin expression between wild-type and $P2X_7R^{-/-}$ mice, the major contribution of $P2X_7R$ to acute neutrophil sequestration likely lies in the dissipation of soluble VCAM-1 rather than integrin expression (Figure 3.6). Given the high abundance of soluble VCAM-1 on the surface of alveolar epithelial cells, one can envision alveolar epithelium is not only a responder to microenvironments, but also incept the inflammatory cell sequestrations in lung injury.

The current immunoablation studies demonstrate that $P2X_7R$ on AEC I, critically regulates neutrophil influx into injured lung tissue. Complementary to our findings, targeting VCAM-1 associated pathways in disease models significantly reduces tissue damage, presumably due to reduced neutrophil influx (Tabary *et al.*, 2006;Ibbotson *et al.*, 2001). Furthermore, in various models of injury, infection, and inflammation the influx of leukocytes are significantly impaired in mice deficient for the VCAM-1 (Cybulsky *et al.*, 2001) or in mice treated with anti-VCAM-1 antibodies (Bowden *et al.*, 2002;Miyao *et al.*, 2006). In previous studies, α4/CD18-independent neutrophil influx has been reported to

play an important role during bacterial pneumonia (Kumasaka *et al.*, 1996a;Tasaka *et al.*, 2002). Association of α4-integrin on activated neutrophils with VCAM-1 substrate increases rolling and adherence, independent of selectins and β2-integrins (Ibbotson *et al.*, 2001;Reinhardt *et al.*, 1997;Reinhardt & Kubes, 1997). The shear forces in pulmonary capillaries are less and sufficient to support the α4β1-integrin mediated tethering and adhesion interactions (Reinhardt *et al.*, 1997). Nevertheless, the α4-integrin/VCAM-1-pathway is rapidly induced irrespective of bone marrow response and is transferrable on neutrophils (Ibbotson *et al.*, 2001). Functional blocking of VCAM-1 activity is protective in our model of acute lung injury as evidenced by reduced neutrophil sequestration, and IL-1β and IL-6 production in BAL (Figure 3.5). This was due to the fact of VCAM-1 binding to alveolar macrophages intensifies the already activated inflammatory response. Moreover, *in vitro* migration of neutrophils toward neutralized BAL with anti-VCAM-1 antibody or from $P2X_7R^{-/-}$ mice was reduced significantly (Figure 3.4). The present demonstration of a clear predisposition to enhanced BAL neutrophil sequestration and BAL cytokinemia in $P2X_7R^{-/-}$ mice following recombinant VCAM-1 reconstitution may also lie in its rescued-phenotype to shed sVCAM-1 (Figure 3.5). In the $P2X_7R^{-/-}$ mice, reconstitution of VCAM-1 accelerated the neutrophil sequestration to levels equal to those in wild-type mice. In addition, conditioned media from stimulated alveolar epithelial cells strikingly increased the number of chemotaxed neutrophils and was significantly reduced in $P2X_7R^{-/-}$ (Figure 6). This suggests that the depleted neutrophil sequestration in $P2X_7R^{-/-}$ was linked to the reduced VCAM-1 shedding from alveolar epithelium. Thus, $P2X_7R$ is likely to accelerate leukosequestration via VCAM-1 shedding. Together with our data, these findings

indicate that sVCAM-1 is critical for directing the movement of neutrophils in inflamed lung tissues. This finding is particularly important given that soluble VCAM-1 is a critical chemoattractant for neutrophil and in light of the previous finding that α4-integrin/VCAM-1 pathway conceivably induces inappropriate neutrophil sequestration (Ibbotson *et al.*, 2001).

Albeit the *in vivo* significance of VCAM-1 cleavage and shedding is incompletely understood, the observation of high levels of soluble VCAM-1 in BAL suggests a likely pathophysiological role in lung injury (Levesque *et al.*, 2000). Recent studies report that VCAM-1 shedding can be mediated by two distinct metalloproteinase activities, a PMA inducible protease like TNF-α-converting enzyme (ADAM-17, TACE) and a constitutive VCAM-1 sheddase that is active under normal cell culture conditions (Garton *et al.*, 2003). In addition several juxtamembrane sheddase like neutrophil elastase, cathepsin G and proteinases have also been implicated in the generation of soluble VCAM-1 (Levesque *et al.*, 2001). However, a definitive role of these proteases for the generation of soluble VCAM-1 *in vivo* is not clear. In this study we show for the first time that VCAM-1 shedding is functional in AEC I and is increased in acute lung injury via $P2X_7R$ mediated activation of ADAM-17. Several lines of evidence support the model that the activation of $P2X_7R$ couples ADAM-17 induced soluble VCAM-1 generation from AEC I. First, VCAM-1 expression is specifically induced in trans-differentiated AEC II by IL-1β and *in vivo* in freshly isolated AEC by LPS+MV, and is less in $P2X_7R^{-/-}$. Secondly, the shedding of VCAM-1 from AEC surface is increased by IL-1β and was blocked in presence of metalloproteinase inhibitor. Third, there was concomitant increase of ADAM-17 activity in AEC I by LPS+MV and is reduced in $P2X_7R^{-/-}$ mice. Fourthly,

BzATP stimulation increases the ADAM-17 activity in HEK-$P2X_7R$ cells, indicating ADAM-17 activation is mediated by $P2X_7R$ in AECI.

In summary, our experimental results demonstrate a direct link between $P2X_7R$ and control of neutrophil migration into injured lung tissue. This occurs via a previously unrecognized mechanism by which $P2X_7R$ on AEC I regulate the flux of neutrophils through shedding of VCAM-1 into local alveolar microenvironments by cellular activation of ADAM-17 (Figure 3.9). Previously, $P2X_7R$ has been demonstrated to be the major regulatory system for mature IL-1β release from alveolar macrophage (Myrtek *et al.*, 2008); these new data add to the pleiotropic properties of $P2X_7R$, demonstrating that $P2X_7R$-bearing AEC I can contribute acute lung injury. Furthermore, these new data indicate a prime role for $P2X_7R$ in modulating the expression of VCAM-1 receptors on the surface of AEC I. Thus, $P2X_7R$ resides at the critical nexus of cytokine regulation, neutrophil recruitment and inflammation as a vital regulator of alveolar function. Targeting $P2X_7R$ and VCAM-1 may provide a new therapeutic strategy to reduce neutrophil sequestration without altering yet critical mediators in lung injury.

3.6 References

1. Altemeier WA, Matute-Bello G, Gharib SA, Glenny RW, Martin TR, & Liles WC (2005). Modulation of lipopolysaccharide-induced gene transcription and promotion of lung injury by mechanical ventilation. *Journal of Immunology* **175**, 3369-3376.

2. Altemeier WA, Matute-Bello G, Frevert CW, Kawata Y, Kajikawa O, Martin TR, & Glenny RW (2004). Mechanical ventilation with moderate tidal volumes synergistically increases lung cytokine response to systemic endotoxin. *American Journal of Physiology-Lung Cellular and Molecular Physiology* **287**, L533-L582.

3. Atsuta J, Sterbinsky SA, Plitt J, Schwiebert LM, Bochner BS, & Schleimer RP (1997). Phenotyping and cytokine regulation of the BEAS-2B human bronchial epithelial cell: Demonstration of inducible expression of the adhesion molecules VCAM-1 and ICAM-1. *American Journal of Respiratory Cell and Molecular Biology* **17**, 571-582.

4. Bowden RA, Ding ZM, Donnachie EM, Petersen TK, Michael LH, Ballantyne CM, & Burns AR (2002). Role of alpha(4) integrin and VCAM-1 in CD18-independent neutrophil migration across mouse cardiac endothelium. *Circulation Research* **90**, 562-569.

5. Bregeon F, Delpierre S, Chetaille B, Kajikawa O, Martin TR, Autillo-Touati A, Jammes Y, & Pugin A (2005). Mechanical ventilation affects lung function and cytokine production in an experimental model of endotoxemia. *Anesthesiology* **102**, 331-339.

6. Burns JA, Issekutz TB, Yagita H, & Issekutz AC (2001). The alpha(4)beta(1) (very late antigen (VLA)-4, CD49d/CD29) and alpha(5)beta(1) (VLA-5, CD49e/CD29) integrins mediate beta(2) (CD11/CD18) integrin-independent neutrophil recruitment to endotoxin-induced lung inflammation. *Journal of Immunology* **166**, 4644-4649.

7. Chen J, Chen Z, Chintagari NR, Bhaskaran M, Jin N, Narasaraju T, & Liu L (2006). Alveolar type I cells protect rat lung epithelium from oxidative injury. *Journal of Physiology* **572**, 625-638.

8. Chin JE, Hatfield CA, Winterrowd GE, Brashler JR, Vonderfecht SL, Fidler SF, Griffin RL, Kolbasa KP, Krzesicki RF, Sly LM, Staite ND, & Richards IM (1997). Airway recruitment of leukocytes in mice is dependent on alpha(4)-integrins and vascular cell adhesion molecule-1. *American Journal of Physiology-Lung Cellular and Molecular Physiology* **272**, L219-L229.

9. Chiumello D & Cressoni M (2009). Respirator management of sepsis-related respiratory failure. *Current Infectious Disease Reports* **11**, 365-371.

10. Cicko S, Lucattelli M, Muller T, Lommatzsch M, De Cunto G, Cardini S, Sundas W, Grimm M, Zeiser R, Durk T, Zissel G, Boeynaems JM, Sorichter S, Ferrari D, Di Virgilio F, Virchow JC, Lungarella G, & Idzko M (2010). Purinergic Receptor Inhibition Prevents the Development of Smoke-Induced Lung Injury and Emphysema. *Journal of Immunology* **185**, 688-697.

11. Clausen P, Jacobsen P, Rossing K, Jensen JS, Parving HH, & Feldt-Rasmussen B (2000). Plasma concentrations of VCAM-1 and ICAM-1 are elevated in patients with Type 1 diabetes mellitus with microalbuminuria and overt nephropathy. *Diabetic Medicine* **17**, 644-649.

12. Corti M, Brody AR, & Harrison JH (1996). Isolation and primary culture of murine alveolar type II cells. *American Journal of Respiratory Cell and Molecular Biology* **14**, 309-315.

13. Cybulsky MI, Iiyama K, Li HM, Zhu SN, Chen M, Iiyama M, Davis V, Gutierrez-Ramos JC, Connelly PW, & Milstone DS (2001). A major role for VCAM-1, but not ICAM-1, in early atherosclerosis. *Journal of Clinical Investigation* **107**, 1255-1262.

14. Dhanireddy S, Altemeier WA, Matute-Bello G, O'Mahony DS, Glenny RW, Martin TR, & Liles WC (2006). Mechanical ventilation induces inflammation, lung injury, and extra-pulmonary organ dysfunction in experimental pneumonia. *Laboratory Investigation* **86**, 790-799.

15. Doerschuk CM, Mizgerd JP, Kubo H, Qin L, & Kumasaka T (1999). Adhesion molecules and cellular biomechanical changes in acute lung injury. *Chest* **116**, 37S-43S.

16. Doerschuk CM, Tasaka S, & Wang Q (2000). CD11/CD18-dependent and -independent neutrophil emigration in the lungs - How do neutrophils know which route to take? *American Journal of Respiratory Cell and Molecular Biology* **23**, 133-136.

17. Downey GP, Worthen GS, Henson PM, & Hyde DM (1993). Neutrophil sequestration and migration in localized pulmonary inflammation - capillary localization and migration across the interalveolar septum. *American Review of Respiratory Disease* **147**, 168-176.

18. Elices MJ, Osborn L, Takada Y, Crouse C, Luhowskyj S, Hemler ME, & Lobb RR (1990). VCAM-1 on activated endothelium interacts with the leukocyte integrin VLA-4 at a site distinct from the VLA-4/fibronectin binding-site. *Cell* **60**, 577-584.

19. Erzurum SC, Downey GP, Doherty DE, Schwab B, Elson EL, & Worthen GS (1992). Mechanisms of lipopolysaccharide-induced neutrophil retention - relative contributions of adhesive and cellular mechanical-properties. *Journal of Immunology* **149**, 154-162.

20. Ferrari D, Pizzirani C, Adinolfi E, Lemoli RM, Curti A, Idzko M, Panther E, & Di Virgilio F (2006). The P2X7 receptor: a key player in IL-1 processing and release. *Journal of Immunology* **176**, 3877-3883.

21. Folkesson HG & Matthay MA (1997). Inhibition of CD18 or CD11b attenuates acute lung injury after acid instillation in rabbits. *Journal of Applied Physiology* **82**, 1743-1750.

22. Gao XP, Liu QH, Broman M, Predescu D, Frey RS, & Malik AB (2005). Inactivation of CD11b in a mouse transgenic model protects against sepsis-induced lung PMN infiltration and vascular injury. *Physiological Genomics* **21**, 230-242.

23. Gao XP, Xu N, Sekosan M, Mehta D, Ma SY, Rahman A, & Malik AB (2001). Differential role of CD18 integrins in mediating lung neutrophil sequestration and increased microvascular permeability induced by Escherichia coli in mice. *Journal of Immunology* **167**, 2895-2901.

24. Garton KJ, Gough PJ, Philalay J, Wille PT, Blobel CP, Whitehead RH, Dempsey PJ, & Raines EW (2003). Stimulated shedding of vascular cell adhesion molecule 1 (VCAM-1) is mediated by tumor necrosis factor-alpha-converting enzyme (ADAM 17). *Journal of Biological Chemistry* **278**, 37459-37464.

25. Gerritsen ME & Bloor CM (1993). Endothelial-cell gene-expression in response to injury. *Faseb Journal* **7**, 523-532.

26. Goke M, Hoffmann JC, Evers J, Kruger H, & Manns MP (1997). Elevated serum concentrations of soluble selectin and immunoglobulin type adhesion molecules in patients with inflammatory bowel disease. *Journal of Gastroenterology* **32**, 480-486.

27. Green LC, Wagner DA, Glogowski J, Skipper PL, Wishnok JS, & Tannenbaum SR (1982). Analysis of Nitrate, Nitrite, and [N-15]-Labeled Nitrate in Biological-Fluids. *Analytical Biochemistry* **126**, 131-138.

28. Gu BJ & Wiley JS (2006). Rapid ATP-induced release of matrix metalloproteinase 9 is mediated by the P2X7 receptor. *Blood* **107**, 4946-4953.

29. Hamzaoui A, Ammar J, El Mekki F, Borgi O, Ghrairi HE, Ben Brahim M, & Hamzaoui K (2001). Elevation of serum soluble E-selectin and VCAM-1 in severe asthma. *Mediators of Inflammation* **10**, 339-342.

30. Hogg JC & Walker BA (1995). Polymorphonuclear leukocyte traffic in lung inflammation. *Thorax* **50**, 819-820.

31. Ibbotson GC, Doig C, Kaur J, Gill V, Ostrovsky L, Fairhead T, & Kubes P (2001). Functional alpha(4)-integrin: A newly identified pathway of neutrophil recruitment in critically ill septic patients. *Nature Medicine* **7**, 465-470.

32. Kallet RH, Jasmer RM, Pittet JF, Tang JF, Campbell AR, Dicker R, Hemphill C, & Luce JM (2005). Clinical implementation of the ARDS network protocol is associated with reduced hospital mortality compared with historical controls. *Critical Care Medicine* **33**, 925-929.

33. Kataoka A, Tozaki-Saitoh H, Koga Y, Tsuda M, & Inoue K (2009). Activation of P2X7 receptors induces CCL3 production in microglial cells through transcription factor NFAT. *Journal of Neurochemistry* **108**, 115-125.

34. Kumasaka T, Doyle NA, Quinlan WM, Graham L, & Doerschuk CM (1996a). Role of CD11/CD18 in neutrophil emigration during acute and recurrent Pseudomonas aeruginosa-induced pneumonia in rabbits. *American Journal of Pathology* **148**, 1297-1305.

35. Kumasaka T, Quinlan WM, Doyle NA, Condon TP, Sligh J, Takei F, Beaudet AL, Bennett CF, & Doerschuk CM (1996b). Role of the intercellular adhesion molecule-1 (ICAM-1) in endotoxin-induced pneumonia evaluated using ICAM-1 antisense oligonucleotides, anti-ICAM-1 monoclonal antibodies, and ICAM-1 mutant mice. *Journal of Clinical Investigation* **97**, 2362-2369.

36. Levesque JP, Hendy J, Takamatsu Y, Williams B, Winkler IG, & Simmons PJ (2001). VCAM-1 cleavage and release of neutrophil serine proteases elastase and cathepsin G in the bone marrow are common features of hemopoietic progenitor cell mobilization induced by G-CSF or chemotherapy. *Blood* **98**, 1242.

37. Levesque JP, Takamatsu Y, Nilsson SK, Haylock DN, & Simmons PJ (2000). Mobilization of hemopoietic progenitor cells into peripheral blood is associated with VCAM-1 proteolytic cleavage in the-bone marrow. *Blood* **96**, 221A.

38. Li X, Zhou L, Feng YH, Abdul-Karim FW, & Gorodeski GI (2006). The P2X7 receptor: a novel biomarker of uterine epithelial cancers. *Cancer Epidemiol Biomarkers Prev* **15**, 1906-1913

39. Lopez-Aguilar J, Quilez ME, Marti-Sistac O, Garcia-Martin C, Fuster G, Puig F, Flores C, Villar J, Artigas A, & Blanch L (2010). Early physiological and biological features in three animal models of induced acute lung injury. *Intensive Care Medicine* **36**, 347-355.

40. Matsuno O, Miyazaki E, Nureki S, Ueno T, Ando M, Ito K, Kumamoto T, & Higuchi Y (2007). Elevated soluble ADAM8 in bronchoalveolar lavage fluid in patients with eosinophilic pneumonia. *International Archives of Allergy and Immunology* **142**, 285-290.

41. McDonald B, Pittman K, Menezes GB, Hirota SA, Slaba I, Waterhouse CCM, Beck PL, Muruve DA, & Kubes P (2010). Intravascular danger signals guide neutrophils to sites of sterile inflammation. *Science Signaling* **3**.

42. McDonnell GV, McMillan SA, Douglas JP, Droogan AG, & Hawkins SA (1998). Raised CSF levels of soluble adhesion molecules across the clinical spectrum of multiple sclerosis. *Journal of Neuroimmunology* **85**, 186-192.

43. Mchale JF, Harari OA, Marshall D, & Haskard DO (1999). TNF-alpha and IL-1 sequentially induce endothelial ICAM-1 and VCAM-1 expression in MRL/lpr lupus-prone mice. *Journal of Immunology* **163**, 3993-4000.

44. Mehta VB, Hart J, & Wewers MD (2001). ATP-stimulated release of interleukin (IL)-1beta and IL-18 requires priming by lipopolysaccharide and is independent of caspase-1 cleavage. *Journal of Biological Chemistry* **276**, 3820-3826.

45. Mendez MP, Morris SB, Wilcoxen S, Du M, Monroy YK, Remmer H, Murphy H, Christensen PJ, & Paine R (2008). Disparate mechanisms of sICAM-1 production in the peripheral lung: contrast between alveolar epithelial cells and pulmonary microvascular endothelial cells. *American Journal of Physiology-Lung Cellular and Molecular Physiology* **294**.

46. Mendez MP, Morris SB, Wilcoxen S, Greeson E, Moore B, & Paine R (2006). Shedding of soluble ICAM-1 into the alveolar space in murine models of acute lung injury. *American Journal of Physiology-Lung Cellular and Molecular Physiology* **290**, L962-L970.

47. Mishra A, Chintagari NR, Guo YJ, Weng TT, Su LJ, & Liu L (2011a). Purinergic P2X(7) receptor regulates lung surfactant secretion in a paracrine manner. *J Cell Sci* **124**, 657-668.

48. Mishra A, Chintagari NR, Guo Y, Weng T, Su L, & Liu L (2011b). Purinergic P2X7 receptor regulates lung surfactant secretion in a paracrine manner. *J Cell Sci* **124**, 657-668.

49. Mitsiades CS & Mitsiades N (2003). P2X7 polymorphism and chronic lymphocytic leukaemia. *Lancet* **361**, 1478-1479.

50. Miyao N, Suzuki Y, Takeshita K, Kudo H, Ishii M, Hiraoka R, Nishio K, Tamatani T, Sakamoto S, Suematsu M, Tsumura H, Ishizaka A, & Yamaguchi K (2006). Various adhesion molecules impair microvascular leukocyte kinetics in

ventilator-induced lung injury. *American Journal of Physiology-Lung Cellular and Molecular Physiology* **290**, L1059-L1068.

51. Moon H, Na HY, Chong KH, & Kim TJ (2006). P2X7 receptor-dependent ATP-induced shedding of CD27 in mouse lymphocytes. *Immunology Letters* **102**, 98-105.

52. Muller T, Paula VR, Grimm M, Durk T, Cicko S, Zeiser R, Jakob T, Martin SF, Blumenthal B, Sorichter S, Ferrari D, Di VF, & Idzko M (2010). A Potential Role for P2X7R in Allergic Airway Inflammation in Mice and Humans. *American Journal of Respiratory Cell and Molecular Biology*.

53. Myrtek D, Muller T, Geyer V, Derr N, Ferrari D, Zissel G, Durk T, Sorichter S, Luttmann W, Kuepper M, Norgauer J, Di Virgilio F, Virchow JC, & Ldzko M (2008). Activation of human alveolar macrophages via P2 receptors: Coupling to intracellular Ca2+ increases and cytokine secretion. *Journal of Immunology* **181**, 2181-2188.

54. Nakao S, Kuwano T, Ishibashi T, Kuwano M, & Ono M (2003a). Synergistic effect of TNF-alpha in soluble VCAM-1-induced angiogenesis through alpha 4 integrins. *Journal of Immunology* **170**, 5704-5711.

55. Nakao S, Kuwano T, Ishibashi T, Kuwano M, & Ono M (2003b). Synergistic effect of TNF-alpha in soluble VCAM-1-induced angiogenesis through alpha 4 integrins. *Journal of Immunology* **170**, 5704-5711.

56. Osborn L, Hession C, Tizard R, Vassallo C, Luhowskyj S, Chirosso G, & Lobb R (1989). Direct expression cloning of vascular cell-adhesion molecule-1, a cytokine-induced endothelial protein that binds to lymphocytes. *Cell* **59**, 1203-1211.

57. Parmley LA, Elkins ND, Fini MA, Liu YE, Repine JE, & Wright RM (2007). alpha-4/beta-1 and alpha-L/beta-2 integrins mediate cytokine induced lung leukocyte-epithelial adhesion and injury. *British Journal of Pharmacology* **152**, 915-929.

58. Parvathenani LK, Tertyshnikova S, Greco CR, Roberts SB, Robertson B, & Postmantur R (2003). P2X7 mediates superoxide production in primary microglia and is up-regulated in a transgenic mouse model of Alzheimer's disease. *Journal of Biological Chemistry* **278**, 13309-13317.

59. Pittet JF, Mackersie RC, Martin TR, & Matthay MA (1997). Biological markers of acute lung injury: Prognostic and pathogenetic significance. *American Journal of Respiratory and Critical Care Medicine* **155**, 1187-1205.

60. Reinhardt PH, Elliott JF, & Kubes P (1997). Neutrophils can adhere via alpha(4)beta(1)-integrin under flow conditions. *Blood* **89**, 3837-3846.

61. Reinhardt PH & Kubes P (1997). Emigrated (not circulating) neutrophils adhere to cardiac myocytes via alpha(4)-integrin. *Faseb Journal* **11**, 433.

62. Rice GE & Bevilacqua MP (1989). An inducible endothelial-cell surface glycoprotein mediates melanoma adhesion. *Science* **246**, 1303-1306.

63. Ridger VC, Wagner BE, Wallace WAH, & Hellewell PG (2001). Differential effects of CD18, CD29, and CD49 integrin subunit inhibition on neutrophil migration in pulmonary inflammation. *Journal of Immunology* **166**, 3484-3490.

64. Rizzoni D, Muiesan ML, Porteri E, Castellano M, Salvetti M, Monteduro C, De Ciuceis C, Boari G, Valentini U, Cimino A, Sleiman I, & Agabiti-Rosei E (2003). Circulating adhesion molecules and carotid artery structural changes in patients with noninsulin-dependent diabetes mellitus. *Journal of Human Hypertension* **17**, 463-470.

65. Rose DM, Cardarelli PM, Cobb RR, & Ginsberg MH (2000). Soluble VCAM-1 binding to alpha 4 integrins is cell-type specific and activation dependent and is disrupted during apoptosis in T cells. *Blood* **95**, 602-609.

66. Rubenfeld GD, Caldwell E, Peabody E, Weaver J, Martin DP, Neff M, & Stern EJ (2005). Incidence and outcomes of acute lung injury. *New England Journal of Medicine* **353**, 1685-1693.

67. Ruegg C, Postigo AA, Sikorski EE, Butcher EC, Pytela R, & Erle DJ (1992). Role of Integrin alpha-4-beta-7/alpha-4-beta-P in lymphocyte adherence to fibronectin and VCAM-1 and in homotypic cell clustering. *Journal of Cell Biology* **117**, 179-189.

68. Singh RJR, Mason JC, Lidington EA, Edwards DR, Nuttall RK, Khokha R, Knauper V, Murphy G, & Gavrilovic J (2005). Cytokine stimulated vascular cell adhesion molecule-1 (VCAM-1) ectodomain release is regulated by TIMP-3. *Cardiovascular Research* **67**, 39-49.

69. Skerrett SJ, Liggitt HD, Hajjar AM, Ernst RK, Miller SI, & Wilson CB (2004a). Respiratory epithelial cells regulate lung inflammation in response to inhaled endotoxin. *American Journal of Physiology-Lung Cellular and Molecular Physiology* **287**, L143-L152.

70. Skerrett SJ, Liggitt HD, Hajjar AM, Ernst RK, Miller SI, & Wilson CB (2004b). Respiratory epithelial cells regulate lung inflammation in response to inhaled endotoxin. *American Journal of Physiology-Lung Cellular and Molecular Physiology* **287**, L143-L152.

71. Solle M, Labasi J, Perregaux DG, Stam E, Petrushova N, Koller BH, Griffith J, & Gabel CA (2001). Altered cytokine production in mice lacking P2X(7) receptors. *Journal of Biological Chemistry* **276**, 125-132.

72. Spragg RG, Bernard GR, Checkley W, Curtis JR, Gajic O, Guyatt G, Hall J, Israel E, Jain M, Needham DM, Randolph AG, Rubenfeld GD, Schoenfeld D, Thompson BT, Ware LB, Young D, & Harabin AL (2010). Beyond Mortality Future Clinical Research in Acute Lung Injury. *American Journal of Respiratory and Critical Care Medicine* **181**, 1121-1127.

73. Tabary O, Corvol H, Boncoeur E, Chadelat K, Fitting C, Cavaillon JM, Clement A, & Jacquot J (2006). Adherence of airway neutrophils and inflammatory response are increased in CF airway epithelial cell-neutrophil interactions. *American Journal of Physiology-Lung Cellular and Molecular Physiology* **290**, L588-L596.

74. Tasaka S, Richer SE, Mizgerd JP, & Doerschuk CM (2002). Very late antigen-4 in CD18-independent neutrophil emigration during acute bacterial pneumonia in mice. *American Journal of Respiratory and Critical Care Medicine* **166**, 53-60.

75. Vanderstocken G, Bondue B, Horckmans M, Di Pietrantonio L, Robaye B, Boeynaems JM, & Communi D (2010). P2Y(2) receptor regulates VCAM-1 membrane and soluble forms and eosinophil accumulation during lung inflammation. *Journal of Immunology* **185**, 3702-3707.

76. Velikova G, Banks RE, Gearing A, Hemingway I, Forbes MA, Preston SR, Hall NR, Jones M, Wyatt J, Miller K, Ward U, Al-Maskatti J, Singh SM, Finan PJ, Ambrose NS, Primrose JN, & Selby PJ (1998). Serum concentrations of soluble adhesion molecules in patients with colorectal cancer. *British Journal of Cancer* **77**, 1857-1863.

77. Velikova G, Banks RE, Gearing A, Hemingway I, Forbes MA, Preston SR, Jones M, Wyatt J, Miller K, Ward U, AlMaskatti J, Singh SM, Ambrose NS, Primrose JN, & Selby PJ (1997). Circulating soluble adhesion molecules E-cadherin, E-selectin, intercellular adhesion molecule-1 (ICAM-1) and vascular cell adhesion molecule-1 (VCAM-1) in patients with gastric cancer. *British Journal of Cancer* **76**, 1398-1404.

78. Walsh GM, Symon FA, Lazarovits AI, & Wardlaw AJ (1996). Integrin alpha(4)beta(7) mediates human eosinophil interaction with MAdCAM-1, VCAM-1 and fibronectin. *Immunology* **89**, 112-119.

79. Wellicome SM, Kapahi P, Mason JC, Lebranchu Y, Yarwood H, & Haskard DO (1993). Detection of a circulating form of vascular cell-adhesion molecule-1 - raised levels in rheumatoid-arthritis and systemic lupus-erythematosus. *Clinical and Experimental Immunology* **92**, 412-418.

80. Woodside DG, Kram RM, Mitchell JS, Belsom T, Billard MJ, McIntyre BW, & Vanderslice P (2006). Contrasting roles for domain 4 of VCAM-1 in the regulation of cell adhesion and soluble VCAM-1 binding to integrin alpha(4)beta(1). *Journal of Immunology* **176**, 5041-5049.

81. Wosten-van Asperen RM, Lutter R, Specht PAC, van Woensel JB, van der Loos CM, Florquin S, Lachmann B, & Bos AP (2010). Ventilator-induced inflammatory response in lipopolysaccharide-exposed rat lung is mediated by angiotensin-converting enzyme. *American Journal of Pathology* **176**, 2219-2227.

CHAPTER IV

SUMMARY AND CONCLUSION

AEC I play important roles in alveolar barrier protection and fluid homeostasis. Earlier studies indicated that purinergic P2X7 receptors were specifically expressed in AEC I. However, their implication in lung functions has not been studied. The present study was hence designed to study the pathophysiological role of P2X7 receptor in AEC I.

We studied the AEC I and AEC II communications as they relate to surfactant secretion. Our results indicated that P2X7 receptors are functionally active in AEC I. The stimulation of P2X7 receptors in AEC I releases soluble mediator, ATP, which acts in a paracrine fashion on AEC II. Activation of P2Y2 receptors by extracellular ATP increases surfactant secretion from AEC II via a PKC–dependent signaling pathway. Moreover, the paracrine regulation of surfactant exocytosis by P2X7 receptor is a physiologically relevant phenomenon as the P2X7 receptor knock-out mice are less responsive to hyperventilation-induced surfactant release. We conclude that P2X7 receptors in AEC I are an important regulator of surfactant secretion and AEC I and AEC II communications.

Next, we explored the pathological function of P2X7 receptor in AEC I. We compared the P2X7 receptor knock-out and wild-type mice for their susceptibility to ALI. Our results identified that P2X7 receptor knock-out mice are less susceptible to LPS and mechanical ventilation-induced ALI. Furthermore, delving into the mechanism, we

found that P2X7 receptor-mediated sVCAM-1 release from AEC I is crucial for the recruitment of neutrophils in the alveolar space. Moreover, the metalloprotease, ADAM17 are responsible for VCAM-1 shedding from AEC I surface.

In summary, we for the first time implicated the roles of P2X7 receptors in surfactant regulation and neutrophil infiltrations in ALI. Thus, $P2X_7R$ resides at the critical nexus of surfactant regulation, cytokine modulation, neutrophil recruitment and inflammation.

APPENDIX

PERMISSION GRANTED FOR THE PURPOSE INDICATED

Mishra, A., Chintagari, N. R., Guo, Y. J., Weng, T. T., Su, L. J., and Liu, L. (2011) *J Cell Sci* **124,** 657-668

[http://jcs.biologists.org/content/124/4/657.full.pdf+html]

OFFICIAL JOURNAL OF THE COMPANY OF BIOLOGIST

VITA

Amarjit Mishra

Candidate for the Degree of

Doctor of philosophy

Thesis: Purinergic P2X7 receptor: Pathophysiological Role in Alveolar Functions

Major Field: Veterinary Biomedical Sciences

Biographical:

EDUCATION:

Bachelor of Veterinary Science & Animal Husbandry, India, July.1998-July. 2003

Master of Veterinary Science (Animal Biochemistry): Indian Veterinary Research Institute, Bareilly, UP, India, August 2003- July 2005. (Major Advisor: Dr. Sanat K. Meur). Thesis: Influence of induced heat stress on HSP 70 in buffalo lymphocytes.

Ph.D: Completed the requirement for Doctor of Philosophy degree with major in Veterinary Biomedical Sciences (Physiology) at Oklahoma State University, December, 2011.

EXPERIENCE:

Junior Research Fellow (July 2003- July. 2005)
Teaching Associate (July 2006-December. 2011)

PROFESSIONAL MEMBERSHIPS:

American Physiological Society
American Association for Advancement of Science
Society for Experimental Biology and Medicine

Name: AMARJIT MISHRA Date of Degree: December, 2011

Institution: Oklahoma State University Location: Stillwater, Oklahoma

Title of Study: PURINERGIC P2X7 RECEPTOR: PATHOPHYSIOLOGICAL ROLE IN ALVEOLAR FUNCTIONS

Pages in Study: 166 Candidate for the Degree of Doctor of Philosophy

Major Field: Veterinary Biomedical Sciences (Physiology)

Scope and Method of Study:

The present study was initiated to elucidate the role of P2X7 receptor in alveolar functions. P2X7 receptor function was studied in AEC I. P2X7 receptor stimulation in AEC I was examined for its role in ATP release and modulating the surfactant secretion from AEC II. Finally, we studied the novel function of P2X7 receptors in acute lung injury. We used a variety of techniques including cytokine array, ELISA, immunoblotting, histopathology to address the biological questions.

Findings and Conclusions:

1. P2X7 receptor are functional in AEC I.
2. Activation of P2X7 receptor in AEC I releases ATP.
3. P2X7 receptor stimulation in AEC I increases surfactant secretion from AEC II via paracrine release of ATP.
4. P2X7 receptor knock-out mice release less surfactant in response to hyperventilation.
5. P2X7 receptor antagonism and P2X7 receptor knock-out mice are less susceptible to acute lung injury.
6. The release of soluble VCAM-1 (sVCAM-1) from AEC I surface is P2X7 receptor-dependent.
7. Soluble VCAM-1 attracts neutrophils into the alveolar space in acute lung injury.

ADVISER'S APPROVAL: Dr. LIN LIU